FUNCTIONAL ANALYSIS OF THE CELLULOSE SYNTHASE GENE FAMILY IN MAIZE: FROM BIOINFORMATICS TO ASSESSMENTS AT WHOLE-PLANT, TISSUE, CELL, AND PROTOPLAST LEVELS

By

BRENT A. O'BRIEN

A DISSERTATION PRESENTED TO THE GRADUATE SCHOOL
OF THE UNIVERSITY OF FLORIDA IN PARTIAL FULFILLMENT
OF THE REQUIREMENTS FOR THE DEGREE OF
DOCTOR OF PHILOSOPHY

UNIVERSITY OF FLORIDA

2011

To my grandfather, S. Allen Poole, for his love, guidance, and undying support of my academic endeavours

ACKNOWLEDGMENTS

I thank my advisor, Karen Koch, and supervising committee, Drs., Ken Boote, Alice Harmon, Gary Peter, and Wilfred Vermerris for their guidance and scientific insight throughout my graduate career. I also thank my labmates (past and present) and our lab manager, Wayne Avigne, for all of their help and support throughout my time in graduate school. Finally, I thank my family and friends for their support and encouragement.

TABLE OF CONTENTS

page

.

LIST OF TABLES

LIST OF FIGURES

Abstract of Dissertation Presented to the Graduate School
of the University of Florida in Partial Fulfillment of the
Requirements for the Degree of Doctor of Philosophy

FUNCTIONAL ANALYSIS OF THE CELLULOSE SYNTHASE GENE FAMILY IN MAIZE: FROM BIOINFORMATICS TO ASSESSMENTS AT WHOLE-PLANT, TISSUE, CELL, AND PROTOPLAST LEVELS

By

Brent A. O'Brien

December 2011

Chair: Karen Koch
Major: Plant Molecular and Cellular Biology

Cellulose is "the most abundant polysaccharide on earth," and predominates in the primary cell wall of almost every plant cell. Cellulose is also central to formation of secondary cell walls in vascular tissues and wood. Since the function of cellulose in these walls varies with tissue and development, we hypothesized that these roles would be reflected in differential regulation of cellulose synthase genes. We utilized four approaches to test this hypothesis in the diverse cellulose-synthase gene family of maize, a species critical to human needs for food, fuel, and fiber. First, bioinformatic analysis of the cellulose synthase (*CesA*) gene family revealed several, potentially-functional paralogs in this ancient tetraploid. In most instances, paralogs mapped to chromosomal segments associated with enhanced gene loss, supporting an emerging model for one subgenome remaining resistant to gene loss after a genome duplication event. Second, we quantified expression of 13 *CesAs* at cell-, protoplast-, and tissue-levels. In suspension cultures and *in planta*, three *CesA* family members (C*esA10, CesA11,* and *CesA12)* showed consistent, exclusive co-expression. Each instance of their coordinate, elevated mRNA levels coincided with sites and/or timing of enhanced lignin deposition, consistent with

involvement of these genes in secondary cell wall biosynthesis. Other *CesA's* showed coordinate regulation among some family members, but composition of these subgroups changed during development. Third, we characterized *CesA* responses to induction of secondary cell wall biosynthesis in suspension cells. Expression of most *CesAs* was not altered, but the upregulation of C*esA10, CesA11,* and *CesA12* with onset of secondary cell wall deposition supported their contribution to this process. For our fourth approach, we employed co-segregational analysis to determine if *cesA* mutants were associated with visible phenotypes in maize. No such phenotypes were evident for homozygous mutations in any of the seven *CesA* family members or double-mutant examined, indicating significant functional redundancy within the *CesA* family.

Collectively, results support a model in which three *CesAs* (*CesA10, CesA11, and CesA12*) predominate in deposition of secondary cell walls of maize, and where other C*esAs* function in primary wall formation through combinations of co-expressed *CesA*-subgroups that vary with given tissues and stages of development.

CHAPTER 1
INTRODUCTION

The plant cell wall is a complex structure constructed predominantly from polysaccharides such as cellulose, pectins, and hemicelluloses. In addition to these various carbohydrate constituents, the cell wall also includes proteins, and in some instances, lignin, cutin, and suberin (Fry, 2004). The cell wall protects the cell from damage and pathogens, provides mechanical support for the cell and plant, and ultimately determines plant shape and size through its role in cell expansion. Furthermore, the endosperm cell walls in many species act as storage sites for re-mobilizable, hemicellulosic polysaccharides (Reid and Edwards, 1995; Olsen, 2007).

Cell walls are classified as either primary or secondary, and primary walls are further defined as type I or type II (Schaffner and Sheen, 1991). Primary cell walls are those that are initially laid down around the plasma membrane. Their expansion allows plant cells to increase in size as they grow. In some cell types, secondary layers of cell wall are deposited inside the primary wall once cell growth has stopped. These layers can be distinguished by the pitch, or angle, of the cellulose microfibrils deposited within. Secondary cell walls have greater mechanical strength than primary cell walls, and are often associated with xylem vessels and woody tissues rich in lignin (Boerjan et al., 2003). Secondary cell wall composition typically differs from that of the primary wall in that it often contains substantial amounts of lignin (which adds strength) and waxy substances such as cutin and suberin.

Among primary cell walls, the type I are more taxonomically widespread than the type II, and are standard in gymnosperms, dicots, and many monocots. Type II cell walls occur only in the commelinoid monocots, which include grasses, gingers, and bromeliads (Schaffner and Sheen, 1991; Carpita, 1996; Yokoyama and Nishitani, 2004). The main difference between these

two types of primary cell walls is their chemical composition. Although cellulose is the most abundant component in both types, it is cross-linked primarily with xyloglucans in type I walls and glucuronoarabinoxylans in type II walls (Carpita, 1996). In addition, type I walls contain considerably more pectin and structural protein than do type II walls (Carpita, 1996).

Cellulose is the most abundant component in the cell wall and is largely responsible for its mechanical strength (Saxena and Brown, 2005). Even in woody tissues and cells with abundant lignin, it is the cellulose infrastructure that provides a significant portion of the strength and flexibility to the cell wall. The importance of cellulose in providing durability to cell walls is apparent in the brittle culm mutants of barley and rice, in which tissues are easily broken due to a deficiency of cellulose, even though lignin levels are unchanged or elevated (Tanaka et al., 2003; Burton et al., 2010). This polysaccharide is present as structural units comprised of 36 individual, linear chains of (1→4)-ß-linked D-Glucose that combine to form a single microfibril (Delmer and Amor, 1995). The individual glucan chains can range from 8,000 units long in primary cell walls, to 15,000 units in secondary cell walls (Pear et al., 1996; Brett, 2000; Brown, 2004). In addition, individual glucan chains overlap (with regard to chain ends) within a microfibril (Carpita, 1996). The orientation of deposition for these microfibrils determines the direction that the cell can elongate (Saxena and Brown, 2005), thus regulation of cellulose deposition is central to plant architecture.

Cellulose is a semi-crystalline molecule that can be polymorphic (Saxena and Brown, 2005). The crystal state of cellulose depends on the positioning of the individual glucan chains relative to one another. Cellulose I, which is found in plants (as opposed to synthetic cellulose II), consists of parallel glucan chains packed side by side. The two crystalline configurations of cellulose I are I_{α} and $I_{ß}$. The cellulose molecules in both configurations show the same skeletal conformation, but their hydrogen bonding patterns differ (Atalla and VanDerhart, 1989;

Nishiyama et al., 2003). This results in each type having a different lattice structure (Atalla and VanDerhart, 1989). Plant cellulose is generally richer in cellulose $I_ß$, whereas the cellulose of more primitive organisms has more of the I_α configuration. Chemical perturbation experiments have shown that cellulose $I_ß$ is the more stable form, but microfibrils can contain both types, and the ratio of each configuration can influence physical properties of cellulose (Atalla and VanDerhart, 1989; Saxena and Brown, 2005).

Cellulose crystallization is believed to occur at the same time the strands are synthesized in the rosette (Herth, 1983). This mode of action is supported by a correlation between the size of rosette arrays and the microfibrils they form. Whereas individual rosettes in plants yield 36-chain fibrils, the algae *Micrasterias* produces much larger fibrils from arrays of up to 175 rosettes (Giddings et al., 1980). Additionally, the *radial swelling 1-1* mutant in *Arabidopsis* is a temperature sensitive *CesA* mutant that, upon exposure to nonpermessive temperature, shows dissociation of individual rosettes and production of amorphous, noncrystalline cellulose (Arioli et al., 1998). Mechanisms underlying these configurations of cellulose in plants and their balance in a given microfibril have remained a subject of intensive interest for many years (Vietor et al, 2002; Nishiyama et al., 2002 and 2008; Tanaka and Iwata, 2006).

The first successful investigation into the biochemical mechanism of biological cellulose synthesis demonstrated that a lyophilized preparation from the cellulose-producing bacteria, *Acetobacter xylinum,* could produce cellulose in the presence of glucose and oxygen (Hestrin and Schramm, 1954). A few years later the substrate required for cellulose synthesis by this same system was specifically determined to be UDP-glucose by providing different forms of C-14-glucose (Glaser, 1957). These results were also supported by the observation that *A. xylinum* mutants lacking capacity to produce UDP-glucose were also cellulose deficient (Valla et. al., 1989). Although much subsequent effort focused on elucidating mechanisms of cellulose

biosynthesis, progress has been slow due to the lability of membrane protein complexes, the difficulty associated with characterizing them, and the extent of required cofactors. Furthermore, and perhaps more importantly, callose contamination of preparations to be used for study of cellulose synthesis has remained a problem for many years. The basis for this difficulty included the similarity in structures of callose and cellulose (callose being 1-3 β-D- glucose and cellulose being 1-3 β-D- glucose), production of both compounds at the plasma membrane, and synthesis of both from the same substrate (Pear et al., 1995).

The enzyme responsible for providing this UDP-glucose substrate remained elusive for some time, however sucrose synthase was considered a strong candidate due to its likelihood of contributing the same substrate for callose synthesis (Frost et al., 1990; Nolte and Koch, 1993). Further investigation by Amor et al. (1995) initially indicated that as much as 50% of sucrose synthase could be located at the plasma membrane, and that this immunolocalized to helical arrays with patterns that paralleled cellulose deposition (Amor et al., 1995). Similar observations were reported for dense localization of sucrose synthase in the plasma membrane at sites of cellulose deposition in tips of rapidly-growing cotton trichomes (Nolte et al., 1995) and at points of wall thickening in hypoxic wheat roots (Alberecht and Mustroph, 2003). The *shrunken1* maize mutant, which is deficient in an endosperm-specific sucrose synthase, lacks cell walls in its interior, consistent with a possible role of sucrose synthase in their formation (Chourey et al., 1991). Only recently has evidence emerged that directly links sucrose synthase with cellulose synthase machinery. Work by Fujii et al. (2010) has demonstrated through immunogold labeling with sucrose synthase antibodies, that sucrose synthase can bind to rosettes in vitro and synthesize cellulose, thus supporting previous observations that sucrose synthase is likely essential for cellulose production *in planta*.

Cellulose synthase was first identified as an 83-kD polypeptide using a product-entrapment approach in *Acetobacter xylinum* (Lin and Brown, 1989). This cellulose synthase gene was subsequently cloned (Saxena et al., 1990). Concurrent, yet independent experiments involving complementation of a cellulose-deficient, *A. xylinum* mutant led to the cloning of a four-gene operon, with one gene (*BcsA*) being homologous to the cellulose synthase cloned by Saxena et al.(1990) (Wong et al., 1990). Another cellulose synthase gene (*CelA*) was then cloned from *Agrobacterium tumefaciens* in 1995 (Matthysse et al., 1995), but identification of cellulose synthase genes in plants proved more challenging. Most researchers sought *BcsA/CelA* homologs in plants using the bacterial *BcsA* gene as a probe. This approach was not successful, because cellulose synthases are now known to have significant variation in sequence outside key domains conserved in processive glycosyltransferases (Saxena et al., 1994; Delmer and Amor, 1995).

The first plant cellulose synthase (*CesA*) was cloned in cotton by sequencing a cDNA library from cotton fibers at a stage of maximum secondary cell wall deposition (Pear et al., 1996). Identification of two highly conserved genes having regions of high homology to the bacterial *CelA* genes led to the initial conclusion that these were indeed cellulose synthases. Since this discovery, the release of sequenced genomes and databases of gene expression during developmental progression has led to identification of no fewer than 10 *CesA* genes in *Arabidopsis* and at least 12 in maize (Holland et al., 2000). The presence of orthologous *CesA* genes has also been confirmed in other species with sequenced genomes, such as rice and poplar (Burton et al., 2005). Structural data indicate that the *CesA* genes code for integral membrane proteins that assemble into rosettes. This association was first demonstrated in a temperature-dependent *Arabidopsis cesA* mutant, called *radial swelling 1-1*,that showed

disassembly of individual rosettes and production of noncrystalline cellulose at high temperatures (Arioli et al., 1998; Taylor, 2008).

Cellulose synthesizing protein complexes were first observed at the ends of microfibrils in algae by imaging freeze-fractured membranes (Giddings et al., 1980). This highly-ordered, six-particle structure was termed a "rosette", and these have since been observed in high concentration at sites of rapid cellulose synthesis in vascular plants (Herth, 1985). The cellulose synthase complex is only partially exposed on the extracellular side of the plasma membrane, with a more substantial portion exposed to the cytoplasm (Nuhse et al., 2004; Taylor, 2008). Work also suggests that the cellulose synthase complex is associated with other essential molecular factors (Richmond and Somerville, 2000; Saxena and Brown, 2005; Taylor, 2008). These are hypothesized to include proteins that affect organization of the complex, as well as catalyze crystallization of glucan chains, and aid transfer of UDP-glucose (the substrate of cellulose synthase) to the catalytic sites (Albersheim et al., 1999; Saxena and Brown, 2005; Fuji et al., 2010). Cellulose synthase has been observed, *in vitro*, to processively (without stopping or detaching) catalyze the polymerization reaction in one step (Richmond and Somerville, 2000; Saxena and Brown, 2005; Taylor, 2008).

Previous research has shown that different groups of *CesA* genes are expressed in cells synthesizing primary cell walls compared to cells synthesizing the cellulose in secondary cell walls (Taylor et al., 2003; Appenzeller et al., 2004; Saxena and Brown, 2005; Persson et al., 2007). Furthermore, mutant analysis in *Arabidopsis* has shown that expression of three different *CesA* genes is required to form a functional rosette in both primary and secondary cell walls (Burn et al, 2002; Zhong et al, 2003; Taylor et al., 2003; Tanaka et al., 2003). These observations have led to the hypothesis that three distinct, non-redundant cellulose synthases are required to form a functional rosette (Taylor et al., 2003; Saxena and Brown, 2005; Persson et

al., 2007; Jiang et al., 2008)). Although a 3:2:1 stoichiometry of CesA isoforms has been depicted in models representing the heterohexameric CESA complex, there has been no direct evidence to support this specificity in balance of subunits.

Studies of cellulose synthesis in plants suggest that initiation of this process may require a sitosterol-glucoside primer to initiate glucan chain elongation (Peng et al., 2002; Endler and Persson, 2011). Data indicate that sitosterol-glucosides are synthesized on the cytosolic face of the plasma membrane (Cantatore et al. 2000), which is consistent with work showing a plasma-membrane association for the enzyme responsible for its synthesis, UDP-Glc:sterol glucosyltransferase (Elbein and Forsee, 1975). Furthermore, cotton fiber membranes can synthesize sitosterol-cellodextrins in vivo when supplied with UDP-glucose (Peng et al., 2002). Once cellulose synthesis has been initiated, current models suggest the sitosterol is cleaved from the nascent cellulose chain by a specific membrane-bound cellulase called KORRIGAN. This hypothesis is supported by the accumulation of lipid-linked-cellodextrins in *Arabidopsis korrigan* mutants (Sato et al., 2001). Furthermore, cellulose synthase activity is enhanced in naturally-occurring detergent-resistant membranes (Bessueille et al., 2009) . These sections of membrane have especially high levels of sitosterol-β-glucoside, and are similar to lipid rafts in animals because they have altered lipid composition (Lingwood and Simons, 2007).

Although there has been much progress in understanding the mechanism of cellulose synthesis, several significant aspects of this process remain unclear. One of these is the identity and stoichiometry of CesA isoforms that can assemble into CESA complexes. Another is the developmental and tissue-specific regulation of *CesA* gene expression. It is also poorly understood how the identity and stoichiometry of CesA isoforms in a given CESA complex affects its function. Still another challenge to the field is defining the presence and identity of unidentified cofactors required for assembly of complexes or their functioning. These

unidentified cofactors are among suggested reasons for a consistent lack of success in achieving cellulose synthesis through transgenic approaches (using plant *CesAs*) in non-plant systems. Further research employing both genetic and biochemical approaches will be central to enhancing our understanding of how this seemingly simple polysaccharide is synthesized in plants.

Work presented here employs three additional avenues of investigation. The first is a bioinformatic analysis of the maize cellulose synthase family. The second combines molecular-level analysis in isolated tissues, and in suspension-culture and protoplast systems responding to perturbations. The third extends the mutant-analysis approach to the cellulose synthase gene family in maize, a large, C4-panicoid species with immediate commercial value.

Suspension cultures and protoplasts provide ideal platforms for experimental alterations. Both systems can be readily perturbed, and an investigator also has a choice of source tissue from which cultures or protoplasts are generated. This provides a means of addressing properties and/or responses of specific cell types. These systems also offer the benefits of relative cellular uniformity. In addition, suspension cells and protoplasts can be quickly regenerated, and easily perturbed. Age of suspension-cell lines is important, though, since these can become immortalized and perpetuated indefinitely. When they do, cells dedifferentiate and their genomes undergo major epigenetic modifications (Tanurdzic et al., 2008). However, when used and interpreted carefully, suspension cultures can provide a valuable avenue of inquiry.

Protoplasts are also useful and can be readily released from whole tissues and cultured cells. They have successfully facilitated studies of diverse biological processes, from cell-wall regeneration (Shea et al., 1989) to C4 metabolism (Shatil-Cohen et al., 2011). Protoplasts are also ideal for genetic transformation, as the lack of a cell wall facilitates gene transfer through electroporation and/or microinjection (Potrykus, 1991; Dong-Yoo et al., 2007). Cautions in use

of protoplast systems include their mechanical delicacy, which often results in high mortality rates, and the cell-wall-removal process, which can activate wounding- and pathogen-infection responses (Moreno et al., 2005; Walley et al., 2007). The latter can occur as a result of the mechanical stress of cell wall removal, exposure to fungal elicitors (cell wall degrading enzymes), or the presence of small oligosaccharides released from the cell wall during digestion (Cordero et al., 1994; Moreno et al., 2005; Walley et al., 2007). Changes in gene expression can also occur in response to sugar-starvation while cells are incubating in cell wall-digestion medium (Yu, 1999).

The third, new avenue of investigation used here aids current research endeavors by bringing *Zea mays* L. ssp *mays* into the realm of species with mutations altering genes for cellulose synthesis. Our current understanding of cellulose synthesis has come from characterization of mutants deficient in one or more of the cellulose synthase genes, but has focused mainly on *Arabidopsis*, rice and barley (Turner and Somerville, 1997: Tanaka et al. 2003; Taylor et al., 2003, Burton et al., 2010). Additional insights have also been gained through transgenic approaches in tobacco and aspen (Wu et al., 2009; Joshi et al., 2011). There are currently no reports associating a *CesA* mutation in maize with a phenotype. Work here characterizes new mutations in most of the maize *CesA* gene family, with the goal of determining which family members are essential to normal physiology, morphology, and development.

The source of these new maize mutants has been a transposon-mutagenic population that enables identification of insertion sites. Transposable elements provide a useful mechanism for naturally generating and characterizing mutants. These elements, or transposons, are small, mobile DNA sequences that can insert into genes, often causing them to lose function. Although many transposons have the capacity to insert anywhere in the genome, the *Mutator* (*Mu*) class typically inserts in the 5′ regions of functional genes (Dietrich et al., 2002). Since transposons

were first discovered by Barbara MClintock in the 1940's (McClintock, 1947), several transposon families and subclasses have been defined. All transposable elements can be broadly categorized as being "Class I" or "Class II", depending on whether they transpose using an RNA (Type I), or DNA (TypeII) intermediate (Wicker, 2007). Furthermore, transposons are classified as either autonomous or nonautonomous. Autonomous transposons are those with sequences that code for a transposase enzyme having the capacity to mediate movement of a transposon sequence to a new location. In some instances the original sequence is excised for reinsertion, and in others, the original transposon remains in position while a copy is transposed to a new locale (Wicker et al., 2007). Nonautonomous transposons can contain as little as the essential *cis*-elements needed for recognition and transposition by the transposase. Autonomous transposons must be present in order for nonautonomous elements to transpose.

Among some of the best characterized transposons in maize are the *Mutator*, or *Mu*, family of transposable elements. These transposons are particularly useful for genetic studies because they contain terminal inverted repeat (TIR) sequences from which primers can be designed, and sequences flanking insertion sites can be identified (Dietrich et al., 2002). This approach provides a convenient method for identifying disrupted genes and associating them with a phenotype. The *Mu*-TIRs are generally about 215 base pairs long and are highly conserved within each of the 12 subclasses of *Mu* transposable elements, termed *Mu1* to *Mu12.* More recent work has revealed that these initial 12 sub-classes account for over 300 separate *Mu* insertions in the B73 maize genome, and that these group into five overall *Mu* clades (C. Hunter., Univ. of Florida, PhD dissertation 2010). Several research groups have used the *Mutator* family of transposons to generate and tag new mutations in maize (Walbot, 2000; Raizada et al., 2001; Meeley and Briggs, 1995; McCarty and Meeley, 2009; Williams-Carrier et al., 2010). The

largest and most active at present is the UniformMu maize population developed at the University of Florida (McCarty et al., 2005; Settles et al., 2007).

The UniformMu population was generated by introgressing a highly (*Mu*) transposon-mutagenic line, called Robertson's Mutator, into the maize W22 inbred. Along with the active *Mu* transposon system, a *Mu*-associated *bz-mum9* color marker was also introgressed into the population. This marker allows easy determination of whether a given plant has inherited the transposase and can still generate new mutations. In the absence of transposase, kernels carrying *bz-mum9* are bronze, whereas wild type kernels are dark purple. Kernels carrying *bz-mum9* and an active transposase are bronze with a varying amount of small purple spots. Other benefits of the UniformMu population are its high mutation frequency, low mutant load, moderate total *Mu* TE copy number, a database of pedigreed insertions, and a uniform background of plant material that allows easy identification of novel phenotypes (McCarty et al., 2005).

Here, bioinformatic and evolutionary analyses have identified four new *CesA* paralogs (homologous genes arising directly from duplication within a genome), and shown that at least one copy of each unique *CesA* is retained on chromosomal regions associated with resistance to gene degradation. Only redundant *CesA* paralogs were found on chromosomal regions associated with gene loss. This observation is consistent with a recent hypothesis that suggests gene loss after a genome duplication event, such as occurred long ago in maize, will occur preferentially from one "copy" of the genome that is more resistant to gene degradation (Schnable et al., 2010). Phylogenetic analysis has also revealed that one, and only one paralog was retained (and not subfunctionalized) from each of the three *CesA* subclades associated with primary cell wall synthesis in maize. A Gene Balance Hypothesis (Birchler and Veitia, 2010) suggests that this balance between gene dosage from *CesA* subclades may reflect a functional balance between

isomers in CESA heterohexamers. Gene retention and loss after polyploidization events in diverse species appears responsive to the stoichiometry of isomers in multimeric complexes when this balance has been essential to functionality. Further support for such a relationship among the CesA's of maize comes from the observation that in *Arabidopsis*, primary cell wall biosynthesis depends on the presence of three different CesAs, one from each of the three sub-clades associated with primary wall formation.

We also show that although expression of the *CesA* genes in maize is typically a coordinated process, mRNA profiles show that co-regulated groups of *CesA* transcripts vary across tissues and throughout development. Three *CesAs* (*CesA10, CesA11*, and *CesA12*) are consistently coexpressed at all stages of development, and are predominantly associated with tissues developing secondary cell walls. Also, these three genes are strongly upregulated in suspension cells that have been hormonally induced to differentiate into tracheary element-like cells rich in secondary wall. The other, primary cell-wall-associated *CesAs* form discreet expression profiles that cluster together, but change at different stages of development. Additionally, we show that these co-expression clusters observed *in planta* can change in response to perturbations of protoplasts and suspension cells, thus indicating plasticity in the co-expression modules and transcription-level responses of *CesAs*.

Finally, mutant analysis has demonstrated that several of the primary-wall-associated maize *CesAs* are functionally redundant, and do not cause visible phenotypes when mutated. This is likely a result of the proliferation of the maize *CesA* family, which would add to the high level of functional redundancy observed among the primary wall-*CesAs* in *Arabidopsis*.

CHAPTER 2
ANALYSIS OF THE CELLULOSE SYNTHASE GENE FAMILY IN MAIZE

Background

Cellulose represents roughly 50% of total plant-based biomass, making it one of the most abundant renewable resources on the planet. This biopolymer is also integral to plant structure, fiber quality, digestibility, and carbon partitioning. As food and fossil fuels become limiting, a central importance emerges for better utilizing cellulosic resources. Gaining greater understanding of the mechanisms underlying cellulose synthesis at the genetic and molecular level will provide potentially invaluable avenues for improving composition of cellulosic biomass (for use as bioreactor feedstock) and other cell wall-based aspects of plant yield.

The cellulose synthase (*CesA*) genes of plants derive from an ancient lineage, and are present in numerous taxonomically diverse organisms from vascular plants to algae, bacteria, protists, fungi, and urochordate animals (Richmond, 1991; Hirose et al., 1999). Although sequences of *CesAs* in vascular plants do not have a high degree of overall homology, they do share several conserved regions implicated in CesA function. The D,D,D,QxxRW domain (with conserved aspartate residues) appears essential for catalytic activity (Saxena et al., 1995; Delmer and Amor, 1995; Taylor, 2008). Also, an N-terminal LIM (Lin11, Isl-1 & Mec-3)-like Zinc-binding domain/RING (or Cys3HisCys4 containing) domain is hypothesized to mediate protein-protein interaction (Kawagoe and Delmer, 1997; Taylor, 2008). In addition, eight transmembrane domains (two N-terminal and four C-terminal) allow orientation within the plasma membrane (Pear et al, 1996; Taylor, 2008) (Figure 2-1). The Zinc-binding domain/RING domain and catalytic D,D,D,QxxRW domain are predicted to lie in cytoplasmic regions of the protein, and both of these domains are associated with a hypervariable region (HVR) not seen in the CesAs of bacteria or cyanobacteria (Delmer, 1999). One of these HRVs is N-terminal,

positioned between the Zinc-binding domain and the first two transmembrane domains. The other HVR is in the central region of the cytoplasmic loop that contains the D,D,D,QxxRW domain (Figure 2-1 and Taylor, 2008). This region of the cytoplasmic loop is also termed the Class Specific Region (CSR), because these sequences are conserved between related sub-clades of CesAs from different species, but not among the diverse CesA family members from within the same species (Vergara and Carpita, 2001; Taylor 2008). Mutation of residues affecting phosphorylation in the hypervariable regions has resulted in directionally asymmetric movement of rosettes, and discrepancy in the velocity of bi-directional movement of these structures along cortical microtubules (Chen et al., 2010). This aberrant movement of rosettes leads to abnormal patterns of microfibril deposition and loss of anisotropic cell expansion (Chen et al., 2010). In contrast, rosettes in wild type plants move bidirectionally along cortical microtubules in roughly equal numbers (Paredez et al., 2006; Yoneda et al., 2007). Chen et al. (2010) thus suggest that the phosphorylation status of CesA proteins can affect polar interaction with microtubules.

Cellulose synthases are processive enzymes classified as family 2-inverting-nucleotide diphospho-sugar glycosyltransferases (Campbell et al., 1997). Using UDP-glucose as a substrate, CesAs form β-(1-4)-linked glucose chains estimated to range from as long as 8,000 residues in primary cell walls, up to 15,000 residues in secondary walls (Pear et al., 1996; Brett, 2000; Brown, 2004). Individual cellulose chains can then associate through hydrogen bonds and form the highly-structured, crystalline cellulose of the microfibrils in cell walls. The CesAs function in vivo as membrane-bound heterohexamers that require at least three different CesA isoforms to assemble (Taylor et al, 2003). Research using an *Arabidopsis* (GFP)-CesA3 fusion protein has shown that CesAs also localize to the Golgi, however this observation could be an artifact of overexpression (Crowell et al., 2009). Furthermore, insertion of CesAs into the plasma membrane is regulated by the movement of microtubule-associated, CesA-Golgi bodies

(Crowell et al., 2009). Currently, the mechanism of assembly and stoichiometry of isoforms within a complex remains unknown (Taylor, 2000, 2003; Taylor, 2008). Visualization of CesA super-complexes through freeze-fracture microscopy has shown that the functional, microfibril-producing unit, or "rosette," is a symmetric hexamer comprised of six (heterohexameric) CesA protein complexes (Haigler and Brown, 1986). Dimensions of individual cellulose chains and the terminal rosette complexes indicate that each CesA isoform produces one cellulose chain, and each hexameric rosette is made from six CesA hexamers. The microfibrils formed from each rosette are thus comprised of 36 individual cellulose chains (per diameter) (Ha et al., 1998; Somerville et al., 2004).

Maize has undergone two major genome duplication events. The first occurred about 70 million years ago (mya), before the lineage of maize and rice diverged, and the second was relatively recent (5 to 12 mya) (Swigonova et al., 2004). Although the maize genome has returned to an essentially diploid state, there is still an abundance of gene duplications (Schnable et al., 2011). The maize *CesA* gene family has 12 members with published cDNA sequences, however pseudo-genes are also common within the *CesA* gene family. In addition, tandem duplications of genes are common in maize (Dooner and Kermicle, 1971; Veit et al., 1990), and may well have affected the *CesA* family. The prevalence tandem duplications poses a challenge for genome assembly, so their extent and locale may not yet be evident in the current version of the maize genome. In addition, there are small (presumably non-coding) gene fragments with high sequence identity to several of the *CesAs*. A complete appraisal of the maize *CesA* gene family is continuing to emerge and may include additional functional genes and non-coding sequences. All of these are relevant to our understanding of this complex family, and for genetic approaches to discern functional roles among them.

A central aspect of CesA function is learning which family members act together, possibly through assembly of heterohexamers. Research in *Arabidopsis* indicates that three specific *CesAs (AtCesA4, AtCesA7, AtCesA8)* are required for secondary cell wall synthesis (their maize orthologs being *CesA10*, *CesA11*, and *CesA12*), and that other family members are likely involved in synthesis of the primary cell wall (Taylor et al., 2003). Additional work shows that in *Arabidopsis* and rice, each of the individual *CesAs* contributing to secondary cell wall biosynthesis is essential. Null mutations in any of these genes result in severe phenotypes that include reduced biomass, irregular xylem, and/or brittle tissues (Turner and Somerville, 1997; Tanaka et al., 2003; Taylor et al., 2003). In contrast, synthesis of the primary wall involves a high level of functional redundancy among the *CesAs* that contribute predominantly to this process, with null mutations in *AtCesA1* and *AtCesA3* being the only ones associated with phenotypes (Persson, 2007; Taylor, 2008). These include an embryo lethality and temperature-dependent radial swelling of cells for *cesA1* mutants, and a gametophytic lethality associated with defective pollen formation for mutants of both *cesA1* and *cesA3*.

Here we present an in-depth analysis of the maize cellulose synthase gene family, profile expression of its members under diverse conditions, and identify co-regulated isoforms. Results will be useful in future efforts to alter quality or quantity of cellulose in plant tissues. In the current work, we show that *ZmCesA10, ZmCesA11,* and *ZmCesA12* are expressed coordinately, and almost exclusively in tissues undergoing secondary cell wall synthesis. Furthermore, expression of *ZmCesA10, ZmCesA11,*and *ZmCesA12* in these tissues is elevated relative to other tissues where expression is detected. Previous work has indicated that the maize *ZmCesA10, ZmCesA11*, and *ZmCesA12* belong to the same phylogenetic sub-clade of *CesAs* as the *Arabidopsis AtCesA4, AtCesA7, AtCesA8* (secondary wall genes), and are most highly expressed in stalk and root tissue (Appenzeller et al., 2004). Here we test the hypothesis that the cellulose

synthases are differentially regulated, with specific isoforms being coordinately expressed as a result of subfunctionalization to perform specific tasks. To this end, we quantify mRNA levels in diverse tissues at key stages of development.

Results

Identification and Characterization of *CesA* Paralogs

A bioinformatic approach was used to characterize the structure, phylogeny, and possible regulatory features of the *CesA* family in maize. The size of this family was determined by using published cDNA sequences from the 12 known *CesAs* to search the maize reference genome (B73 RefGen_v2.: maizesequence.org) with the basic local alignment search tool (BLAST) (Altschul et al., 1990). Results showed several additional sequences in the genome with high homology to *CesA* family members. In addition, four of these sequences encoded potentially functional proteins. When predicted protein sequences from these putative family members were included in phylogenetic analysis of the 12 known *CesAs*, four new sequences were found to group with respective paralogs of *CesA7*(one), *CesA11*(one) and *CesA12*(two) (Figure 2-2). These paralogs are hereafter referred to as *CesA7-a*, *CesA11-a*, *CesA12-a* and *CesA12-b*. Together, the published *CesAs* and paralogs in maize group into six subclades, consistent with organization of *CesA* families in other plant species (Carrol and Specht, 2011).

A closer comparison of *CesA7* and *CesA7-a* was undertaken to determine the types of differences that distinguish closely-related family members. The cDNA sequence for *CesA7-a* was predicted by aligning its genomic sequence with the published cDNA of *CesA7.* Assuming that splice sites were conserved, a 93.8% sequence homology was observed, along with numerous single nucleotide polymorphisms (SNPs), plus 11 small insertions (< 5 bp), and two deletions (relative to *CesA7*) (Figure 2-3A). When the predicted *CesA7-a* cDNA was translated in the correct frame, it encoded an open reading frame without premature stop codons, and

shared 98.5% amino acid sequence similarity with CesA7 (Figure 2-3B). Additionally, qRTPCR results show that *CesA7-a* is expressed at levels comparable, but not identical, to *CesA7*.

Evolution of *CesA* Genes in Maize

Previous work suggests that the maize genome arose from gradual diploidization of an ancient tetraploid, giving rise to chimeral chromosomes with segments of both the original genomes (Swignova et al., 2004; Schnable et al., 2011). To determine the role this could have played in the current structuring of the *CesA* family, we mapped all family members, including paralogs, to their approximate chromosomal locations (Figure 2-4A). One of the ancestral genomes dominated in retention of *CesA* genes, and included at least one gene copy of each unique *CesA* from each of the six subclades. Conversely, *CesAs* from the other genome were either lost, or retained only where detectable paralogs were present. (Figure 2-4B). The maize *CesA*-family thus provides a model for exploring the functional implications of an evolutionary mechanism recently proposed by Schnable et al. (2011) to have affected the tetraploid to diploid conversion in *Zea mays*.

Micro-RNA Targets in the *CesA* Gene Family

Micro-RNAs (miRNA) can contribute to regulation of protein expression through degradation of messenger-RNA (mRNA), and/or inhibition of protein translation (Chen and Rajewsky, 2007). To assess the potential for miRNA-based regulation of the *CesAs*, we identified putative target sites among the *CesA* family members using the miRNAFinder program from the Noble Foundation (bioinfo3.noble.org/mirna/). The number of miRNA target sites for each *CesA* varied greatly, ranging from two to 28, in *CesA2* and *CesA12*, respectively (Figure 2-5). Cluster analysis based on miRNA sequence similarity showed little to no relationship with sub-clades of their putative *CesA* targets. However, one cluster of miRNAs showed a significant enrichment of those potentially targeting *CesA10* and *CesA12* (Figure 2-6).

Expression of the *CesA* Gene Family During Development

To better understand how cellulose synthases function in vivo, and the relationships between them, we quantified mRNA levels from diverse tissues at the seedling- vegetative- and anthesis (reproductive maturity)-stages (Table 2-1). Tissue was harvested at 3 days after germination (DAG) for the seedling-stage, 40 DAG for the vegetative-stage, and 72 DAG for the anthesis-stage (Figure 2-7). Results showed that expression of the maize cellulose synthases was highly dynamic, with mRNA levels from different *CesAs* varying many-fold between different tissues and during development (Figures 2-7 and 2-8). Effects of developmental stage were prominent and determined the proportion of tissues in which a given family member was abundantly expressed (mRNA levels greater than 50% of the gene-specific maximum) (Figure 2-7). Maximum and minimum mRNA levels from a given gene varied markedly and were especially apparent for *CesA10*, *CesA11*, and *CesA12* during the transition from the vegetative- to anthesis-stage (Figure 2-8). At the anthesis-stage, most of the *CesA*'*s* mRNA levels were at or near their minima in leaf blades and pollen. However, *CesA3* and *CesA5* consistently had the most abundant mRNAs in these tissues, which raises the question of whether these genes have a "housekeeping" function (Figure 2-9).

To facilitate comparative analysis of these expression profiles, and the inter-relationship among *CesA* family members, we explored the extent to which responses of different *CesAs* could be clustered. We used the Modulated Modularity Clustering (MMC) program (Stone and Ayroles, 2009) to test family member groupings based on similarity of expression patterns in all tissues examined at a given developmental stage. Each cluster was defined based on the degree of correlation observed among expression profiles of its members. The most highly-correlated group was designated, "Cluster I," with successive numbering used for less-strongly-clustered groups. At the seedling- and vegetative-stages, *CesA10*, *CesA11*, and *CesA12* grouped clearly

into Cluster I. Furthermore, levels of mRNA from these genes rose by several orders of magnitude in rapidly-growing tissues that were developing vascular tissue (Figure 2-10). Cluster II included *CesA7* and *CesA7-a*. With the exception of *CesA8*, which was essentially independent, the remaining family members showed similar-enough patterns of expression at this stage to group collectively into Cluster III (Figure 2-10).

At anthesis, Cluster I again included *CesA10*, *CesA11*, and *CesA12* (Figure 2-9). Here too, respective mRNA levels were notably higher in tissues that were becoming lignified and/or developing vascular tissue (Figures 2-11 and 2-12). These results are consistent with a role for *CesA10*, *CesA11*, and *CesA12* in secondary cell wall synthesis. Four *CesAs* grouped in Cluster II, where responses of *CesA4* and *CesA6* at anthesis joined those of the previously-grouped *CesA7* and *CesA7-a* (Figure 2-11). Although expression patterns of *CesA3* and *CesA5* were independent of those from other family members at this stage, responses of all remaining family members grouped together in Cluster III (Figure 2-11).

Developing kernels warranted separate analysis, and were harvested at 15 days after pollination. Samples were dissected into embryo, endosperm, pericarp, and pedicel fractions. In these kernel tissues, *CesA10, CesA11*, and *CesA12* again showed a similar expression pattern, and here too, maximal mRNA levels coincided with deposition of secondary cell walls in the pedicel (Figure 2-13B). Phloroglucinol staining of a longitudinal kernel section showed the abundance of lignin in the pedicel, and indicated the extent of "woodiness" that develops in this tissue of the kernel (Figure 2-13A). These data are consistent with the hypothesis that *CesA10, CesA11*, and *Cesa12* have a role in secondary cell wall synthesis in maize.

Discussion

Bioinformatic Analysis Reveals Additional *CesA* Paralogs

At the outset of this study, there were 12 named cellulose synthases with published cDNA sequences in maize. The sequencing and updating of the maize genome (B73 RefGen_v2, 2010) facilitated further analysis presented here, including identification of four additional *CesA* genes by BLAST alignment of published *CesA* cDNAs with newly emerging sequences. In most instances, many unknown sequences aligned to each individual cDNA used as a query sequence, and E-values indicated high levels of homology. However, most of these sequences were considerably shorter than full length cDNAs, and many had deletions and stop codons, thus indicating that they were likely pseudogenes and not encoding functional proteins. Nonetheless, this does not rule out their potential to serve as templates for generation of regulatory RNA sequences (possible roles of miRNA and siRNA are discussed below, but they were not analyzed here). Additionally, the presence of pseudogenes can complicate interpretation of results when using PCR-based genetic approaches, depending on placement of primer pairs. Related issues of gene-specificity are also involved for the full length, potentially protein-coding paralogs identified here for *CesA7*, *CesA11*, and *CesA12*, respectively designated *CesA7-a*, *CesA11-a*, *CesA12-a*, and *CesA12-b* (Figure 2-2).

To investigate the extent of sequence divergence and protein-coding potential of *CesA* paralogs, we aligned paralog genomic sequences to the cDNAs of corresponding family members. Assuming conservation of intron-exon boundaries, the paralog *CesA7-a* had limited sequence divergence relative to *CesA7*, maintaining 93.8% cDNA sequence identity (Figure 2-3) that translated to 98.5% identity at the protein level. These results raise questions regarding a possible evolutionary advantage to retention of some paralogs, especially where full-length cDNAs are highly conserved. Although there are three *CesA12* paralogs in total, these showed

somewhat less strong sequence similarity and included possible premature stop codons. The *CesA12-a* and *CesA12-b* genes may still encode functional proteins if nucleotide sequence divergence altered intron-exon splice sites, thus causing a frame shift.

Sequences of *CesA11* and *CesA11-a* unexpectedly aligned to one another with 100% identity. Further investigation showed that genomic sequences flanking both genes also aligned with 100% identity until roughly 3 kilobases (kb) upstream, and 5kb downstream of the *CesA11* sequence. Outside the boundaries where 100% homology was lost, the sequences diverged completely. Initially, assignment of these identical sequences to different chromosomal locales seemed the possible result of a genome assembly in progress. However, further investigation traced these sequences to two, fully-independent bacterial artificial chromosomes (BACS) from which the maize genome was assembled, thus supporting a valid assignment of these sequences to both genomic locations. Because this duplication is large (roughly 13 kb), identical, and probably recent, it is unlikely to have resulted from a long-terminal-repeat retrotransposon or a translocation. A remaining possibility is that this unusual duplication may have been mediated by a helitron, which can transpose while carrying genomic fragments of 15 kb or greater (Kapitonov and Jurka, 2001; Yang and Bennetzen, 2009).

Phylogenetic Analysis of the *CesAs*

Phylogenetic analysis of the *CesAs* and paralogs noted above indicated that several of the previously named *CesAs* (e.g. *CesA1+CesA2* and *CesA4+CesA9*) are probable paralogs of one another (Figure 2-2). At least one paralog (two genes total) can be found in each of the six subclades of the *CesA* family except for that represented by *CesA10* alone. This may indicate that *CesA10* gene has a unique role in the assembly or functionality of the CesA complex, and possibly one for which multiple copies of the gene are disadvantageous. Other *CesAs* lacking paralogs are not alone in their clades (as is *CesA10*), and include *CesA3, CesA5, CesA6,* and

CesA8. In addition, these family members are found in clades that include only *CesAs* thought to be involved in primary cell wall synthesis. Furthermore, many of these family members share more than 88% sequence identity, and the three subclades in which they are found all share a similar overall structure (Figure 2-4B). This observation indicates that the original genes may have once been closely related paralogs, but have since diverged without major change function.

Evolution of the *CesA* Gene Family

Work thus far suggests that the modern maize genome has resulted from two ancient tetraploidization events followed by subsequent diploidization. Both of the genomes that arose from tetraploidization are represented in portions of the chimeral chromosomes of modern maize (Figure 2-4A) as a result of numerous crossovers, translocations between duplicated genomes, transposition events, and significant gene loss. Chromosomal segments deriving from each of the two ancestral genomes were determined by alignment with the sorghum genome (Schnable et al., 2011). The ancestral genomes were then named Maize-1 and Maize-2 based on the amount of detected gene loss, with Maize-1 retaining more genes (Schnable et al., 2011).

To better understand how gene duplication and loss could have affected evolution of the *CesA* family, we mapped each family member to the maize genome and determined its position-based association with one or the other ancestral genomes (Figure 2-4A). We then applied this genome designation to the phylogenetic tree (Figure 2-4B). At least one *CesA* gene from each subclade was mapped to a chromosomal region designated as Maize-1, whereas *CesAs* mapping to components of the Maize-2 genome exist only as paralogs. Results were consistent with the recent suggestion that one genome, either in its entirety or segment-by-segment, dominates with respect to resisting gene deterioration (Schnable et al., 2011). Interestingly, *CesA11* and *CesA12* have paralogs that appear to have originated in Maize-1, either before or after the tetraploidization event. We favor a relatively recent origin for these *CesA11* and *CesA12*

gene duplications due to their positioning and the extent of their sequence similarity. However, the possibility remains that these genes may already have had two copies in the original genome before tetraploidization, and their paralogs have since deteriorated.

Potential for Micro-RNAs to Affect Differential Regulation of *CesA* Genes

Short, 22-nucleotide miRNA sequences can regulate mRNA degradation and inhibit translation (Chen and Rajewsky, 2007). Degradation of mRNAs occurs through miRNA recruitment of the RNA-induced-silencing-complex, which then cleaves the mRNA and dissociates. An initial appraisal of predicted mRNA target sites showed a highly variable number of these among the maize cellulose synthases, ranging from two in *CesA2* to 28 in *CesA12* (Figure 2-5). The number of potential target sites could reflect the degree to which a given family member is miRNA-regulated, since more target sites would increase opportunity for interaction with various miRNAs being expressed in different tissues. We initially hypothesized that *CesAs* sharing a high degree of homology would be targeted by the same miRNAs, however this was not observed. Instead, only two miRNA target sites appeared in more than one family member, one was present in both in *CesA4* and *CesA9*, and the other was in *CesA10* and *CesA12*. Coordinate expression was observed to varying degrees within both gene pairs (see below). Results thus indicated that miRNA-mediated regulation was "fine-tuned" to each particular gene. Additionally, when the predicted miRNAs that targeted *CesAs* were clustered based on sequence similarity, they grouped randomly with regard to which *CesA* family member they targeted. The only exception was in one clade of miRNAs, where approximately 30% of sequences targeted *CesA10*, another 36% targeted *CesA12*, and the remainder targeted five other family members. Taken together, these observations indicate that *CesA10* and *CesA12* may share some degree of miRNA-dependant regulation.

Expression of *CesAs* Varies with Tissue and Development

Expression profiles of the *CesA* family members in diverse tissues sampled at each developmental time point, show a wide range in mRNA levels for any given gene. These differences in expression vary markedly from tissue to tissue, and also over time in like tissues. The identity of maximally expressed family members at any given time or in any given tissue is variable (Figures 2-7 and 2-8). We suggest that expression of the *CesA* gene family in maize, and consequently cellulose deposition, is under complex regulation, involving diverse heterohexamers with different characteristics and functions depending on contributions from different *CesA* isoforms.

Cluster Analysis of Gene Expression Among the *CesAs*

Application of clustering analysis to the *CesA* expression data from each time point revealed groups of family members that shared a high degree of similarity in expression pattern, thus indicating some level coordinate regulation (Figures 2-10 and 2-11). With the exception of Cluster I (*CesA10, CesA11,* and, *CesA12*), whose members shared the highest degree of correlated expression, the family members belonging to a given cluster changed at different time points. For example, Cluster II consistently included *CesA7* and *CesA7-a*, but *CesA4* and *CesA6* also joined this group at the anthesis-stage (Figures 2-10 and 2-11). One might initially expect that within a gene family, highly similar sequences such as *CesA7* and *CesA7-a* would be similarly expressed. However, genes with clear, consistent differences in their sequences were also frequently coexpressed. This issue is especially important when the genes code for isoforms of a heterogenous protein complex like that of CESA. Our data show more support for the conserved-differences scenario, considering that Cluster I (*CesA10, CesA11,* and, *CesA12*) was the only group to consistently represent the same family members, and each of these genes represents its own subclade on the *CesA* family tree. Furthermore, even though expression

profiles of *CesA7* and *CesA7-a* group consistently together, the same can not be said for other paralogs such as *CesA4* and *CesA9* (Figures 2-10 and 2-11).

As noted above, the only family members with expression patterns that clustered together exclusively and consistently throughout development were *CesA10, CesA11,* and, *CesA12*. The variation in expression levels of these genes between tissues was also more extreme than for other family members, sometimes increasing coordinately by up to 60-fold (Figure 2-6). At all stages of development, the tissues in which *CesA10, CesA11,* and, *CesA12* were most highly expressed were also those where vascular tissue was developing or tissues were becoming lignified (Figures 210- , 2-11, and 2-12). Analysis of mRNA levels of *CesA* family members in the developing kernel are consistent with whole-plant observations, since mRNAs of *CesA10, CesA11,* and, *CesA12* were several-fold more abundant in the highly-lignified pedicel than in other kernel tissues (Figure 2-13). Earlier studies also showed that maize CesA10, CesA11, and, CesA12 had closest homology to CesAs in *Arabidopsis* and rice that were necessary for secondary cell wall synthesis (Tanaka et al., 2003; Taylor et al., 2003; Appenzeller et al., 2004). Collectively, research presented here indicates that *CesA10, CesA11,* and *CesA12* are primarily, although not exclusively, associated with secondary cell wall synthesis in maize.

Methods

Bioinformatic Analysis of the Maize Genome for Identification of *CesA* Paralogs

Paralogs of named *CesA* family members were identified by using BLAST (Altschul et al., 1990) to compare the cDNA sequence from each named *CesA* to the maize genome (B73 RefGen_v2 : maizesequence.org). Output was screened to identify sequences most likely to encode functional *CesA* paralogs. Sequences were considered paralogs if they 1) had high homology to the query sequence (E-value of 0), and 2) included sufficient alignment to encode a potential protein of similar length to the *CesAs*. Each newly-identified, putative paralog was

characterized by aligning its genomic sequence with the cDNA of its respective, homologous *CesA* gene. For each paralog, cDNA sequence was predicted assuming a conservation of mRNA splice sites, followed by removal of introns. Each of these predicted cDNAs was then aligned with cDNA from its corresponding *CesA* family member (multalin.toulouse.inra.fr) to manually map SNPs, insertions, and deletions (Figure 2-3).

Phylogenetic Analysis of the *CesA* Family

Phylogeny of the *CesA* family, including paralogs, was analyzed using the MEGA4 program (Tamura et al., 2007). Sequences of proteins and predicted-proteins (in the case of paralogs) were aligned, and used to build an unrooted, neighbor-joining, phylogenetic tree based on homology. The tree was constructed using a pairwise deletion option with 1000 bootstrap replications (Figure 2-2).

Evolutionary Analysis of the *CesA* Family

The evolutionary origin of the maize *CesAs* and their paralogs was estimated by mapping each gene on the maize genetic map, and ascertaining which portion of the ancient tetraploid genome was represented in the corresponding chromosomal segment. This provided a means of designating which *CesA* genes resided on each of the two sub-genomes generated by ancient tetraploidization and subsequent diploidization (Figure 2-4A). The positions of chromosomal regions derived from each subgenome have been described in previous work (Swignova et al., 2004; Wei et al., 2007; Schnable et al., 2011). Assigning a genome designation to each CesA protein in the phylogenetic tree facilitated interpretation of the evolutionary relationship between *CesA* family members and their paralogs.

Prediction of miRNA Target Sites in the *CesAs*

Micro-RNA target sites within the *CesA* genes were predicted by the miRNAFinder program (bioinfo3.noble.org). Genomic sequence of each *CesA* family member was used to

query the rice Expressed Sequence Tags (EST) collection, and the rice genome was then used to make target site predictions. Predicted miRNAs for each gene were compiled, and redundant miRNAs, or those mapping to the same location in a gene (i.e. identical pre-miRNA sequences appearing multiple times in the output), were eliminated. All 154 predicted miRNAs were then aligned and clustered using the MEGA4 program (Tamura et al., 2007) to determine if (predicted) miRNAs targeting co-expressed *CesAs* were related. The resulting tree was constructed using pairwise deletion with 1,000 bootstrap replications. Each *CesA* was assigned a unique color that was shared by all miRNAs targeting that gene (Figure 2-6).

Plant Material

Maize inbred W22 was used for all expression analyses. Plants were grown in the laboratory for samples dissected at the seedling-stage, and under field conditions for samples harvested at the vegetative- and anthesis-stages. All material was frozen immediately in liquid nitrogen.

Isolation of RNA and cDNA Synthesis

Approximately 200 mg of tissue from each sample was finely ground in liquid nitrogen, and incubated in 1ml Trizol (Invitrogen Cat # 15596-018) for 5 min at 25°C with frequent vortexing (15 s). Chloroform (200 mL) was added and the solution vortexed for 15 sec, allowed to incubate for 1 min at 25°C, and vortexed again for 15 sec. Samples were then centrifuged at 13,200 rpm for 10 min to separate phases, and 200mL was transferred from the top phase to 700 mL Qiagen RLT buffer (RNeasy Plant Mini kit, Qiagen Cat # 74904). Ethanol (100%, 500 mL) was added before vortexting (15 sec). Total RNA was then cleaned and eluted using the RNeasy Plant Mini kit (Qiagen Cat # 74904), as per the manufacturer's protocol. Any contaminating DNA was removed by treatment with DNase-1(Ambion Cat # AM1906). Total RNA concentration was quantified using a (Bio-Rad) SmartSpec 3000 spectrophotometer, followed by

dilution to 50 ng/µL. Diluted RNA was used to synthesize cDNA with a SuperScript One-Step kit (Invitrogen Cat # 10928-042). Resulting cDNA was diluted 10-fold.

Real Time Quantitative RT-PCR

Levels of mRNA in tissues sampled throughout development were quantified using a Step One Plus Real-Time PCR System (ABI). Gene-specific primers for each *CesA* were designed manually, and specificity was checked by ensuring that primers did not closely align to any other family members, paralogs, or closely-related genes (see appendix, Table B-1). Three biological replicates, and two technical replicates were quantified for each tissue sampled. Reactions used the SYBR Green platform, with each 20µL-reaction containing 10µL Fast SYBR Green Master Mix (ABI Lot # 1003024), 5µL cDNA, and 100nM of both forward and reverse primers. Transcript abundance was normalized using 18S ribosomal RNA (Taqman Ribosomal RNA Control Reagents, ABI Lot # 0804133) as a control. Optimization of the control reactions resulted in a final reaction volume of 20µL that contained 10µL Fast SYBR Green Master Mix, 1µL forward and reverse control primers (diluted 1:18 from the ABI kit concentration), and 2.5µL cDNA. Each 96-well PCR plate represented one of the tissues sampled, and contained the 84 reactions necessary for two technical replications of three biological replications (tissue samples) for each of the 14 genes tested (13 *CesAs* and 18S rRNA). Amplification curves were closely monitored to ensure the kinetics of each run were comparable. Results were analyzed using the Modulated Modularity Clustering program (Stone and Ayroles, 2009) to assign coregulated family members to modules based on similarity in expression patterns. This program was chosen because it was specifically designed to seek community structure in graphical data.

Phloroglucinol Staining

Whole kernels were harvested at 15 DAP, and fresh tissue was longitudinally hand-sectioned. Other tissues were harvested at anthesis and sectioned in diverse planes.

Samples were then immersed in saturated phloroglucinol solution containing 20% ethanol and 20% HCl. After a 2-min incubation at 25°C, sections were washed with water and images obtained using a RT SPOT camera (Diagnostic Instruments, Sterling Heights, MI) mounted on a Leica MZ 12-5 dissection microscope.

Table 2-1. Tissues sampled at key developmental stages

Seedling	Vegetative	Anthesis
Coleoptile	Developing leaf	Pith
First leaf	Young leaf	Leaf blade
Scutellum	Node	Leaf sheath
Primary root	Stem	Husk
	Sheath	Ligule
	Root	Midrib
	Prop root initial	Stem (heavily lignified)
	Tassel initial	Stem (moderately lignified)
	Ear initial	Mature prop root
		Developing prop root
		Prop root tip
		Lateral root
		Lat. Root initiation zone
		Spikelet
		Pollen
		Floret
		Silk
		Cob

Seedlings were grown on a growth bench under lab conditions and sampled at 3 days after germination (DAG). Vegetative-stage and anthesis-stage plants were grown under field conditions (spring, 2008 at the UF-Plant Science Research Unit, Citra, FL) and sampled at 40 and 72 DAG, respectively.

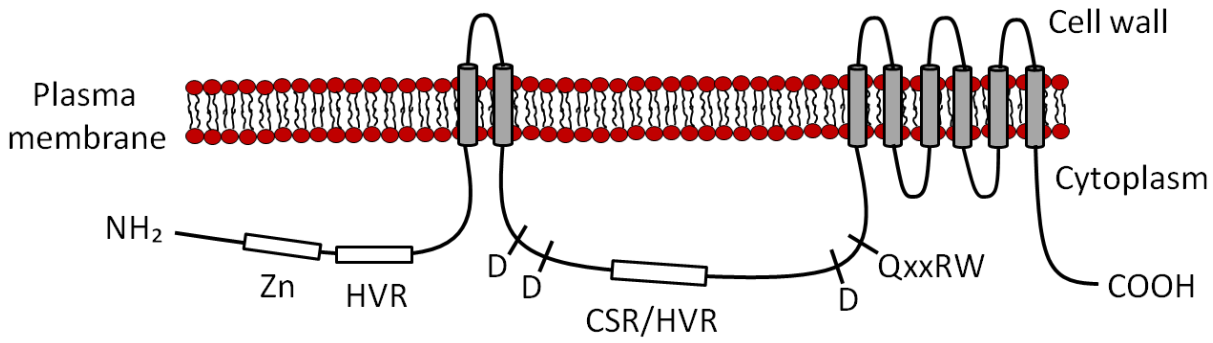

Figure 2-1. Diagram of a canonical CesA protein. The approximate locations of transmembrane domains are represented by grey cylinders. Cytoplasmic domains are designated; Zn (Zinc-binding/RING); HVR(hypervariable region); and CSR (class specific region). The D,D,Q,X,XR,W glycosyl transferase motif is also shown.

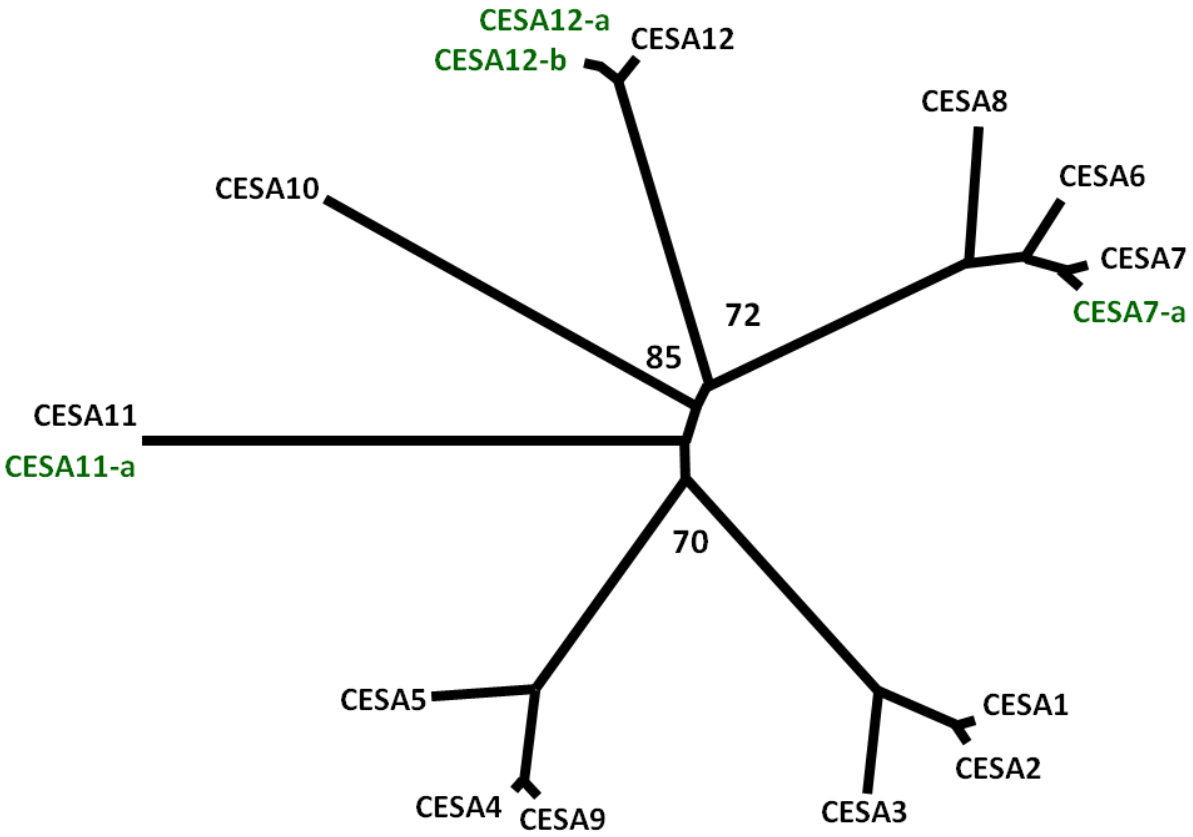

Figure 2-2. Unrooted, neighbor-joining phylogenetic tree of the maize CesA family determined by protein similarity. The CesA1 through CesA12 proteins represent family members with published cDNA sequences. Family members in green are paralogs identified bioinformatically. The tree was constructed using pairwise deletion with 1,000 bootstrap replications in a MEGA4 analysis. Bootstrap values less than 100 are shown.

A

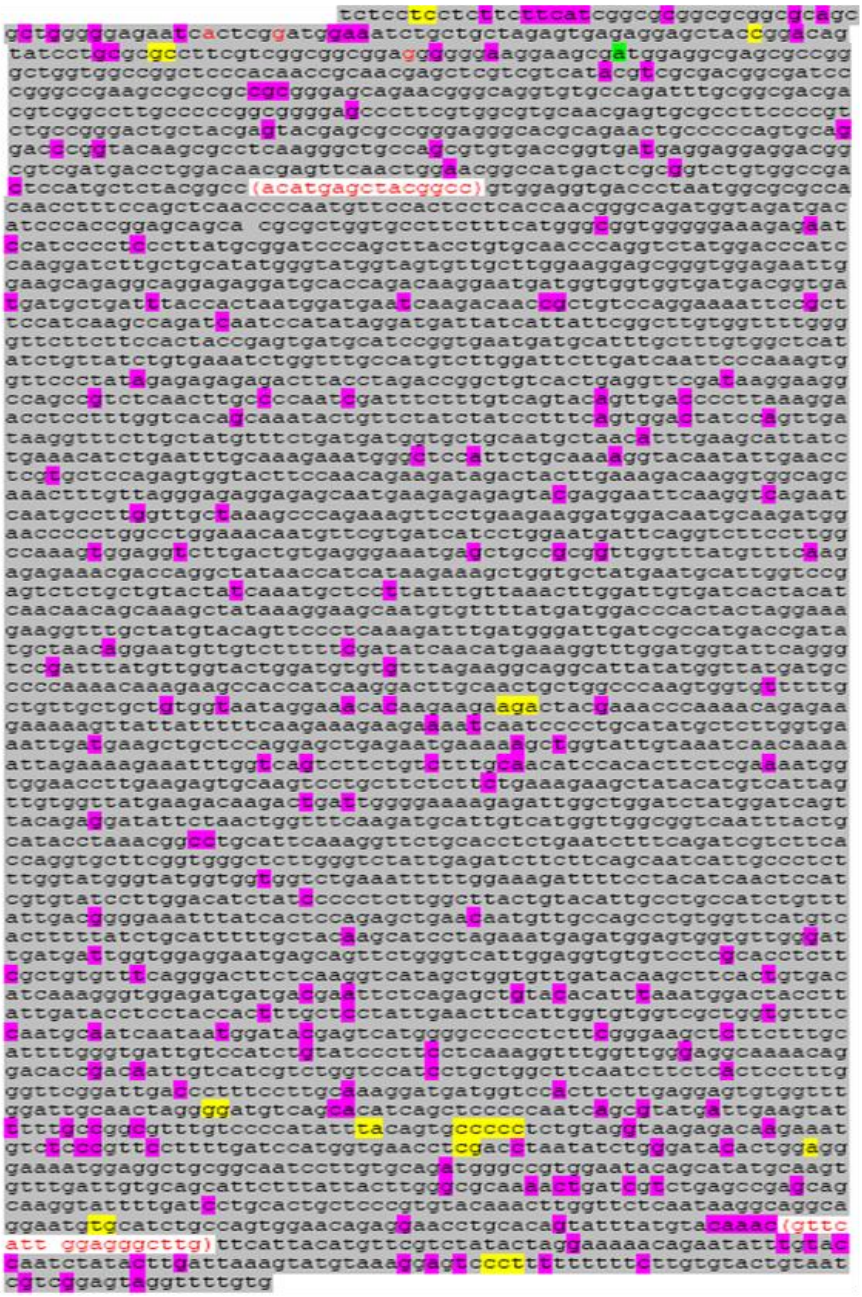

Figure 2-3. Predicted cDNA sequence of *CesA7-a* and its translated protein sequence. A) Assuming conservation of intron-exon boundaries, *CesA7-a* genomic sequence was aligned to *CesA7* cDNA to remove introns. Polymorpmisms (relative to *CesA7*) were mapped, with SNPs highlighted in purple, and insertions in yellow. Deletions are denoted by white background with red text. Overall, the two cDNA sequences share 93.8% homology. B) When translated, the *CesA7-a* predicted cDNA does not introduce premature stop codons, and is 98.5% conserved with CesA7. Met and Stop are written fully to clarify their status.

B

Met E A S A G L V A G S H N R N E L V V I R R D G D P G P K P P P R E Q N G
Q V C Q I C G D D V G L A P G G E P F V A C N E C A F P V C R D C Y E Y E R
R E G T Q N C P Q C R T R Y K R L K G C Q R V T G D E E E D G V D D L D N E
F N W N G H D S R S V A D S Met L Y G H Met S Y G R G G D P N G A P Q P F Q
L N P N V P L L T N G Q Met V D D I P P E Q H A L V P S F Met G G G G K R I H
P L P Y A D P S L P V Q P R S Met D P S K D L A A Y G Y G S V A W K E R V E
N W K Q R Q E R Met H Q T R N D G G G D D G D D A D L P L Met D E S R Q P
L S R K I P L P S S Q I N P Y R Met I I I I R L V V L G F F F H Y R V Met H P V N
D A F A L W L I S V I C E I W F A Met S W I L D Q F P K W F P I E R E T Y L D
R L S L R F D K E G Q P S Q L A P I D F F V S T V D P L K E P P L V T A N T V
L S I L S V D Y P V D K V S C Y V S D D G A A Met L T F E A L S E T S E F A K
K W A P F C K R Y N I E P R A P E W Y F Q Q K I D Y L K D K V A A N F V R E
R R A Met K R E Y E E F K V R I N A L V A K A Q K V P E E G W T Met Q D G T
P W P G N N V R D H P G Met I Q V F L G Q S G G L D C E G N E L P R L V Y V
S R E K R P G Y N H H K K A G A Met N A L V R V S A V L S N A P Y L L N L D
C D H Y I N N S K A I K E A Met C F Met Met D P L L G K K V C Y V Q F P Q R
F D G I D R H D R Y A N R N V V F F D I N Met K G L D G I Q G P I Y V G T G C
V F R R Q A L Y G Y D A P K T K K P P S R T C N C W P K W C F C C C C C G N
R K H K K K T T K P K T E K K K L L F F K K E E N Q S P A Y A L G E I D E A
A P G A E N E K A G I V N Q Q K L E K K F G Q S S V F A T S T L L E N G G T L
K S A S P A S L L K E A I H V I S C G Y E D K T D W G K E I G W I Y G S V T E
D I L T G F K Met H C H G W R S I Y C I P K R P A F K G S A P L N L S D R L H
Q V L R W A L G S I E I F F S N H C P L W Y G Y G G G L K F L E R F S Y I N S
I V Y P W T S I P L L A Y C T L P A I C L L T G K F I T P E L N N V A S L W F
Met S L F I C I F A T S I L E Met R W S G V G I D D W W R N E Q F W V I G G V
S S H L F A V F Q G L L K V I A G V D T S F T V T S K G G D D D E F S E L Y T
F K W T T L L I P P T T L L L L N F I G V V A G V S N A I N N G Y E S W G P L
F G K L F F A F W V I V H L Y P F L K G L V G R Q N R T P T I V I V W S I L L
A S I F S L L W V R I D P F L A K D D G P L L E E C G L D C N Stop G Met S A H
Q L P Q S A Y D Stop S I F A G V C P H I Y S A P S V G K R Q E Met S P V P F D
P W Stop T S T Stop Y L G Y T G G K Met E A A A I L V Q Met G R G I Q H Met
Q V F D C A A F F I T W A Q N Stop S S E P S S K V F Stop S C T A P V Y K L G
S Q Stop G R Q E C A S A S G T E E P A Q Y L C T N V H W R A C S L H V R L Y
Stop E K Q N I C T N L Y L I K V C K G V P F F F L C T V I V G V G F V

Figure 2-3. Continued

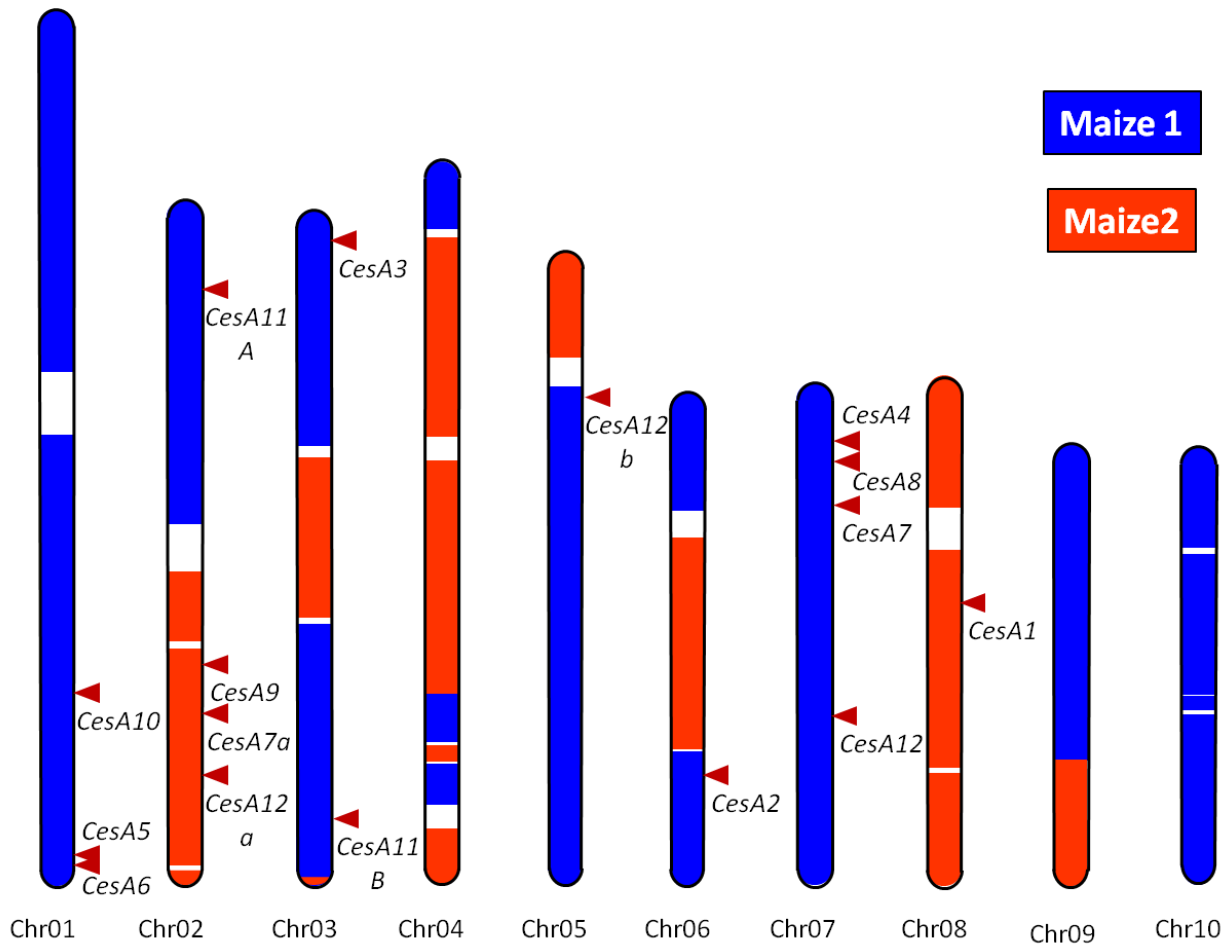

Figure 2-4. Approximate distribution of the *CesA* family and close paralogs within the maize genome. A) Representation of *CesA* positions alongside the chimeral chromosomes of the modern maize genome that resulted from an ancient tetraploidization event and subsequent diploidization. Genome copies (resulting from tetraploidy) are termed Maize-1 and Maize-2, and are represented by blue and orange, respectively. Chromosomal segments that could not be assigned to either genome are white. Note that several *CesA* genes are paralogs of others (see Figure 2-4B). Newly-identified paralogs are named after the family member they are paralagous to, followed by a letter (e.g. *CesA7a*). In some instances (*CesA12a* and *CesA12b* for example) paralogs map to different genomic copies. Chromosomal domains are shown as per Schnable et al. (2011). B) A phylogenetic tree showing the relationship between CesA and CesA-paralog proteins relative to the genome copy in which they reside. The tree was constructed using pairwise deletion with 1,000 bootstrap replications in a MEGA4 analysis (Tamura et al., 2007).

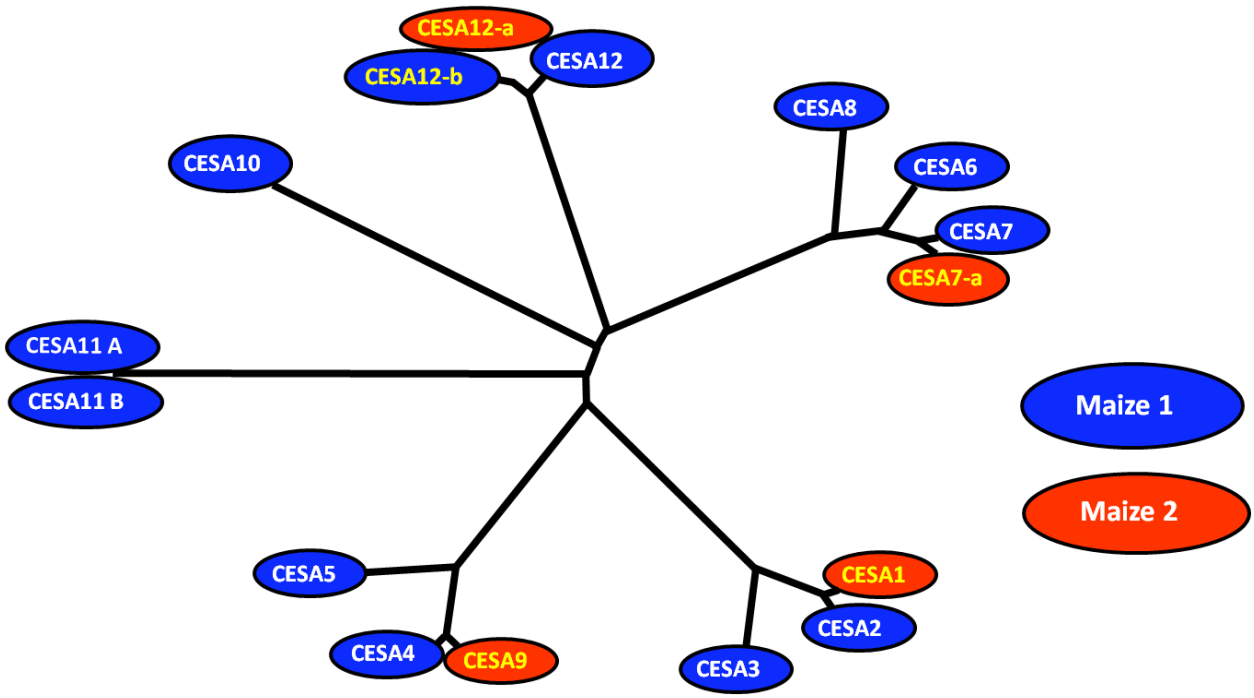

Figure 2-4. Continued

Figure 2-5. Predicted miRNAs targeting each of the maize *CesAs*. Potential target sites and cooresponding miRNAs were predicted using the miRNAFinder program (bioinfo3.noble.org/mirna/). Results were based on similarity of maize *CesA* genomic sequence to the rice EST database and the rice genome. Potential miRNAs that targeted more than one *CesA* are highlighted.

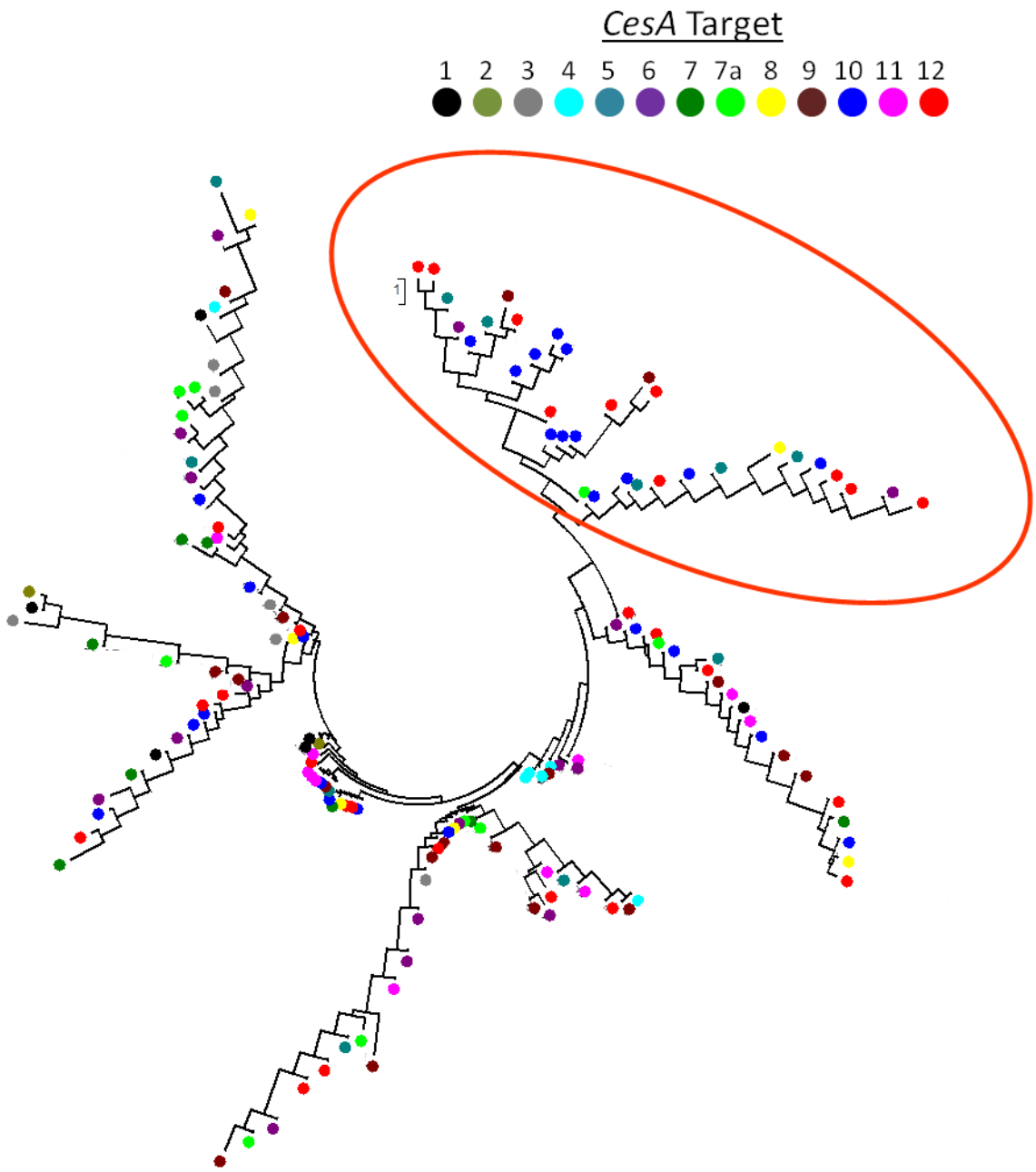

Figure 2-6. Cluster analysis of potentially *CesA*-targeting miRNAs. MicroRNAs were grouped based on sequence similarity, using pairwise deletion with 1,000 bootstrap replications in a MEGA4 analysis (Tamura et al., 2007). The *CesA* family member that each miRNA targets is designated by color. A clade enriched for miRNAs potentially targeting *CesA10* and *CesA12* is circled in orange.

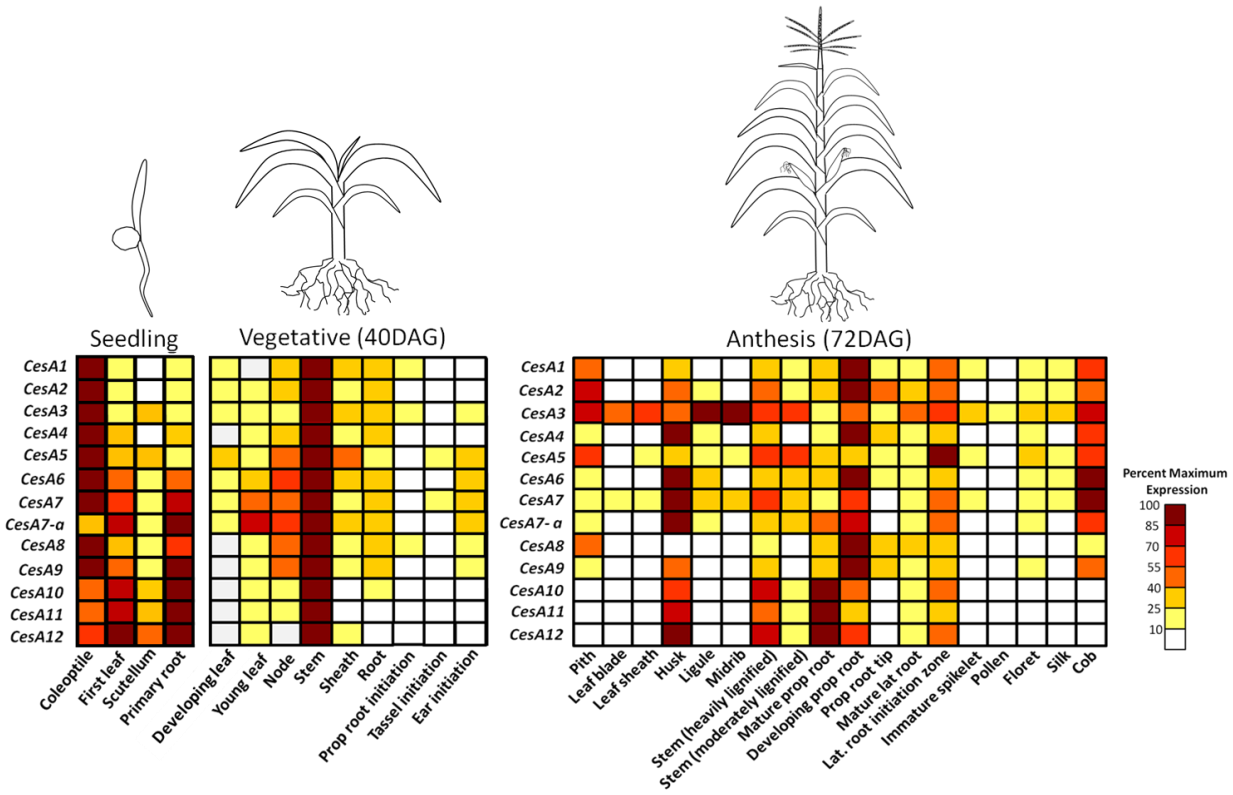

Figure 2-7. Heat maps representing expression of *CesA* family members in all tissues sampled at each time point. Diagrams show relative developmental state of plants sampled at seedling (3DAG), vegetative (40DAG), and reproductive stages of development. Maps show the relative expression of each gene at a given time point as a percentage of its maximum.

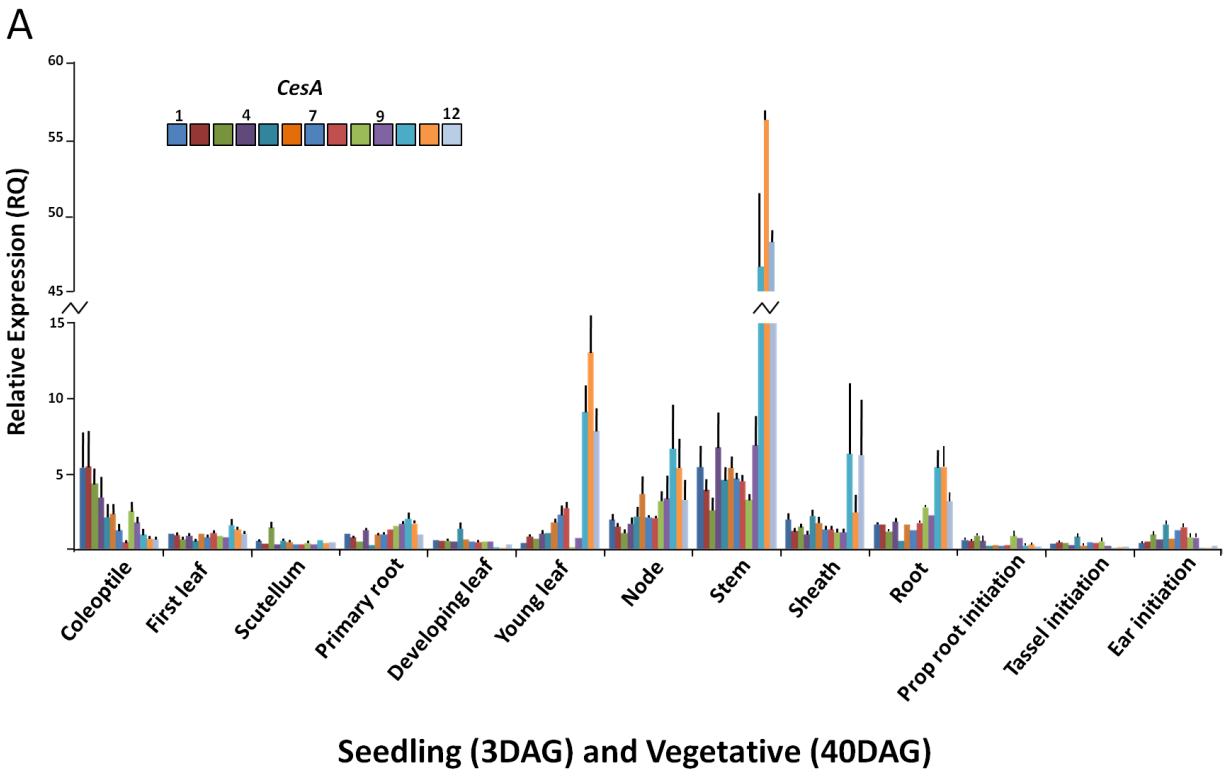

Figure 2-8. Relative expression of the *CesA* family in all tissues samples. A) The seedling- (3DAG) and vegetative- stages (40DAG). B) Anthesis (72 DAG). Expression levels are relative to the amount 18SrRNA measured in each tissue. Data represent three biological replications.

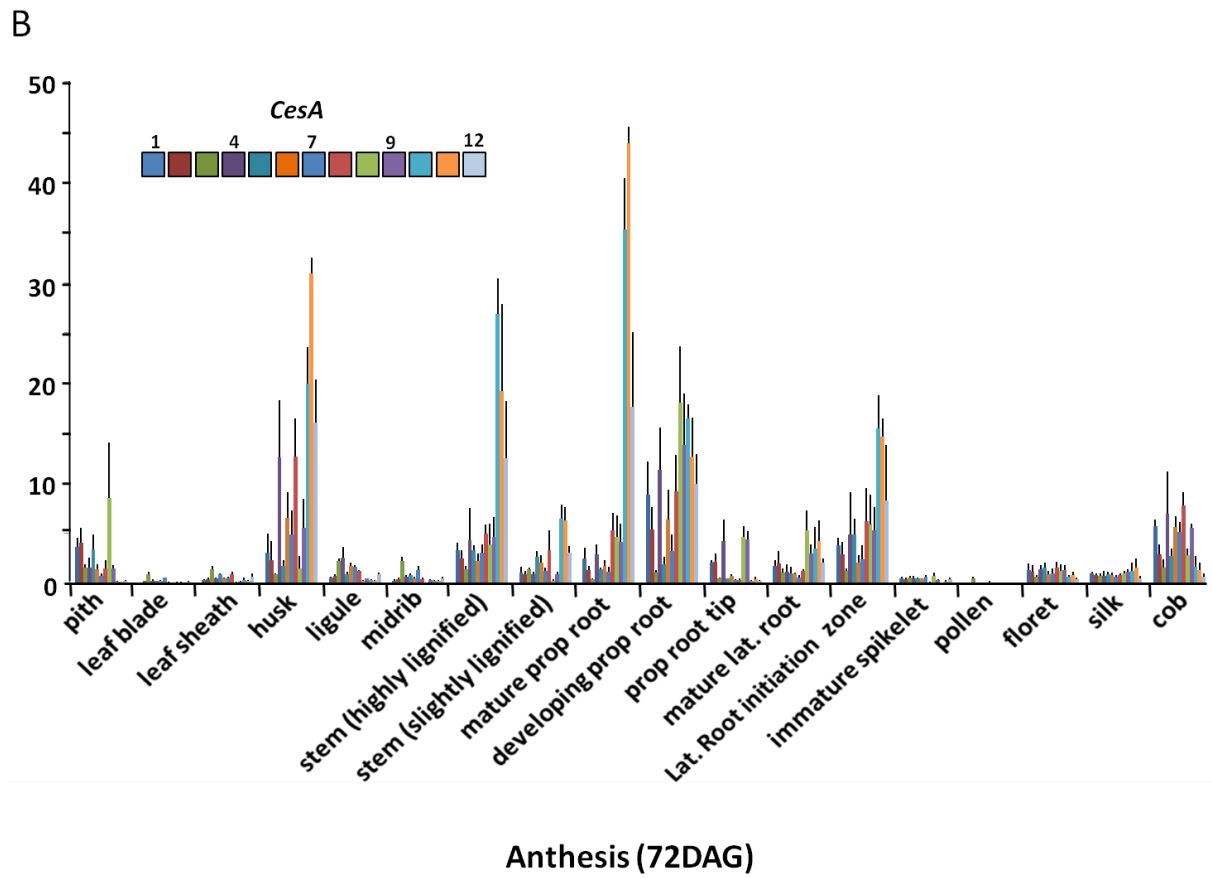

Figure 2-8. Continued

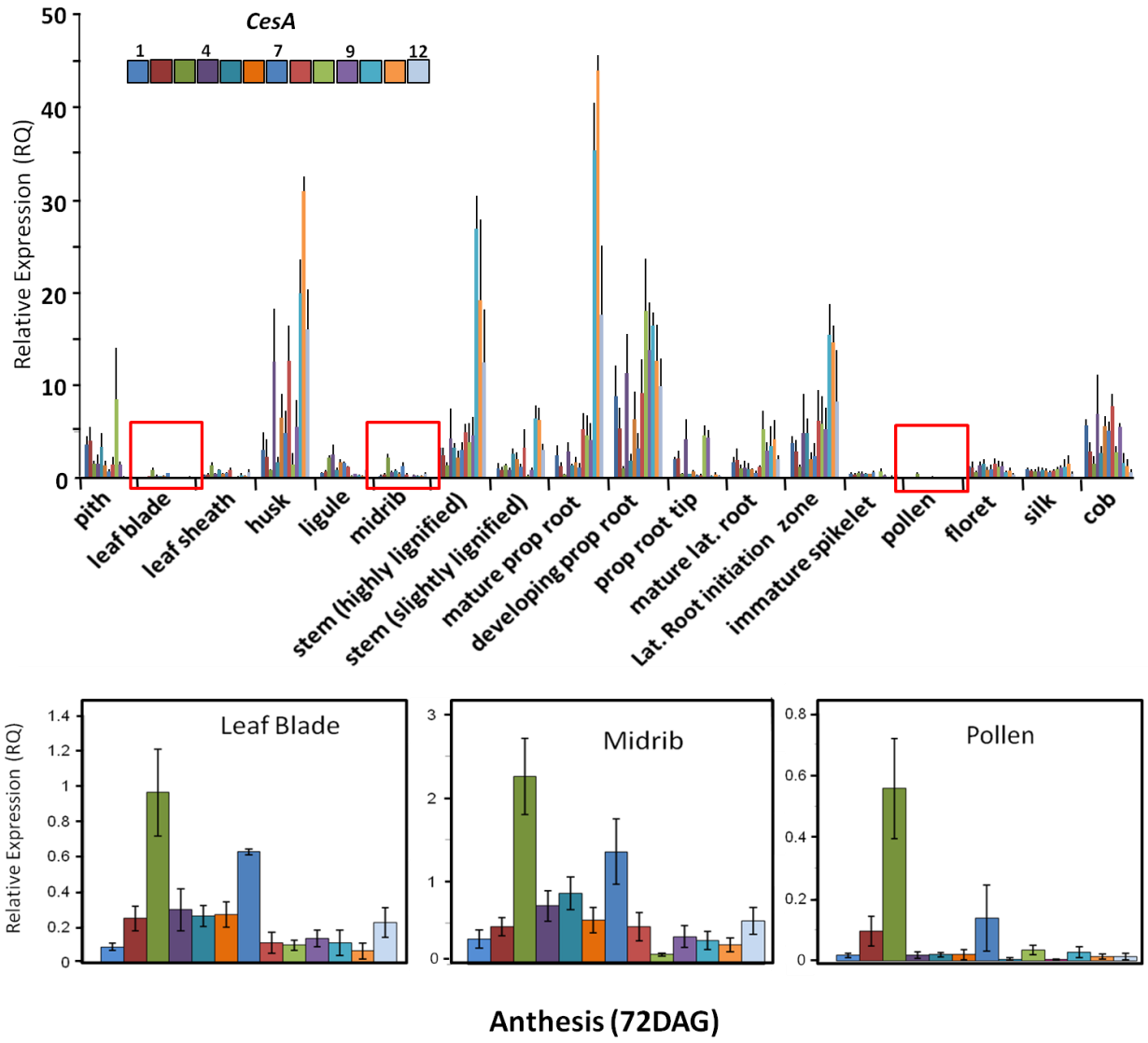

Figure 2-9. Expression of *CesAs* in tissues with low mRNA abundance. In three of the tissues with overall lowest transcript levels, *CesA3*, and then *CesA5* are the dominantly expressed family members. Expression levels are relative to the amount 18SrRNA measured in each tissue. Data represent three biological replicates.

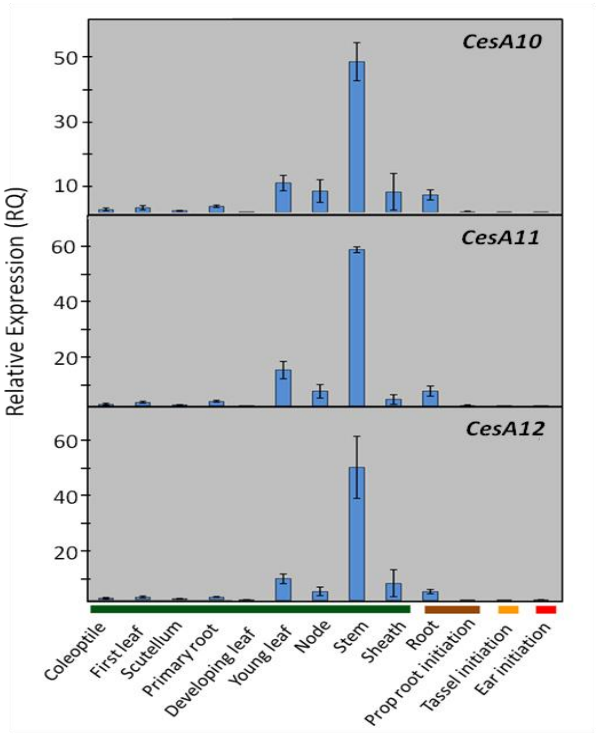

Cluster I

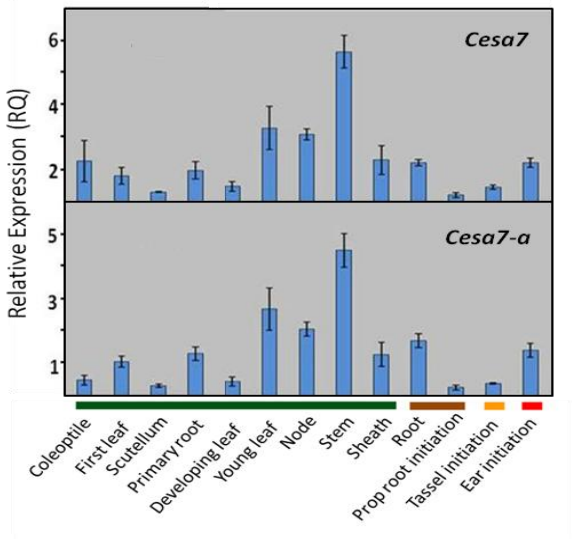

Cluster II

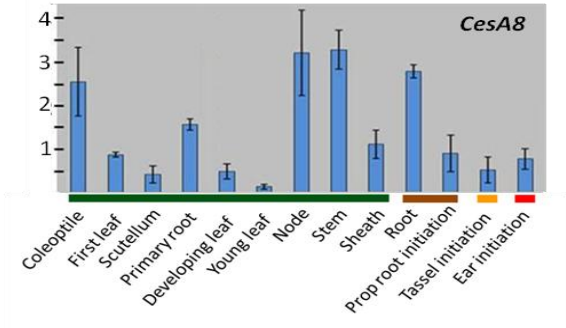

Unclustered

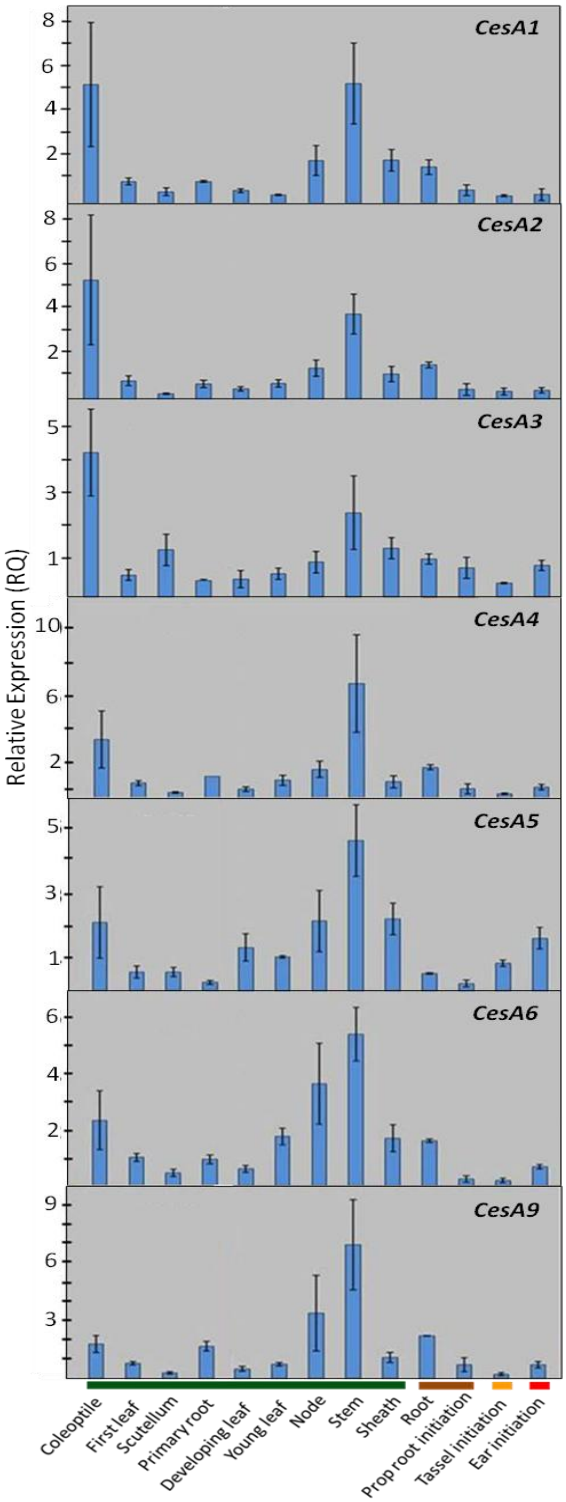

Cluster III

Figure 2-10. Cluster analysis of the *CesA* family at the seedling- and vegetative- stages. A correlation value of 0.8 was used as the cutoff for cluster designation. Genes having insufficient similarity in expression pattern to other family members were considered unclustered. Cluster number indicates strength of correlation between its members. The mean correlation values for cluster I, cluster II, and Cluster III were 0.99, 0.98, and 0.87, respectively. Colored bars along the X-axis indicate tissue type, with green = above ground-, brown = below ground-, yellow = male reproductive-, and red = female reproductive-tissues. The Modulated Modularity Clustering program (Stone and Ayroles, 2009) was used to define clusters. Expression levels are relative to the amount 18SrRNA measured in each tissue. Data represent three biological replicates.

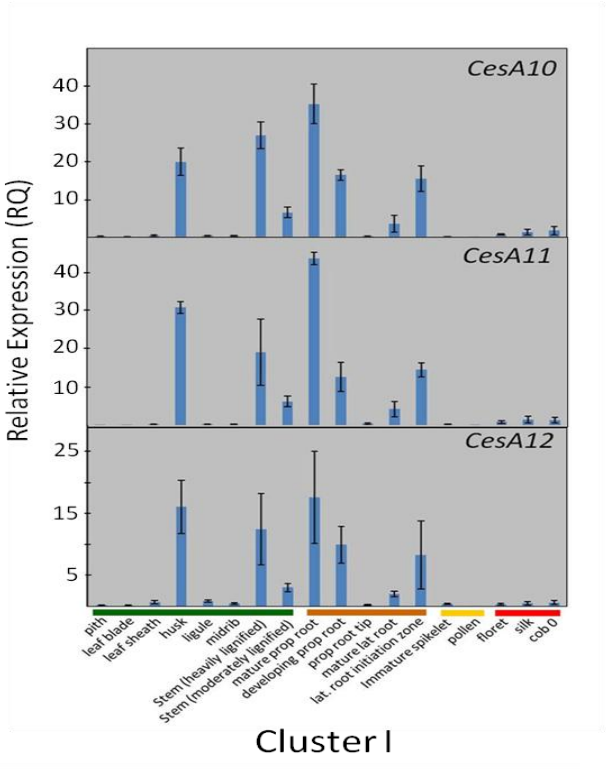

Cluster I

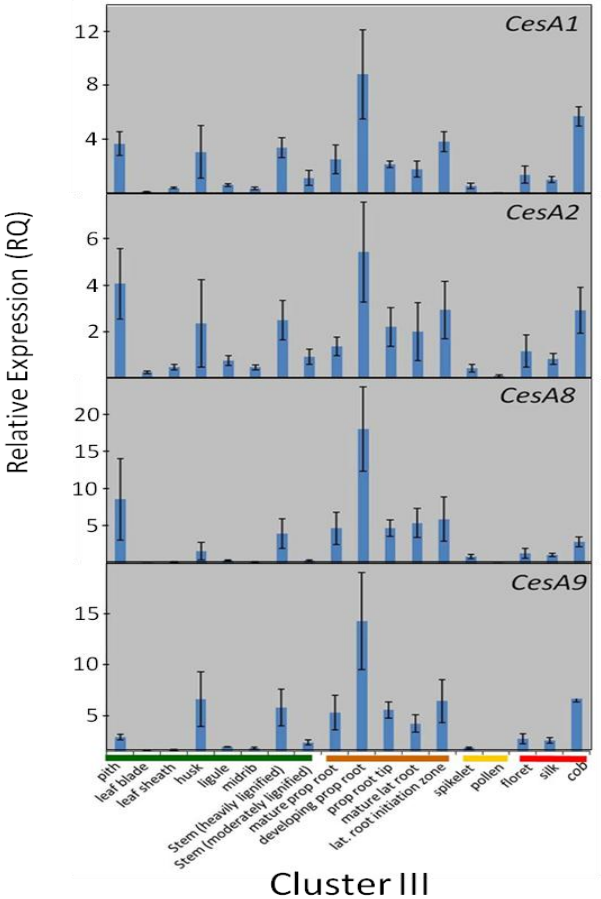

Cluster III

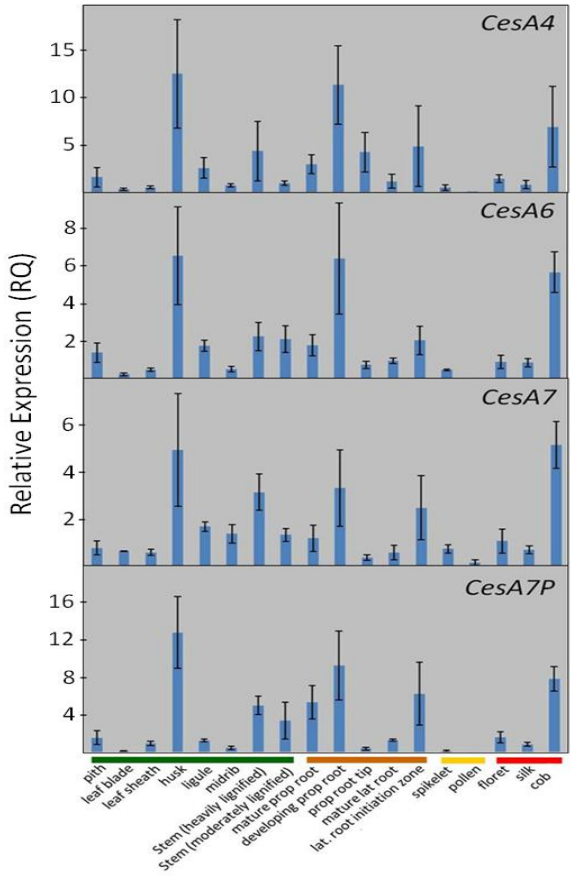

Cluster II

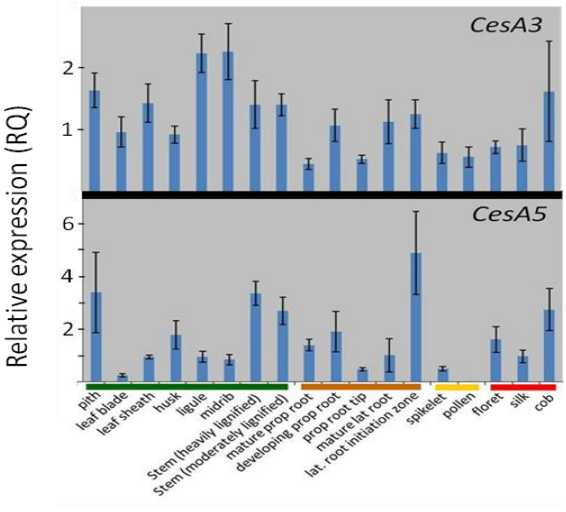

Unclustered

Figure 2-11. Cluster analysis of the *CesA* family at anthesis/reproductive maturity. A correlation value of 0.8 was used as the cutoff for cluster designation. Genes having insufficient similarity in expression pattern to other family members were considered unclustered. Cluster number indicates strength of correlation between its members. The mean correlation values for Cluster I, Cluster II, and Cluster III were 0.96, 0.90, and 0.89, respectively. The Modulated Modularity Clustering program (Stone and Ayroles, 2009) was used to define clusters. Expression levels are relative to the amount 18SrRNA measured in each tissue. Data represent three biological replicates.

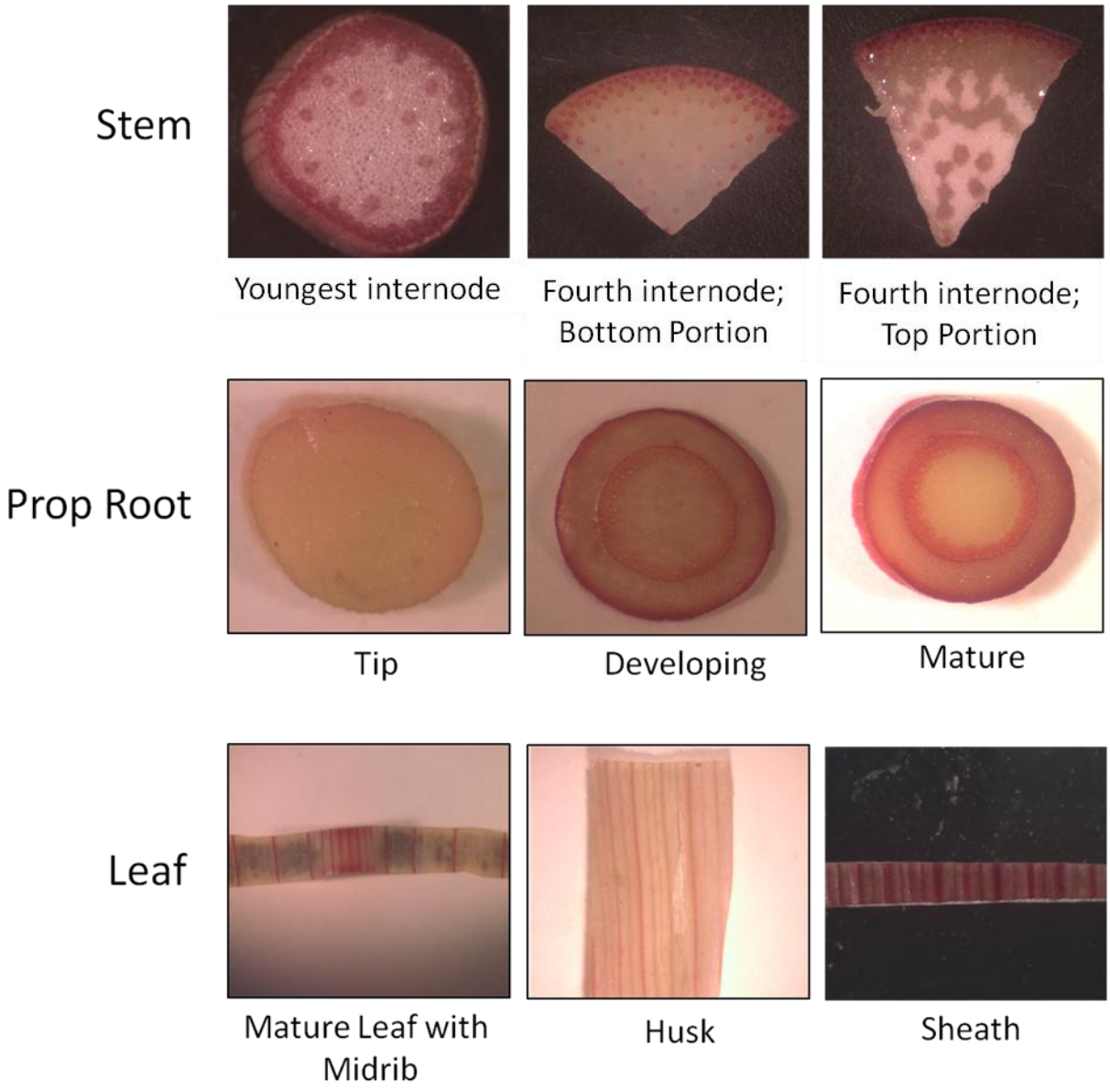

Figure 2-12. Lignin and polyphenol deposition in tissues at the anthesis stage (72 DAG). Cross-sectioned tissues were stained (pink/red) with phloroglucinol/HCl solution to detect the presence of lignin/secondary cell wall deposition. Only tissues showing visible staining are shown.

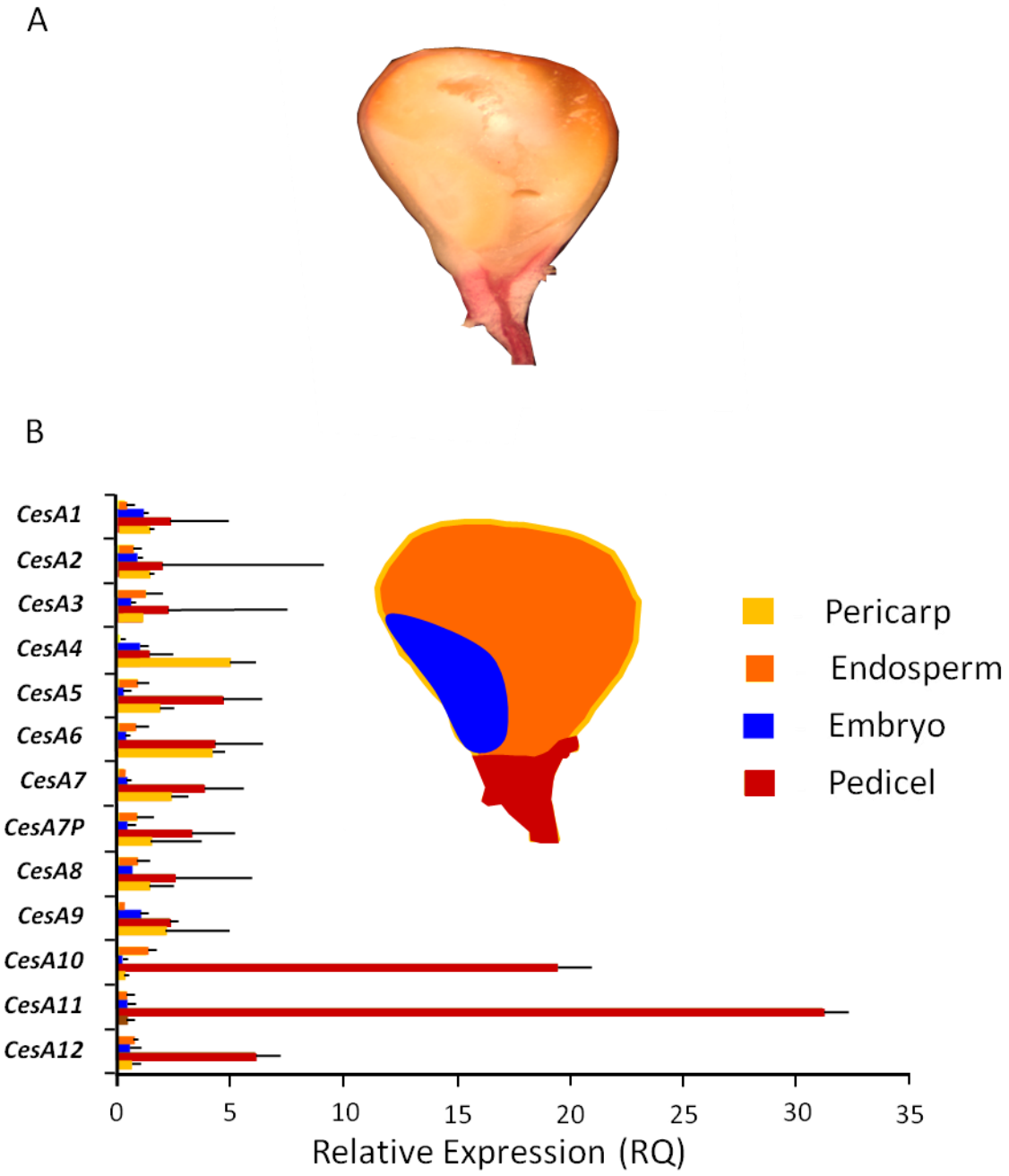

Figure 2-13. Expression of the *CesaA* gene family in kernel tissues 15 days after pollination. A) A longitudinal kernel section stained with phloroglucinol. Pink staining indicates presence of lignin/secondary cell wall. B) Expression of *CesAs* in 4 kernel tissues. Expression levels are relative to the amount 18SrRNA measured in each tissue. Data represent three biological replicates. Photo by Brent O'Brien.

CHAPTER 3
EXPRESSION OF THE CELLULOSE SYNTHASE GENE FAMILY IN A MAIZE SUSPENSION CELL/PROTOPLAST SYSTEM

Background

The plant cell wall is a complex, cellulose-rich structure that serves several essential functions. The cell wall not only provides the cell and whole plant with mechanical strength, but also aids in defense against pathogens, determines cell shape, and participates in signaling (Aziz et al., 2007; Galletti et al., 2009). Because cellulose is the major load-bearing component of the cell wall, considerable effort has been directed towards understanding its synthesis and regulation at the whole-plant and tissue- levels. Most studies have investigated *CesA* expression in tissues of wild-type plants (Pear et al., 1996; Delmer, 1999; Appenzeller et al., 2004; Wang, 2010), or analyzed effects of *CesA* mutations (Tanaka et al., 2003; Taylor et al., 2003; Taylor, 2008). In contrast, comparatively little work has utilized cell-culture or protoplast approaches to investigate cellulose synthase expression in these readily-perturbed systems.

A useful approach to questions of how cellulose synthesis is regulated at the cellular level can be addressed by investigating gene expression in response to perturbations of undifferentiated suspension cells and during cell-wall regeneration by protoplasts. Release of protoplasts from cells of various plant tissues is a common practice, and a widely used approach for diverse fundamental studies. For example, organelles and other cellular constituents can be isolated more readily from protoplasts than from whole tissues (Tallman and Reeck, 1980), and removal of the cell wall facilitates investigations into physical and chemical properties of the plasma membrane (Stafford and Warren, 1991; Yamazaki et al., 2008). Protoplasts can be obtained from specific cell types where they have been invaluable in studies of processes such as the roles of bundle sheath cells in C4 metabolism (Edwards et al. 1979; Shatil-Cohen et al.,

2011), and light effects on guard cell functions (Zeiger and Hepler, 1979; Pandey et al., 2002). Protoplasts have also proven versatile for analysis of transient gene expression, because the accessible plasma membrane makes them ideal for genetic transformation through electroporation or microinjection (Potrykus, 1991; Dong-Yoo et al., 2007). Protoplasts are stressed during the isolation process, however, and resulting changes in gene expression and metabolism necessitate ample controls and cautious interpretation of results.

The cell wall can be effectively removed by use of enzyme treatments that degrade its polysaccharide constituents. The enzymes are typically extracted from fungal sources (parasitic and/or necrotrophic) (Wang et al., 1991; Ling et al., 2010). Liquid medium used to culture cellulytic bacteria has also been shown to degrade cell walls (Tamaru, 2002). Wounding and pathogen response pathways can be induced by exposure of cells to fungal elicitors such as cell-wall-degrading enzymes and contaminants, and/or oligosaccharides released from the cell wall during digestion (Cordero et al., 1994; Moreno et al., 2005). Changes in metabolism and gene expression can also occur as cells and protoplasts respond to 8 hours of incubation in the sugar-free environment of cell wall-digestion medium (Yu, 1999). Furthermore, biotic and abiotic stress responses may result from the mechanical damage and/or stresses associated with the lack of a cell wall (Walley et al., 2007).

Cell wall composition of regenerated protoplasts typically differs from that of walls from either the cell-cultures or plant tissues from which protoplasts were obtained (Blaschek et al. 1981; Pilet et al. 1984; Gould et al. 1986; Wang et al., 1991). During de-novo cell wall synthesis, protoplasts can produce callose (1→3 β-D-glucan) instead of cellulose (1→4 β-D-glucan), and synthesize different polysaccharides than those in cell walls of the source tissue. However, work by Shea et al. (1989) demonstrated that protoplasts derived from carrot suspension cells could regenerate compositionally-similar cell wall to that of normal suspension cells. An exception was

that crystalline cellulose was slower to form, and took 3 days for full regeneration (Shea et al., 1989). The authors suggested that purity of wall-degrading enzymes may be important to prevention of wound responses that could cause abnormal synthesis of callose and other cell wall polysaccharides. Work with maize has demonstrated that protoplasts derived from suspension cells regenerate cell walls more rapidly than those derived from mesophyll (Wang et al., 1991). Furthermore, the regenerated cell walls of protoplasts derived from suspension cells are more evenly distributed, more compact, and better organized than those from mesophyll (Wang et al., 1991). Additionally, when gene expression in potato leaf protoplasts was examined during cell wall regeneration, expression profiles showed no significant upregulation of cell wall-biosynthetic genes relative to shoot tissue *in-planta* (Oomen et al., 2003).

Suspension cells provide yet another approach for fundamental studies of cell wall biosynthesis. Like protoplasts, suspension cells can be derived from diverse tissues, but the tissue from which the suspension cells are initiated must be able to form callus. Suspension cells can also be derived from both differentiated and undifferentiated tissues, thus allowing a choice in the characteristics (i.e. cell wall composition, genetic pre-programming, metabolic properties) of the cell type to be studied. It should be noted that cultured plant cells are often subject to somaclonal variation, and cell lines derived from these variants may have different properties than the source tissue (Lee et al., 1988; Bruneau and Qu, 2010). Application of growth modulators such as phytohormones, phosphates, micronutrients, and sugars has also been shown to control cell differentiation and organ formation (Skoog and Miller, 1957; Oda et al., 2005). Furthermore, research in *Arabidopsis* indicates that in immortalized suspension cell cultures, where cells are continuously proliferating, dedifferentiation occurs concomitantly with clear epigenetic changes (Tanurdzic et al., 2008). Chromatin immunoprecipitation analysis has shown these changes include hypermethylation of euchromatic regions, and hypomethylation of

heterochromatic regions corresponding to transposable elements (TEs). The resulting activation of TEs was accompanied by an increase in 21-nucleotide, small-interfering RNAs, thus implicating RNA interference along with chromatin remodeling in epigenetic restructuring of immortalized suspension cell lines (Tanurdzic et al., 2008).

Plant suspension cell cultures are a highly versatile research platform because one can subject the system to diverse, targeted perturbations. Not surprisingly, they have been used to study a wide variety of cellular processes including specific responses to abcisic acid and gibberelic acid (Xin and Li, 1992; Huang and Lloyd, 1999), aquaporin function (Cavez et al., 2009), mitochondrial release of calcium under anoxia (Subbaiah et al., 1998), and tracheary element formation (Fukuda, 1997).

Suspension cells have been particularly useful for studying cell wall biosynthesis because they can be induced to produce secondary cell walls. Depending on the species and source tissue, different hormone treatments and/or sugar concentrations can induce differentiation of suspension cells to tracheary element-like (TEL) cells that are similar to those found in xylem (Falconer and Seagull, 1985; Fukuda, 1997; Oda et al., 2005; Ohashi-Ito et al., 2010). Induction of TEL formation was optimized in *Zinnia elegans* L. to study xylogenesis, and the characteristics of TELs were remarkably similar to those of intact xylem (Falconer and Seagull, 1985). Tracheary element-like cells had diverse patterns of secondary cell wall deposition typical of xylem such as annular, reticulate, spiral, scalariform, and pitted thickenings. Subsequently, TEL induction in suspension cells has been used to study the relationship between microtubules and secondary cell wall deposition (Oda et al., 2005), expression and regulation of cell wall biosynthetic genes (Ohashi-Ito et al., 2010), and programmed cell death (McCabe and Leaver, 2005; Ohashi-Ito et al., 2010).

Here we employ both protoplast and suspension cell systems to experimentally perturb regulation of gene expression in the maize *CesA* gene family. Relative gene expression was quantified during de-novo cell wall biosynthesis by protoplasts for up to 60 h of regeneration. Expression of the *CesA* family was also assayed in suspension cells undergoing hormone-induced differentiation to TELs. In addition, *CesA* expression was analyzed in both the protoplast and suspension cell systems after specific perturbations. During de-novo cell wall synthesis by protoplasts, *CesAs* from the primary- and secondary-cell wall synthesizing subclades were highly upregulated relative to suspension cells. Also, reducing the sucrose content of protoplast regeneration media showed that the timing and identity of *CesAs* expressed is responsive to sugar availability. Futhermore, induction of secondary cell wall deposition in suspension cells resulted in concurrent increase in levels of *CesA10*, *CesA11*, and *CesA12* mRNAs, consistent with previously described observations in planta (see chapter 2).

Results

Establishment of the Protoplast Regeneration System

Multiple parameters including digestion media, digestion time, agitation speed, harvest methods, purification, and regeneration media were optimized to establish an efficient system for harvest of protoplasts, and develop a suitable environment for cell wall regeneration. The concentrations of cell-wall-degrading enzymes in the digestion medium was adjusted to release the greatest number of protoplasts. Digestion time and agitation speed were adjusted to maximize yield of viable, undamaged protoplasts. Protoplast harvest (centrifugation speed), purification (filtering and flotation methods), and regeneration media (sucrose and 2-4-D concentration) were also optimized, with the end result being a reliable system with reproducible results from a given time course for cell wall regeneration (Figure 3-1). The most essential aspect of this process was

adjusting the digestion media, digestion time, and agitation speed to maximize effective release of protoplasts from suspension cells without compromising viability.

Embryo-derived suspension cells from maize inbred B104 were used as the source of protoplasts. After 8 hours of incubation in digestion media, protoplasts were harvested, purified, and transferred to regeneration media for observation of cell wall biogenesis during the subsequent 60 hours. Prior to protoplast release, light microscopy showed suspension cells were typically present as aggregations of translucent to slightly opaque, irregularly-shaped, ovoid cells. These cells also fluoresced bright, bluish-white under fluorescent light when stained with calcofluor white (Figure 3-1), indicating presence of abundant cellulose. After the 8-hour period of protoplast release in digestion media, nascent protoplasts (0 hours) were transparent, completely spherical, and showed no fluorescence (Figure 3-1). As protoplasts regenerated cell walls, the cells began to aggregate, and at 12 hours of regeneration, slight, patchy calcofluor white fluorescence became evident (Figure 3-1). After 20 hours, most viable cells had aggregated, become translucent, taken on an irregular shape, and showed fluorescence. The fluorescence was not as strong as that of suspension cells, however, indicating that cell wall regeneration was likely still in progress (Figure 3-1).

Expression of *CesAs* and Sucrose Synthases in Protoplasts Regenerating Cell Walls

To determine responses of *CesA* family members to the extreme demands for cell wall biosynthesis by protoplasts, mRNA levels of *CesAs* from the primary and secondary cell wall synthesizing subclades (Figure 2-1) were quantified. Additionally, transcript abundance was determined for three sucrose synthases, since these are hypothesized to associate loosely with the CESA-complex and provide UDP-glucose as substrate for cellulose synthesis (Amor et al., 1995; Fujii et al., 2010). The *CesAs* did not show significant upregulation until about 4 hours after induction of cell wall regeneration, and expression of the sucrose synthases remained low until

20 hours after transfer to induction medium (Figure 3-2). With the exception of *CesA1*, *CesA2*, and *CesA11*, relative expression levels of all other genes analyzed peaked at 44 hours after initiation of cell wall regeneration, and dropped sharply thereafter. In addition, a transient and repeatable peak in mRNA levels occurred at 12 hours for *CesA7 CesA7-a*, *CesA10*, and *CesA11* (Figure 3-2). An additional transient peak for *CesA11* was observed at 28 hours. Relative expression of most other genes increased with each progressive time point, up to 44 hours. With the exception of *Sus1* and *Sus2*, expression profiles were highly variable, thus indicating a lack of coordinate regulation under these conditions (Figure 3-2).

CesA and Sucrose Synthase Expression During Cell Wall Regeneration With Perturbations in Sucrose Concentration

Sugar substrates are necessary for cell wall biosynthesis, and sucrose metabolism is hypothesized to provide substrates to the CESA complex (the reversible sucrose synthase reaction can generate fructose and UDP-glucose). In addition, sugar availability can profoundly affect metabolism and reprogram expression of related genes (Su, 1999; Koch, 2004). We thus investigated the effects of sucrose starvation on *CesA* and sucrose synthase expression during cell-wall regeneration. The sucrose concentration in regeneration media used for both protoplasts and suspension cells was normally 2% w/v, so we compared results under these conditions to responses under 0.5% and 0% sucrose.

Under reduced sucrose conditions (0.5%), sufficient RNA for analysis could be recovered for the first 36 hours after induction of cell wall regeneration (Figure 3-3). Expression of the *CesAs* was comparable (to one another) at each time point between 12 hours and 28 hours of regeneration, with the exception of *CesA12* (Figure 3-3). At 4 hours, mRNAs of all *CesAs* from *CesA1* through *CesA11* were at their lowest levels, whereas expression of *CesA12* was 8-fold higher than its minimum, which did not occur until 20 hours. Transcript levels of *CesA12* peaked

at 28 hours, increasing 32-fold relative to expression at 20 hours. (Figure 3-3). The most prominent change in expression pattern was at 36 hours, where transcript levels of most *CesAs* roughly doubled their previous maxima (Figure 3-3). The sucrose synthases did not share any of these changes in expression. Levels of mRNAs were consistently similar for all three genes (*Shrunken1*, *Sucrose synthase1*, and *Sucrose synthase2*), with transcript abundance increasing slightly throughout the experiment. Overall, expression of the sucrose synthases was relatively low, with mRNA levels at 36 hours roughly double those at 4 hours.

The expression patterns of the *CesAs* and sucrose synthases changed markedly when protoplasts were allowed to regenerate in media without sucrose. Under these conditions, sufficient RNA could only be recovered for the first 28 hours after induction of cell wall regeneration. Expression of the cellulose synthases was most highly upregulated and variable at 12 hours, instead of at the last time point available (28 hours), as was observed under reduced sucrose (Figure 3-3B). The observation that expression levels of *CesA12* fluctuated more than other family members may indicate that some aspect of its regulation is more sensitive to sugar-limiting conditions. The sucrose synthases had expression patterns nearly identical to those observed when protoplasts were grown in reduced sucrose, illustrating that these genes were less responsive to variation in sugar availability than the *CesAs* (Figure 3-3B).

Cellulose Synthase and Sucrose Synthase Expression in Response to Simulated Wounding/Pathogen Infection

Incubation in cell wall-digestion media exposes cells to molecules that stimulate expression of defense response genes. Examples include contaminating fungal toxins, cell wall-degrading enzymes, and oligosaccharides released from the cell walls during digestion. These can all elicit defense responses to wounding and/or pathogen infection (Cordero et al., 1994; Seifert and Blaukopf, 2010). Additionally, removal of the cell wall may initiate signals of

mechanical damage in protoplasts, further enhancing responses to wounding, and altering normal gene expression patterns. To determine the extent of influence potentially exerted on *CesA* expression by defense responses, we simulated wounding and/or pathogen infection in suspension cells, then quantified mRNAs from selected *CesAs* (*CesA1, CesA7,CesA12*) and the systemic wound/pathogen response gene *MPI* (maize proteinase inhibitor) (Cordero et al., 1994). Expression of *MPI* was also assayed in regenerating protoplasts.

The expression profile of *MPI* in regenerating protoplasts was similar to that observed for the *CesAs* and sucrose synthases, with slight upregulation beginning at 4 hours and increasing rapidly through 44 hours (Figure 3-4). Expression levels of test genes were measured at four time points under conditions in which regeneration media contained either 1) no treatment (control), 2) ground whole cells, 3) denatured cell wall-degrading enzymes, or 4) purified partially-digested cell wall. In the control media, *MPI* levels were greatest in freshly-transferred suspension cells, but dropped rapidly during a 12-hour incubation. Cells in media containing ground whole cells showed a peak in *MPI* expression at 2 hours, and slight downregulation of *CesA7,* and *CesA12* (Figure 3-5). In solution containing denatured cell wall-digestion enzymes, all genes were slightly upregulated with peak expression at 2 hours (Figure 3-5). These data show that expression of the *CesAs* is most responsive to simulated pathogen infection. However, this response is transient, with expression levels returning to those of pre-treatment conditions by 12 hours (Figure 3-5).

Expression of the *CesAs* During Induction of Secondary Cell Wall Biosynthesis

With the goal of defining which cellulose synthases may be involved in secondary cell wall biosynthesis, we treated maize suspension cells with phytohormones that were previously shown to induce secondary cell wall formation in *Zinnia* (Falconer and Seagull, 1985; Endo et al., 2009). After 7 days of incubation in secondary-cell-wall-induction media, suspension cells

began to differentiate into tracheary element-like (TEL) cells (Figure 3-6), consistent with results from previous work (Falconer and Seagull, 1985; Fukuda, 1997; Oda et al., 2005; Ohashi-Ito et al., 2010). Concurrent with the appearance of TELs in culture, mRNA levels of *CesA10*, *CesA11*, and *CesA12* were highly elevated relative to the control (Figures 3-6 and 3-7). Upregulation of these genes was maintained, although at lower levels, until 25 days after transfer (DAT) to induction medium. Taken together, these results are consistent with our in-vivo observations indicating that *CesA10*, *CesA11*, and C*esA12* play a role in secondary cell wall biosynthesis.

Discussion

Cellulose Synthase Expression During Cell Wall Regeneration

Expression profiles of the *CesAs* analyzed indicate that family members associated with both primary- and secondary- cell wall formation were involved in de-novo wall biosynthesis by protoplasts (Figure 3-2). This result was contrary to expectations, because the suspension cells used as a source of protoplasts had only primary cell walls, and were derived from undifferentiated embryonic cells that also lacked detectable secondary cell walls. Involvement of both *CesA* classes in cell wall regeneration may be due to concurrent upregulation of all cell wall-biosynthetic genes in response to the severity of complete cell wall removal and signals for its regeneration. Other stresses associated with cell wall digestion may also have been involved, as well as elicitation of defense mechanisms. The impact of stress signals would be consistent with the duration and pattern of observed gene expression, although cell wall regeneration also followed a similar time-course.

Sucrose synthase mRNA levels decreased concurrently with those of most *CesA* genes, indicating a potential reduction in capacity for direct conversion of sucrose to precursors of cellulose biosynthesis. The proposed role of sucrose synthase in cellulose formation may have

been especially important early in cell-wall regeneration, when biosynthesis of cellulose was a major sink for carbon-metabolism. Later, however, the carbon demands for cell wall formation would be expected to lessen, even though mRNAs for some biosynthetic genes remain abundant. Also, mRNA levels of all genes tested did not rise detectably until 4 hours after transfer to regeneration media. This 4 hour-delay may have been due to a period of cellular recovery from the combination of stress and starvation during cell wall removal (digestion medium lacks metabolizable carbohydrate).

Expression of three *CesAs* was distinctive during cell-wall regeneration, with mRNA levels of *CesA1, CesA7* and *CesA11* continuing to rise throughout a 60-hour period, well after transcript levels from other family members had decreased (Figure 3-2). This degree of coordinate regulation was not observed for these selected *CesA* genes under any of the developmental stages or tissues examined *in planta* (Figures 2-10, 2-11, and 2-13). However, their different regulation under these conditions remains consistent with the flexibility observed in vivo for the shifting combinations of expression for members of the *CesA* gene family. The possibility also exists that these *CesAs* may contribute to formation of functional complexes not typically abundant *in planta*.

Expression of *CesAs* During Cell Wall Regeneration Varied with Sucrose Supply

Limiting the concentration of sucrose in protoplast regeneration media changed the expression profiles for *CesA* family members, and also the duration of cell viability (Figure 3-3). Under reduced (0.5% w/v) sucrose, sufficient RNA for analysis could be obtained for 36 hours, but viability was apparently compromised thereafter. The protoplasts may have been unable to form a cell wall, and/or lacked a sufficient energy source. Prior to this point, two distinctive responses were evident among the *CesA* mRNAs. First, transcript levels of *CesA12* fluctuated markedly and independently of the other family members. The basis of this is unknown, but

indicates a clear contrast to the consistent co-regulation of *CesA10, CesA11*, and *CesA12 in planta*. With the exception of *CesA12*, expression of other family members did not increase markedly until 36 hours when mRNA levels of *CesA3, CesA6*, and *CesA10* rose appreciably (Figure 3-3A). Again, these results were unexpected since these genes were not co-expressed *in planta*. It is possible that extreme stress and/or starvation causes co-regulation of specific family members to form CESA complexes with specialized functions. Since these genes were upregulated shortly before loss of detectable mRNAs, the expression of these *CesAs* may have resulted from one or more stress signals and/or been part of a cell-death program. Previous work has provided evidence that programmed cell death is controlled by a signal that concomitantly induces secondary cell wall synthesis (and presumably upregulation of associated genes) (Groover and Jones, 1999).

Similar results were observed during cell wall regeneration in media without sucrose. Under complete starvation, sufficient levels of RNA could not be recovered after 28 hours of cell wall regeneration. Strong upregulation of any *CesA* gene was observed at only 12 hours (Figure 3-3B), which we attribute to duration of cell viability. With the exception of *CesA3*, the identity of the *CesAs* upregulated at 12 hours with 0% sucrose differed from those upregulated at 36 hours under with 0.5% sucrose. This may indicate that the *CesAs* are differentially regulated depending on the availability of nutrients. Also, under both reduced- and no-sucrose conditions, *CesA12* transcript levels varied more often and with greater magnitude than other family members. This may indicate that regulation of this gene is more sensitive to the sugar-status of the environment, and could have a specialized function when carbohydrates become limiting.

Cellulose Synthase Expression in Response to Simulated Wounding/Pathogen Infection

Since cell-wall removal and protoplast formation may involve multiple stresses, we sought to determine the extent of their contribution by testing treatments intended to simulate

exposure to fungal elicitors, wounding, and/or oligosaccharides released from the native wall as a result of pathogen infection. Plants exposed to the aforementioned situations and/or molecules typically undergo a defense response (Cordero et al., 1994; Seifert and Blaukopf, 2010), thus altering gene expression. Transcript levels of all genes increased in the denatured-enzyme treatment, having expression peaks at 2 hours and then rapidly declining (Figure 3-5). Although different treatments had different effects on gene expression of the cellulose synthases and *MPI*, most changes were either modest, transient, or both, indicating that the *CesAs* respond weakly to the treatments applied. Complete removal of the cell wall could have a more severe effect on expression of the *CesAs* than was evident in these cell-culture experiments, since treatments did not include active cell wall-degrading enzymes.

Cellulose Synthase Expression During Induction of Secondary Cell Wall Synthesis

Secondary cell wall deposition was induced when suspension cells were transferred to medium optimal for this purpose in maize. After 10 days of incubation, cells began to differentiate into tracheary-element-like cells (TELs) (Figure 3-6). Direct quantification of differentiated cells was complicated by cell aggregation, but visual quantifications indicated that approximately 20% of cells had become TELs. Transfer to induction media slightly increased mRNA levels of nearly all *CesA*, but by 7 days after transfer (DAT), levels of *CesA10*, *CesA11*, and *CesA12* mRNAs rose strongly (Figure 3-7). This upregulation persisted until 25 DAT, when cells appeared to have entered a stationary phase. Visible differentiation of cells into TELs was not evident until 10 to 14 DAT, but had presumably begun considerably earlier. The strong upregulation of *CesA10*, *CesA11*, and *CesA12* at 7 DAT, followed by a lesser degree of upregulation at subsequent time points, may indicate that transcript and/or protein turnover rates for these genes may be low under the given conditions. In addition, many of the cells capable of differentiating into TELs may have done so relatively early, and subsequently underwent

programmed cell death, as has been previously reported (McCabe and Leaver, 2000; Ohashi-Ito et al., 2010). Considering that the concomitant induction of secondary cell wall synthesis with the increase in transcript levels of *CesA10*, *CesA11*, and *CesA12* is consistent with in-vivo observations indicating that these genes are primarily, although not exclusively, involved in secondary cell wall biosynthesis.

Methods

Generation of the Suspension Cell Line

To initiate a fresh, maize suspension cell line for these experiments, kernels from inbred B104 inbred plants were harvested at 10 to 13 days after pollination and surface sterilized in 3% NaClO for 10 min. Embryos were dissected from the kernel under sterile conditions and those between 1 mm and 2 mm were transferred to 100 x 15 mm petri plates. An N6, callus-initiation medium (pH 5.8) was prepared by combining 4 g/L N6 salts (Chu et al., 1975), 1 mL/L (1000X) N6 vitamin stock, 2 mg/L 2,4-D, 100 mg/L myo-inositol, 2.76 g/L proline, 30 g/L sucrose, 100 mg/L casein hydrolysate, and 2.5 g/L phytagel. Media were autoclaved before adding filter-sterilized (0.2 µm filter) 1 M silver nitrate to a final concentration of 25 µM. Samples were subcultured onto N6 medium as necessary (depending on growth), and Type II, friable calli were selected for additional subcultures. After three months of subculture, Type II, friable calli were transferred to autoclaved liquid regeneration media containing 20 g/L sucrose, 4.4 g/L Murashige & Skoog MS Medium with Vitamins (RPI Corp. Cat# M10400), and 2 mg/L 2,4-D at pH 5.8. Suspension cells were grown in darkness at 25°C in 250-mL flasks with 50 mL medium, agitating at 120 rpm. Cell lines were subcultured (using 10 mL of cells condensed by sedimentation) every 10 days, selecting for cells that formed the smallest aggregates by drawing cells from the top layer after sedimentation. After three months of subculture, approximately

10% of cell lines had become acclimated to the liquid environment. A rapidly dividing cell line that did not form large aggregations was selected for subsequent studies.

Protoplast Isolation, Regeneration, and Characterization

Maize suspension cells derived from B104 embryos were used as the source for generation of protoplasts. Suspension cells (10 DAT) were briefly dried on sterile Whatman paper to remove excess moisture (Schleicher and Schuell CAT# 057145), and 3 g were transferred to sterile Erlenmeyer flasks containing 200 mL (cell wall) digestion media (pH 5.8) containing 1.5% Onazuka RS cellulase (Yakult, Tokyo), 0.3% R-10 Macerozyme (Yakult, Tokyo), 109 g/L mannitol, 1.95 g/L MES, 0.1 g/L calcium chloride, 390 µL β-mercaptoethanol, and 1 g/L BSA. Cells were incubated at 25°C for 8 hours in the dark, shaking at 40 rpm. Protoplasts were released by agitating at 80 rpm for 5 min followed by filtering through 35 µ Nitex nylon mesh (Sefar Prod. Ref. 03-35/16). Protoplasts were collected by centrifugation at 150 x g, retrieving the pellet, and resuspending for washing with regeneration media (described above for suspension cells). This washing process was repeated three times. For subsequent purification, protoplasts were resuspended in 2 mL of 0.6 M mannitol, then layered on 5 mL 0.6 M sucrose in a 10-mL falcon tube. After centrifugation at 225x g for 10 min, floating protoplasts were collected and transferred to regeneration media. The experiments involving cell wall regeneration in "reduced sucrose" or "no sucrose" used the same regeneration media described above for suspension cells, except that only 5 g/L or 0 g/L of sucrose were used instead of 20 g/L. Cell wall regeneration was monitored at 4, 12, 20, 28, 36, 44, and 60 hours after transfer by observation under bright-field and fluorescent microscopes. Samples were also harvested at these time points for qRT-PCR analysis of cellulose synthase mRNA levels. Cellulose deposition was visualized under UV (365 nm) after staining with one drop of calcofluor white (Sigma-Aldrich Prod.# 18909), then adding one drop of 10% potassium hydroxide. Bright field images were

obtained using an RT SPOT camera (Diagnostic Instruments, Sterling Heights, MI) mounted on an Olympus BH2 light microscope, and fluorescent microscopy images were captured with an EvolutionMP camera (Media Cybernetics, Bethesda, MD) mounted on an Olympus BX51 fluorescent microscope.

Simulation of Wounding/Pathogen Infection

Suspension cells (10 DAT) were transferred to three different solutions intended to simulate wounding and/or pathogen infection. Suspension cells (described above) were weighed after blotting to remove excess media, and 1-g samples were transferred to 50 mL of experimental media. Each of these treatments included regeneration media with either 1) boiled cell-wall-degrading enzymes (0.25 g of boiled (5 min) RS cellulase (Yakult, Tokyo) and 0.25 g of boiled (5 min) R-10 macerozyme (Yakult, Tokyo), 2) ground cells (0.5 g of whole cells ground in liquid nitrogen), or 3) cell walls (0.5 g purified cell walls ground in liquid nitrogen). Suspension cells were incubated in darkness at 25°C, shaking at 120 rpm. Samples were harvested at 2, 6, and 12 hours for qRT-PCR analysis. Cell walls were isolated by finely grinding 0.5-g samples of leaf tissue in liquid nitrogen, then adding 9 mL 1% SDS. Samples were then heated to 80°C for 15 min and centrifuged at 3,500 rpm for 5 min. Pellets were washed with 80°C water and recentrifuged a total of three times. Pellets were ground again in 2 mL water before washing three times in 70°C water, three times in 50% ethanol at 70°C, and then three more times in 70°C water.

Induction of Secondary Cell Wall Biosynthesis

Suspension cells (10 DAT) were weighed after briefly blotting away excess moisture, and 1-gram aliquots were transferred to 250-mL flasks with 50 mL of induction media (pH 5.8) containing 20 g/L sucrose, 4.4 g/L Murashige & Skoog MS Medium with Vitamins (RPI Corp. Cat# M10400), 0.2 mg/l 2,4-D, 125 mL 8 µM brassinolide, 1 mg/L BAP(cytokinin), and 10 mL

of 1 M boric acid. Flasks were incubated in darkness at 25°C, shaking at 120 rpm. Samples were harvested at 7, 12, 20 and 25 DAT for qRT-PCR analysis of *CesA* mRNA levels. Images were captured with an RT SPOT camera (Diagnostic Instruments) mounted on an Olympus BH2 light microscope.

Quantitative Real Time RT-PCR

Levels of mRNA were quantified as described in the methods section of chapter 2.

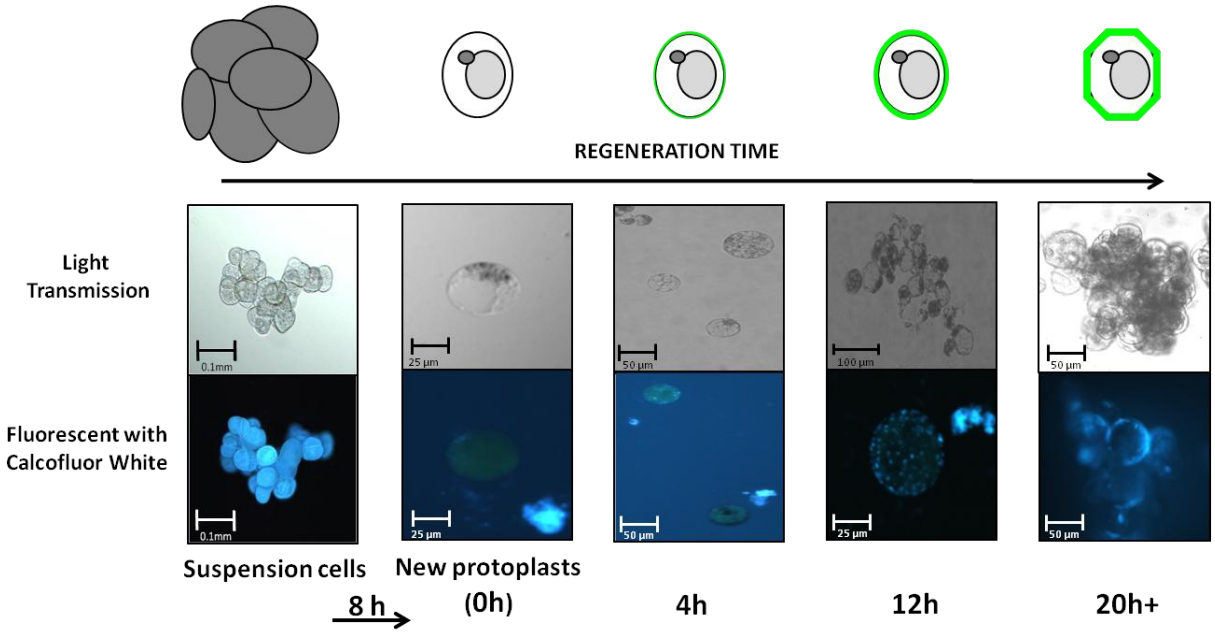

Figure 3-1. Diagram of the protoplast regeneration system. Top; diagram representing the protoplast regeneration system. Grey ovals represent organelles in illustrations corresponding to protoplasts, and cell walls are depicted in green. From left to right; Suspension cells are stripped of their cell walls during 8 h incubation in digestion media; As protoplasts regenerate they begin to stain for cellulose with calcofluor white at 12 h. By 20 h cells assume non-spherical shapes, form aggregations and fluoresce strongly, indicating continued cellulose deposition. Photos by Brent O'Brien.

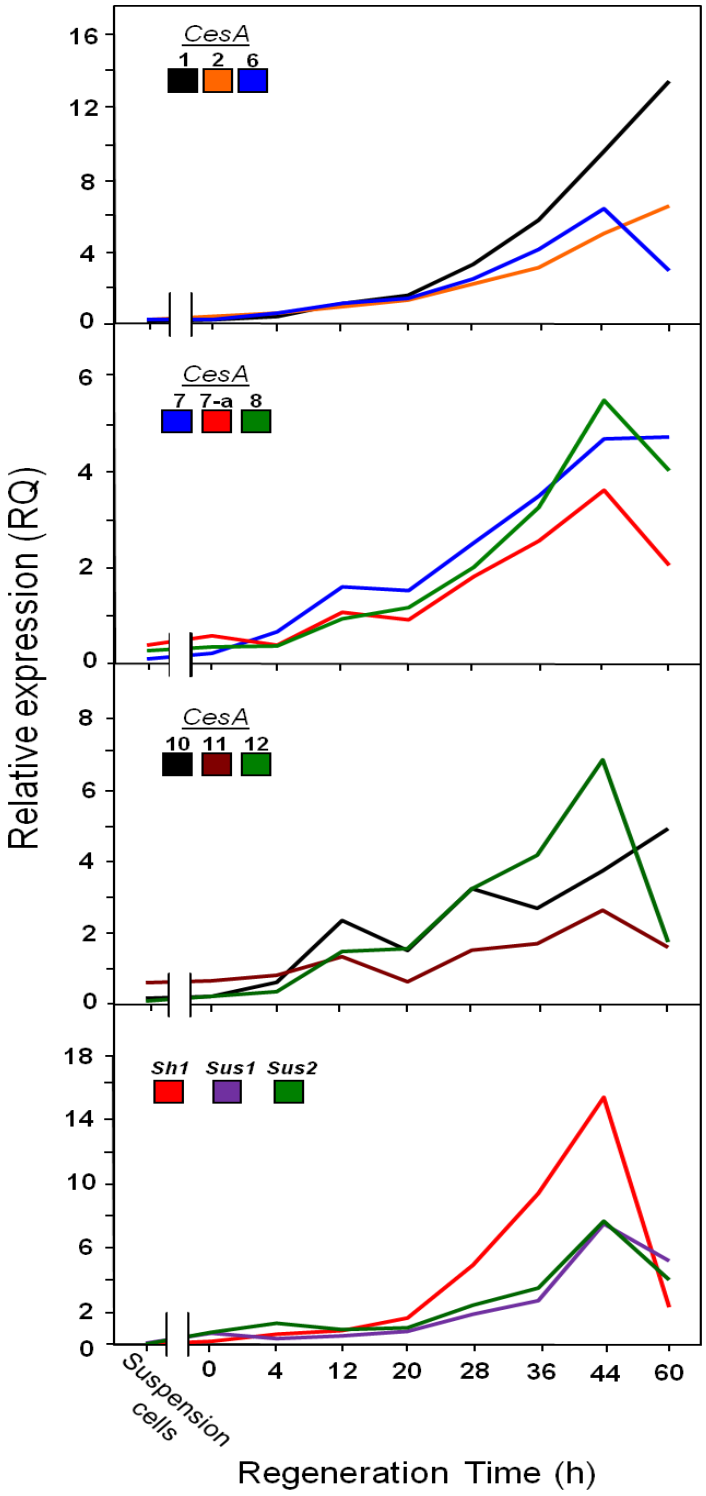

Figure 3-2. Relative expression of select *CesA* family members and sucrose synthases during cell wall regeneration by protoplasts. The x-axis represents time since transfering nacent protoplasts to regeneration media. Suspension cells represent mRNA sampled (from 10-day old cell cultures) immediately before an 8-hour cell wall digestion (indicated by the break). Expression levels are relative to the amount 18SrRNA measured in each tissue.

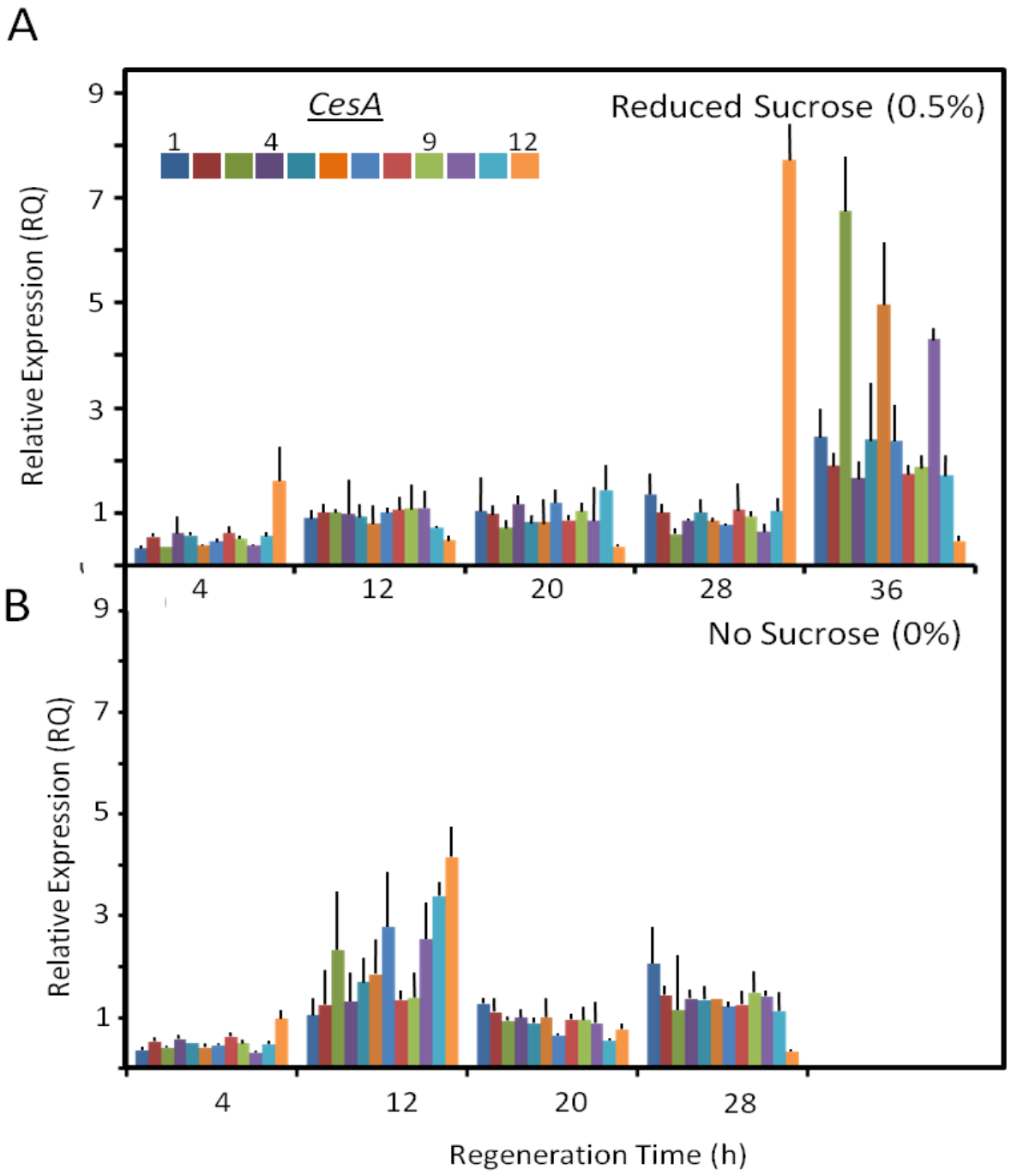

Figure 3-3. Sugar-responsive expression of the *CesA* family during cell wall regeneration by protoplasts. A) Expression in media containing reduced sucrose (0.5% w/v). B) Expression in media without sucrose. Protoplasts were sampled at 8-hour intervals. Expression levels are relative to the amount 18SrRNA measured in each tissue. Data represent three biological replicates.

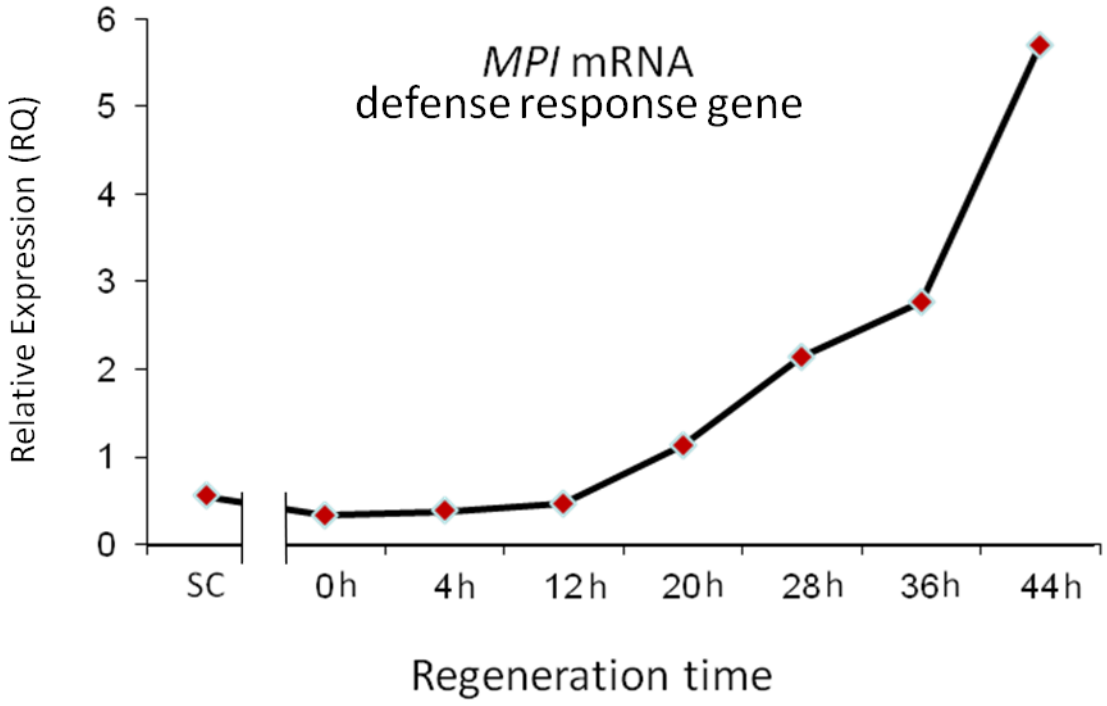

Figure 3-4. Expression of the systemic wound/pathogen response gene *Maize Proteinase Inhibitor* (*MPI*) in suspension cells (SC) and through 44 hours of cell wall regeneration in protoplasts (after an 8-hour digestion). Expression levels are relative to the amount 18SrRNA measured.

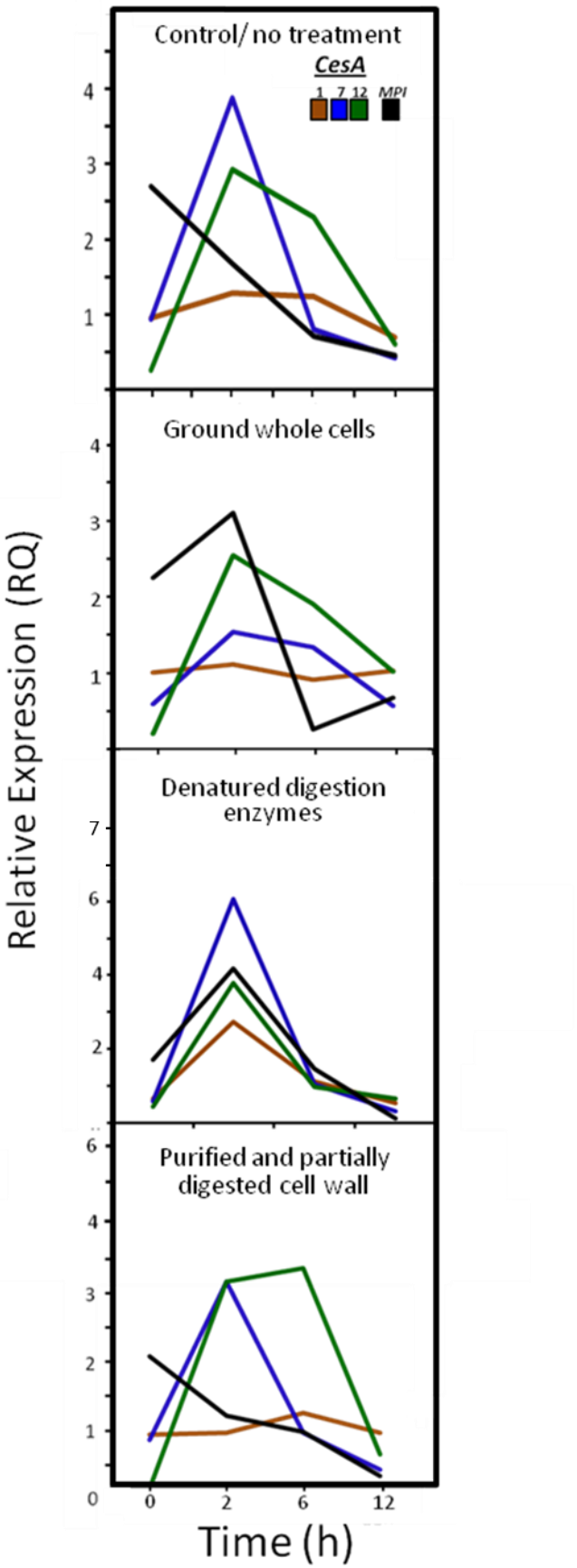
Control/ no treatment
CesA
1 7 12 MPI
Ground whole cells
Denatured digestion enzymes
Purified and partially digested cell wall
Relative Expression (RQ)
Time (h)
0
2
6
12

Figure 3-5. Relative expression of CesA genes and the systemic wound-response gene MPI (Maize Proteinase Inhibitor) in response to simulation of wounding and pathogen infection. The x-axis represents time after transfer of suspension cells (at 7 days after transfer) to fresh regeneration media with the specified treatment.Ground whole cells were intended to mimic mechanical damage whereas denatured digestion enzymes and purified, partially-digested cell wall treatments were intended to simulate pathogen infection. Graphs were not designed for comparison of genes, but to show changes in expression over time for each gene tested. Expression levels are relative to the amount 18SrRNA measured in each tissue. Data represent three biological replicates.

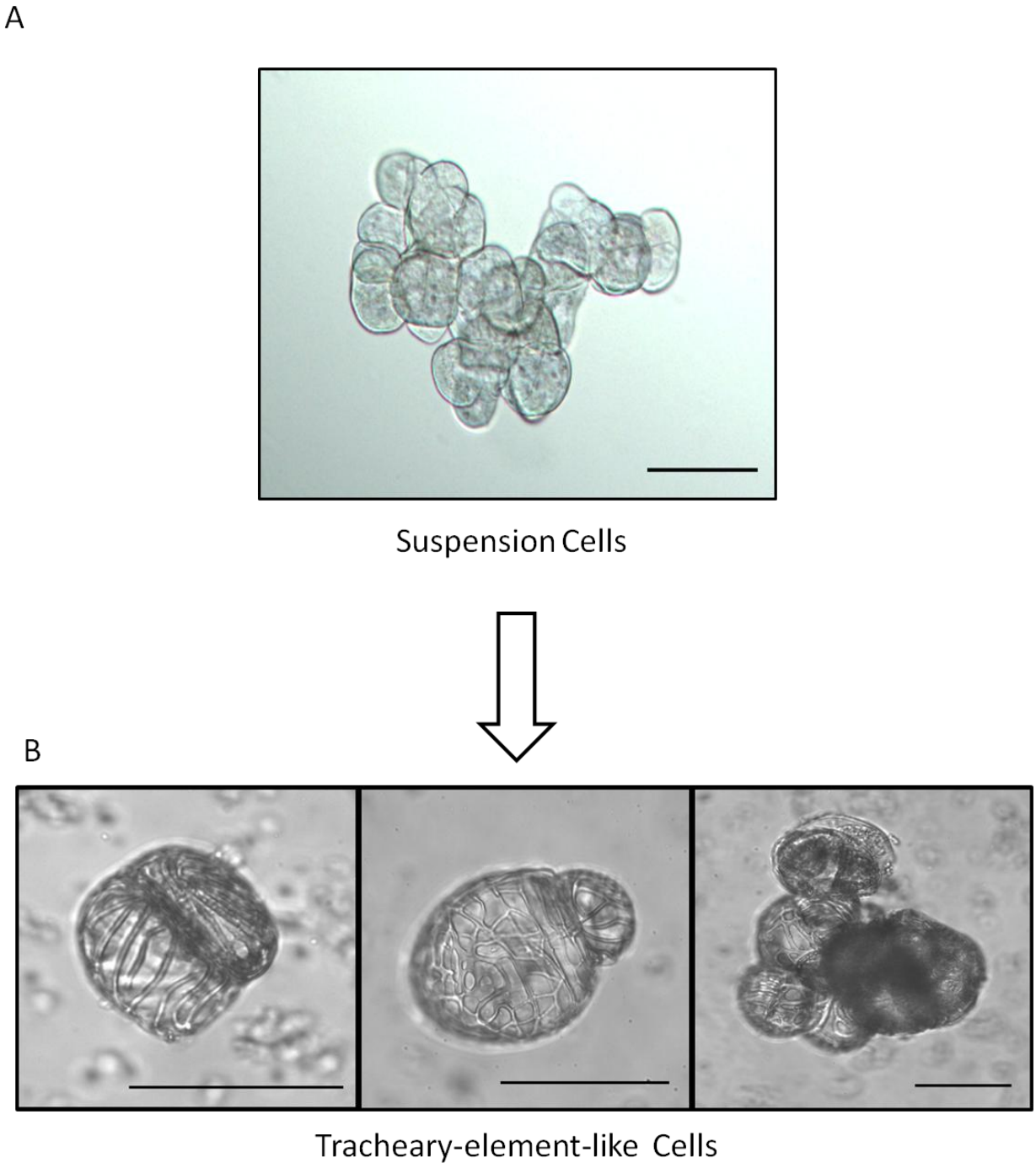

Figure 3-6. Differentiation of suspension cells to tracheary-element like cells after secondary cell wall induction. Maize suspension cells were transferred from regeneration media to either control media or induction media. A) The control group was transferred to normal regeneration media. Scale bar equals 0.15 mm. B) The experimental group was transferred to induction media containing 1% sucrose, 1 µM brassinolide, 10 mM boric acid, 0.1 mg/l 2-4-D, and 0.5 mg/l cytokinin (BAP). Scale bars equal 0.15 mm Photos by Brent O'Brien.

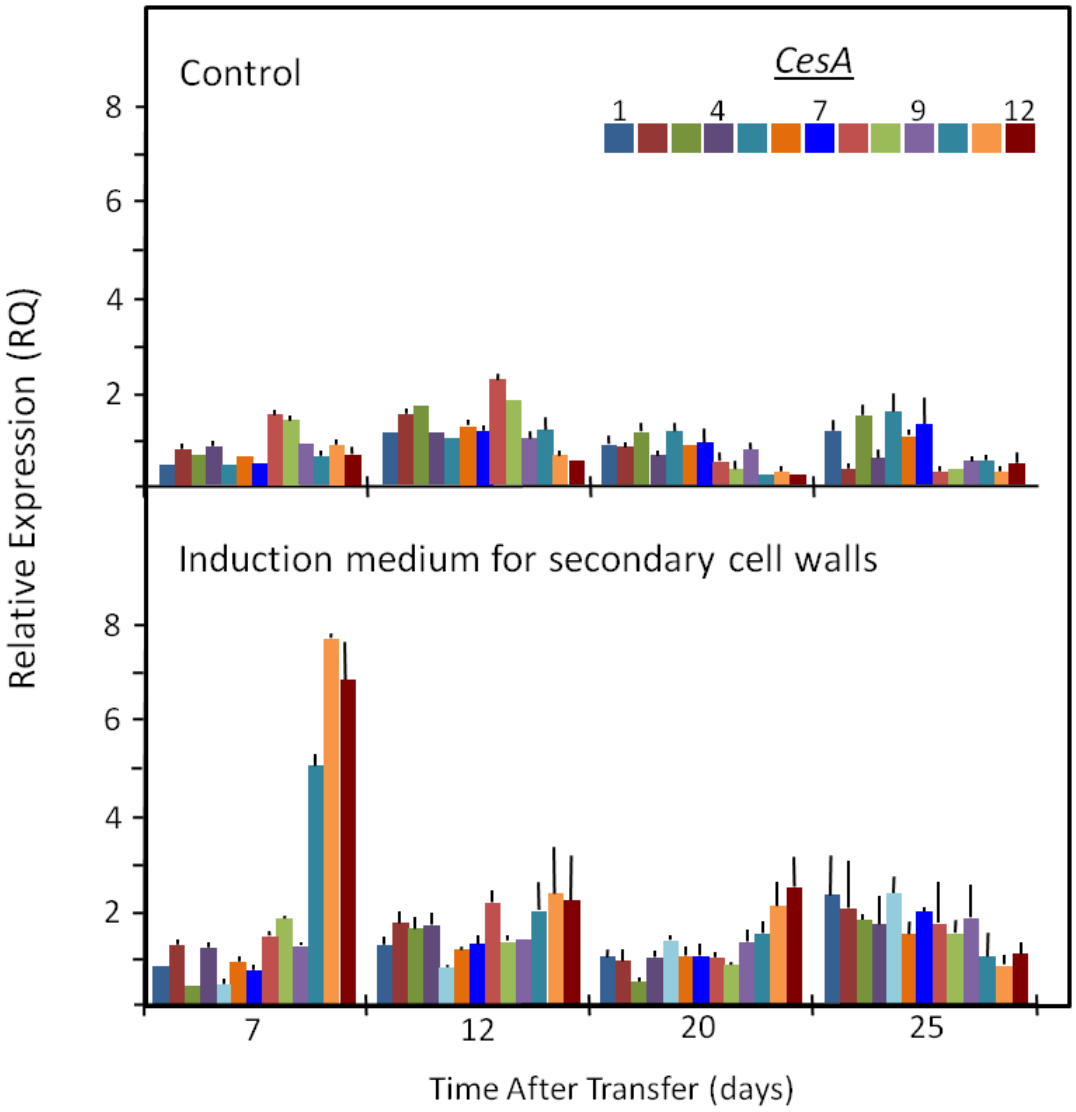

Figure 3-7. Relative expression of *CesA* gene family members during secondary cell wall biosynthesis. Expression of the *CesA* family after maize (embryo-derived B104) suspension cells are transferred to control (untreated) culture medium. In the induction medium (1% sucrose, 1 µM brassinolide, 10 mM boric acid, 0.1 mg/l 2-4-D, and 0.5 mg/l cytokinin [BAP]) expression levels of *CesA10*, *CesA11*, and *CesA12* are highly upregulated relative to the control. Expression levels are relative to the amount 18SrRNA measured in each tissue. Data represent three biological replicates.

CHAPTER 4
CHARACTERIZATION OF MAIZE CESA MUTANTS FROM THE TRANSPOSON-MUTAGENIC UNIFORMMU POPULATION

Background

Transposable elements (TEs), or transposons, are mobile genetic elements of varying size (pieces of DNA or RNA) that have the capacity to move to new sites within the genome. The *Mutator* (*Mu*) class of these elements typically inserts in the coding sequence of genes rather than in the intergenic regions, and thus provide a natural mechanism for mutagenesis. Furthermore, transposable elements can play major roles in genome evolution, because in addition to direct effects of insertion on loss of gene function, transposon action can alter promoters, change intron-exon splice junctions, and modify terminators (Bennetzen, 2000).

Transposons from diverse families (especially retrotransposons) are estimated to make up 85% of the maize genome, and evidence indicates that activity of functional transposon systems is variable in different tissues (Vicient, 2010). Since the discovery of transposons in the 1940's (McClintock, 1947), many types have been characterized, and they can be designated as either class I or class II depending on whether they use RNA (class I) or DNA (class II) as a transposition intermediate (Wicker et al., 2007). Transposons from both classes can also be categorized as either autonomous, which contain sequence that encodes protein(s) necessary to for transposition, or non-autonomous, which contain only the *cis*-elements required for recognition by the transposition protein(s). The transposition protein(s), or transposases, of autonomous elements must be present in a system for non-autonomous elements to transpose.

Many transposons have been well-characterized in maize, particularly because of their usefulness to genetic studies. Especially prominent among them are the *Mu* transposable elements, which include 12 sub-families designated *Mu1* to *Mu12*. These "types" were

designated based on differences between characteristic sequences at their 3′ and 5′ ends. Most transposons are defined, in part, by the presence of terminal inverted repeat (TIR) sequences at both of their ends (Robertson, 1978; Dietrich et al., 2002). Within the *Mu* family, distinctive TIRs are highly conserved, especially within each of the *Mu* subtypes (Brutnell, 2002). The TIRs are roughly 215 bp in length and contain the recognition sequence for the *Mu* transposase (Lisch, 2002; Diao and Lisch, 2007). The vast majority of *Mu* TEs are non-autonomous, but the *Mu9,*or *MuDr*, TEs encode a transposase, and are thus autonomous. In addition to the transposase gene (*MurA*), *Mu9* also includes a *MurB* gene. Although *MurB* function is unknown, transgenic approaches and experiments with deletion derivatives have provided evidence that *MurB* is necessary for *Mu* transposition, possibly aiding stability of transposase function (Walbot and Rudenko, 2002; Diao and Lisch, 2007).

Another characteristic of *Mu* TEs that make them useful in genetic studies is the high rate of forward mutation that they confer. They are more active than any other class-II TE in plants (Brutnell, 2002; Lisch, 2002). Potentially high mutation rates can thus result, depending on the number of autonomous and non-autonomous *Mu's* that are present. In addition, *Mu* elements can insert virtually anywhere in the genome, although evidence indicates a propensity for insertion in the 5′ region of genic sequences (Dietrich et al., 2002; Liu et al., 2009; Vollbrecht et al., 2010). Considering these characteristics, as well as the conservation of *Mu* TIRs, it is not surprising that *Mu* has been the TE family of choice for mutagenesis and transposon tagging research. Such efforts have included the Trait Utility System for Corn (TUSC) developed by Pioneer Hi-Bred Int. (Meeley and Briggs, 1995; McCarty and Meeley, 2009), the Maize-Targeted Mutagenisis (MTM) population developed at Cold Springs Harbor (May et al., 2003), Stanford University's RescueMu project (Walbot, 2000; Raizada et al., 2001), the, the University of Oregon's

Photosynthetic *Mu*'s resource (Williams-Carrier et al., 2010), and the University of Florida's UniformMu population (McCarty et al., 2005; Settles et al., 2007).

The UniformMu maize population was created by introgressing an active *Mu* line called Robertson's Mutator into the maize inbred, W22 (McCarty et al., 2005). Robertson's Mutator is a highly mutagenic line containing a *bz-mum9* color marker. Kernels with the *bz-mum9* gene, in the absence of MuDR, are bronze, whereas W22 kernels are dark purple. When MuDR is present with *bz-mum9*, kernels are bronze with varying amounts of small purple spots. Having this selectable marker provides a convenient, visible means of determining whether a specific line contains an active MuDR. This is important because in the absence of a functional MuDR, mutations in a line will be stable and their effects can be readily studied. Also, any (non-somatic) mutations in this family will be heritable (Chomet et al., 1991). For this reason, bronze kernels are chosen to allow selection for both mutagenic and stable lines in each new generation of the UniformMu population. A key issue has been the exclusion of non-heritable somatic mutations in the database of mutations contained within any given line. Maintenance of the UniformMu population also includes backcrossing new lines to the W22 inbred. This ensures a steady-state mutagenesis, prevents build-up of ancestral mutations, and maintains a uniform background (McCarty et al., 2005).

Sites of *Mu* insertions, which allow identification and mapping of mutations within the UniformMu population, were originally determined by sequencing clones generated through thermal asymmetric interlaced (TAIL) PCR. This method used primers designed to anneal to the conserved TIRs, coupled with arbitrary, degenerate primers to amplify sequences flanking insertions (McCarty et al., 2005). This method was successful in identifying numerous insertion sites, but it did not capture all insertions caused by *Mu*. The basis of this was unclear, but adaptation of next-generation sequencing methods for *Mu*-flanks has proven effective.

Sequencing platforms such as 454 (long read) (Margulies et al., 2005), and Illumina (Illumina Inc., San Diego CA) have since been used, and have provided higher-throughput as well as greater coverage of insertion sites. Methods are currently being refined for additional sub-groups of *Mu's* that had not been previously recognized (C. Hunter, unpublished data).

The defining features of the UniformMu maize population are 1) high mutation frequencies, 2) low mutant load, 3) a selectable color marker for MuDR transposase activity, 4) moderate total *Mu* TE copy number, 5) a database of pedigreed insertions, and 6) a uniform background in plant material (McCarty et al., 2005). The uniform background has been especially valuable in that it provides uniform controls for comparative analyses of newly-generated mutants. Here, we utilized the UniformMu population to characterize mutations in the cellulose synthase gene family (*CesAs*). We employed a reverse genetics approach in which the identity of a disrupted gene is known, and analysis of resulting mutant plants allows the functional role of this gene to be addressed. Forward genetics was also used to determine the causal mutations for lines having phenotypes possibly based on defective cell wall biosynthesis. Results thus far have not associated these phenotypes with known genes, but their study is ongoing (Appendix A).

Results

Reverse Genetics and the UniformMu *CesAs*. To date there are no reports of phenotypes arising from mutations of *CesA* genes in maize. To address the question of whether maize *CesA* mutants can cause a visible phenotype, we searched the UniformMu population for lines carrying insertions in or near *CesA* genes. In total, 16 alleles were analyzed, as well as a double mutant of *CesA7* and *CesA7-a* (Table 4-1). The only family members in which no insertions have yet been identified were *CesA1, CesA3,* and *CesA5*. If mutations in these genes condition a male-lethal phenotype (i.e. defective pollen and/or pollen tube), the absence of associated insertions in the

UniformMu population can be explained by the strategy used for generating and maintaining (UniformMu) lines, where pollen from mutagenic parents was applied to W22 females. In most other instances there were two alleles available and examined for each family member, although *CesA7-a*, *CesA10*, and *CesA11* were represented by a single family member each (Table 4-1). The location of insertions included exons (5′ to 3′), introns, and 5'UTRs. At least 30 plants were examined from lines carrying each of these *CesA* insertions. Plants were grown under field conditions at the UF Plant Science Research Unit (Citra, FL) during spring and fall planting seasons beginning in spring 2008, and continuing through fall 2011. New mutants were acquired during the course of this period and each was added to ongoing investigations.

Phenotypic analyses were focused using two overall criteria. First, for a given *CesA* mutant, we looked at the plant tissues and developmental stages where maximum expression was observed for the *CesA* in wild-type plants, our hypothesis being that loss-of-function mutants would show visible phenotypes at these locations (Table 4-2). Second, we watched for responses similar to those observed in other species (mainly *Arabidopsis* and rice) if any loss-of-function mutations had been identified in similar *CesAs* (Figure 4-1). Ultimately, no visible phenotypes were clearly associated with any of these mutants. However, a recently-obtained *cesA11* line segregated for a phenotype that has been previously described by Postlethwait and Nelson (1957). Characteristics of this mutant are similar to the *brittle culm* mutants of rice and include; severely reduced biomass, brittle stalk and leaf tissue, delayed development, and chronically wilted leaf tips (Figure 4-2). Preliminary PCR genotyping has indicated that these plants are heterozygous for *cesA11*, but this result may be due to the maize genome having two, identical copies of this gene.

Discussion

Reverse genetics and the UniformMu *CesAs*. The lack of visible phenotypes associated with the 16 *Mu* insertions in maize *CesA*s examined thus far may be due to several factors. First, the extent of gene duplications in the maize genome, and especially *the CesA* family, may buffer the species from severe consequences of otherwise deleterious mutations. Paralogs, or even more distantly related family members, may be functionally redundant, in which case multiple null mutants might need to be created before a visible phenotype is apparent. This is a strong possibility, considering a similar situation has been observed with the *Arabidopsis CesAs* (Desprez et al., 2007). The lack of phenotype observed here for maize *cesA12* mutants, and complexities associated with co-segregational analysis of *cesA11*, may both be due to the presence of nearly identical paralogs. Such paralogs may compensate to varying degrees for the loss-of-function mutation. The high degree of sequence similarity also poses considerable challenges to determinations of when one of the genes is potentially "knocked out".

Another possible explanation for the lack of phenotype in certain lines could be the location of insertions. Transposons residing in introns may simply be spliced out of the gene without causing any disruption, particularly if the *Mu* insertion is not a large one. In addition, insertions in the 5′ untranslated region can sometimes only partially disrupt transcription, resulting in "leaky" genes that may still function sufficiently, and therefore do not condition a phenotype. In several instances, no heritable homozygous insertions could be obtained for the alleles examined, which could be due to wild-type copies of near-identical paralogs, or lethality of the homozygous state, as was observed for some alleles in *Arabidopsis* (*AtcesA1*, *AtcesA3*). Considering that *CesA* mutants in other species are recessive, the possibility exists that maize phenotypes may be evident in those homozygous mutants not yet accessible at the time of the present study.

Although we are unable to determine (through PCR) if *cesA11* is the causal insertion for the mutants segregating in that line, similarity of the mutant phenotype to *brittle culm* mutants in rice indicates that *cesA11* is a good candidate. In addition, three of the brittle culm mutants result from disruption of the rice *CesAs* (*OsCesA4*, *OsCesA7,* and *OsCesA9*) involved in secondary wall synthesis (Tanaka et al., 2003), one of which (*OsCesA4*) is homologous to *ZmCesA11*. Phenotypic characteristics shared between *brittle culm* mutants and those in the *cesA11* line include severely reduced biomass, and brittle stem and leaf tissue. In addition, the mutants segregating in the *cesA11* line examined here had chronically wilted leaf tips. If *cesA11* is the causal mutation, wilting may be a result of irregular xylem preventing adequate water transport. This hypothesis seems reasonable considering that maize is a panicoid, C4 grass with a larger architecture, more rapid growth rate, and a higher rate of transpiration than rice. Considering that the maize genome contains two, identical copies of *CesA11* (both from the Maize I genome), additional approaches will be needed for future work, including restriction-enzyme digestion followed by Southern blotting, quantification of *CesA11* mRNAs in mutants, and possible re-sequencing of selected BAC regions will be necessary to determine the relationship between the two *CesA11s*, and whether one of them is associated with the mutant phenotype.

Mutations in any of the secondary-wall-associated *CesAs* in *Arabidopsis* also lead to reduced biomass and irregular xylem formation. Other phenotypic features of *CesA* mutations in *Arabidopsis CesAs* that could emerge in maize homologs include 1) the embryo lethality and radial root swelling (that occurs under high temperature) in *AtcesA1,* 2) defective pollen formation in both *AtcesA1* and *AtcesA3*, and reduced root elongation in *AtcesA6* (Figure 4-1). The other *Arabidopsis CesAs* are functionally redundant, with phenotypes arising only in double or triple mutants. This scenario is likely to apply to maize as well, and may explain the lack of phenotypes in several of the mutants reported here.

Methods

Plant Material

All mutant lines were obtained from the UniformMu population at the University of Florida. Plants were grown under field conditions at the UF Plant Science Research Unit (Citra, FL) during spring and fall planting seasons beginning in spring 2008, and continuing through fall 2011. Lines have been, or are in the process of being backcrossed to W22 to separate the mutation and/or phenotype of interest from other insertions within a given line. Map locations of insertion sites associated with the *CesAs* were determined by aligning flanking sequences to gene models through the MaizeGDB website (maizegdb.org).

Genotyping

Presence of insertions in lines potentially harboring *CesA* mutants was determined by PCR, using primers that target the TIR sequences of *Mu* transposons in combination with forward- and reverse-orientated, gene-specific primers.

Table 4-1. Cellulose synthase mutants identified in the UniformMu population for reverse genetics screening.

	Homozygous mutation (+/-)	Phenotype (+/-)	Allele/s	Insertion location
CesA2	+	-	mu1005736	exon
	+	-	mu1015515	5'utr
CesA4	+	-	mu1016007	exon
	+	-	mu1041689	intron
CesA6	-	?	mu1040612	5'utr
	+	-	mu1037352	intron
CesA7	+	-	mu1016043	exon
CesA7-a	+	-	454AC190931	exon
CesA7xCesA7-a	+	-	mu1016043	exon
	+	-	454AC190931	exon
CesA8	+	-	mu1011353	5'utr
	-	?	mu1039702	exon
CesA9	+	-	mu 1019324	intron
	-	?	mu1031574	5'utr
CesA10	-	?	mu00193	exon
CesA11	-	+/?	mu1007966	5'utr
CesA12	-	?	mu1039500	intron
	-	?	mu1041598	5'utr

At least 30 plants were grown and characterized from each of the segregating families carrying a given insertion. Material was grown to maturity at the UF-Plant Research Unit (Citra, FL) and examined closely for visible phenotypes. Presence of the insertions was confirmed by PCR with TIR-specific and gene-specific primers, as was the zygosity of insertions. In lines heterozygous for the *Mu*-insertion, the possibility of a mutant phenotype could not be determined. Lines that clearly do not have a phenotype are highlighted.

Table 4-2. Sites of maximum expression for the maize CesAs at each developmental stage.

Gene	Seedling Maximum Expression	Vegetative Maximum Expression	Anthesis Maximum Expression
CesA1	Coleoptile	Stem	Developing prop root
CesA2	Coleoptile	Stem	Developing prop root
CesA3	Coleoptile	Stem	Ligule and midrib
CesA4	Coleoptile	Stem	Husk and developing prop root
CesA5	Coleoptile	Stem	Lat. root initiation zone
CesA6	Coleoptile	Stem	Husk, developing prop root, and cob
CesA7	Primary root	Stem	Husk and cob
CesA7-a	Primary root	Stem	Husk and developing prop root
CesA8	Coleoptile	Stem, node, and root	Developing prop root
CesA9	Coleoptile and primary root	Stem	Developing prop root
CesA10	Primary root	Stem	Mature prop root, husk, and stem
CesA11	Primary root	Stem	Mature prop root, husk, and stem
CesA12	Primary root	Stem	Mature prop root, husk, and stem

Sites of maximum expression were focused on when appraising mutants for phenotypes.

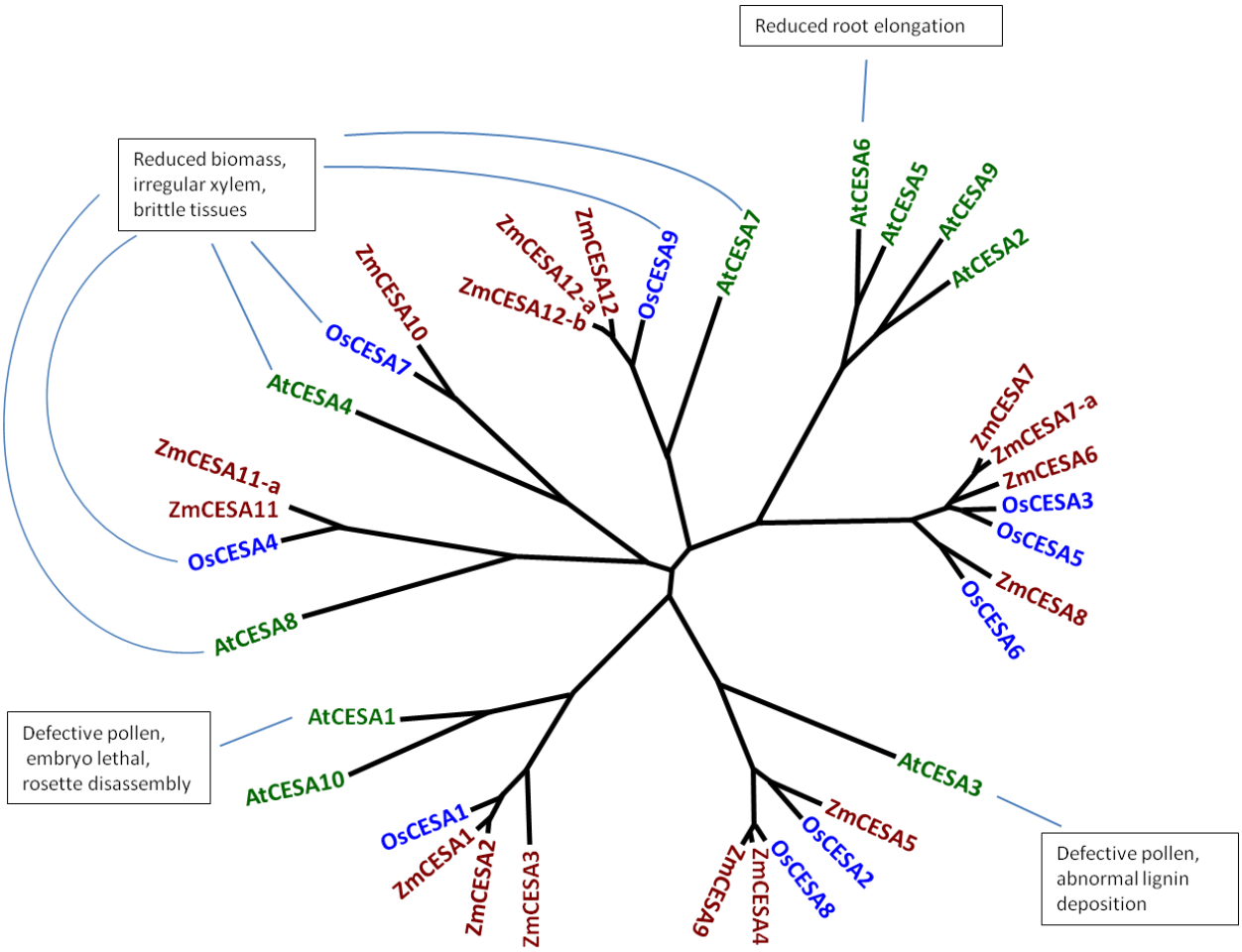

Figure 4-1. Unrooted, neighbor-joining, interspecies phylogenetic tree with descriptions of *cesA* mutant phenotypes. Related cellulose synthases from maize (red), rice (blue), and *Arabidopsis* (green) are represented by six clades, with four *Arabidopsis* genes forming a sub-clade. Phenotypes of characterized *cesA* mutants are described in the boxes. The *radial swelling 1-1*, *isoxaben resistant-1*, and *procuste*, mutants are represented by *AtcesA1*, *AtcesA3*, and *AtcesA6*, respectively. The tree was constructed using pairwise deletion with 1,000 bootstrap replications in a MEGA4 analysis.

Figure 4-2. The mutant phenotype possibly associated with *CesA11*. Mutants are phenotypically identical to the *wilty1* mutant described in 1957 by Nelson and Postlethwait, having chronically wilted leaves, reduced biomass (relative to the wild type), and brittle tissues.

CHAPTER 5
SUMMARY AND FUTURE DIRECTIONS

A two-fold rationale motivated this investigation of the evolution and regulation of genes for cellulose biosynthesis in maize (*Zea mays* L.). The first was the importance of cellulose to both plant biology and human needs. The prominence of cellulose in the cell wall of virtually every plant cell is fundamental to the strength and architecture of plants, and also makes cellulose the most abundant polymer on earth. As such, its uses by humankind has extended from food and fiber, to the rapidly increasing demand for bio-fuels. Recent research has thus focused intensely on the genetics, and regulation of cellulose formation, yet this area has remained notoriously challenging and complex (Taylor et al., 2003 and 2008; Tanaka et al., 2003, Persson et al., 2007; Burton et al., 2010; Fujii et al., 2010). The second motivation was that maize provides not only a valuable model for the grain- and grass-type cell wall, but also constitutes the largest single crop in the nation and world. Here we 1) investigate the structure and evolution of the maize *CesA* gene family, 2) analyze *CesA* expression *in planta* and use suspension-cell and protoplast systems to test responses to experimental perturbations, and 3) characterize *cesA* mutants in maize.

Bioinformatic analyses included the identification of four, previously-undescribed *CesA* paralogs. This indicated that the maize *CesA* family may be more functionally redundant than that in many other species, possibly leading to enhanced expression. In addition (or alternatively), the prevalence of paralogs could also increase the robustness of the maize *CesAs* by allowing subfunctionalization of duplicated genes. We also show that the maize *CesAs* group into six distinct subclades, consistent with phylogenetic analyses of *CesAs* from other plant species (Carrol and Specht, 2011). These subclades can be further divided, with three containing primary wall-associated *CesAs*, and three having members that are predominantly involved in

secondary cell wall synthesis. This division of subclades may reflect the necessity for three different CesAs to be present for assembly of functional CESA complexes, regardless of whether these complexes are associated with primary or secondary wall synthesis (Taylor et al, 2003; Persson et al, 2007).

Our results also show that at least one, each unique *CesA* gene maps to chromosomal regions previously determined to predominate in gene retention. Conversely, genomic segments associated with enhanced gene degradation contain only *CesAs* that are paralogs. These observations are consistent with a recent hypothesis (Schnable et al., 2011) proposing that after a genome duplication event (such as occurred in maize), one "copy" of the genome will be more resistant to gene degradation. The mechanisms behind this observed bias in gene retention remain unclear, however some form of epigenetic labeling of one genome copy is likely. We also observed that one paralog was retained from each of the subclades associated with primary cell wall synthesis, and expression analysis of these paralagous pairs showed there was little or no subfunctionalization. These results are consistent with the Gene Balance hypothesis proposed by Birchler and Veitia (2010) that suggests gene retention and loss will be constrained by the stoichiometry of isoforms in multi-subunit complexes where this balance affects the function of the whole. It thus follows that if essential members from each of these subclades were duplicated, then essential paralogs from each subclade would be retained due to the selective advantage of preserving the balance of potentially interacting isoforms required for proper CESA complex assembly.

In-planta analyses revealed a high level of coordinate expression among members of the maize *CesA* gene family. However, clusters of coordinately-expressed genes varied in different tissues and at different stages of development. Three groups of family members that clustered together based on similarity of overall expression profiles, indicated a co-regulation of genes that

contributed to cellulose synthesis at a given developmental stage. Clustering analysis showed that *CesA10*, *CesA11*, and *CesA12*, were the only family members to exclusively and consistently group together based on expression pattern. In addition, this group of genes invariably showed the tightest correlation among any family members tested, and they were most highly expressed in tissues undergoing secondary cell wall biosynthesis. Furthermore, when suspension cells were induced to differentiate into (secondary wall-rich) tracheary-element-like cells, only these genes were highly upregulated relative to untreated controls. Together these data indicate that *CesA10*, *CesA11*, and *CesA12* function predominantly in secondary cell wall deposition, supporting the subdivision of *CesA* clades.

Expression patterns of diverse maize *CesAs* during cell wall regeneration by protoplasts generally followed comparable trends, maintaining relatively high mRNA levels that peaked at 44 h. Unexpectedly, three family members that did not appear to be co-regulated *in planta* had similar profiles during wall regeneration, indicating that atypical clustering modules are possible under extreme conditions. Additionally, the responses of *CesA* gene family members during wall regeneration with little (0.5%) to no sucrose, further supported plasticity in the co-expression modules observed for the *CesA* genes. Also, transcript levels of *CesA10*, *CesA11*, and *CesA12* were comparable to other family members even though protoplasts do not form secondary cell walls. These results could be explained by two scenarios. First, protoplasts may initially form abnormal cell walls that are not "secondary" in nature but require participation of *CesA10*, *CesA11*, and *CesA12*. Second, removal of cell walls could elicit stress and/or defense responses, which in turn induce *CesA10*, *CesA11*, and *CesA12*.

To investigate how altering normal *CesA* expression affects plant morphology and development, a reverse genetics approach was used. Homozygous mutations in seven primary-wall-associated maize *CesAs*, and one double-mutant did not show a readily visible

phenotype. This may have been due to the prevalence of paralogs in the maize genome, which would add to the high level of functional redundancy reported for some of the primary wall-*CesAs* in *Arabidopsis* (Burton et al., 2004; Persson et al, 2007). In addition, four of the alleles tested contained insertions in the 5'UTR region or an intron, possibly leaving gene function at least partially intact in some of these instances.

Overall, research described here has shown that groups of *CesA* gene family members are co-expressed, with subgroups being fine-tuned to perform specific functions at different developmental stages. Also, the evolution and structure of the *CesA* family indicates that duplications of certain *CesAs* associated with primary-wall synthesis were retained without subfunctionalization, and this proliferation of *CesA* family members in maize is reflected by the high level of functional redundancy observed in *cesA* mutants lacking a visible phenotype.

Work presented here, together with the genetic lines and molecular materials developed during this research, will provide a valuable foundation for future studies. These future directions can range from short- to long-term objectives as follows.

First, combinations of double and even triple mutants can be generated from primary-wall-associated *cesA* mutants produced during these studies. Such materials would provide a means to determine which of the *CesA* family members were functionally redundant.

Second, further analysis of single and double mutants generated here may also be productive. Lines having homozygous insertions in *CesAs* associated with secondary-wall formation have yet to show a clear association with a mutant phenotype in maize, however we have observed a phenotype showing Mendelian segregation in a line carrying an insertion in *CesA11*. Although we have validated the presence of a *cesA11*-insertion, the identical *CesA11* paralogs appear to have prevented accurate genotyping of segregating families by obscuring the presence of homozygous mutants. The nature of the phenotype is promising, however, with

characteristics similar to homologous mutations in rice and *Arabidopsis* (Taylor et al., 2003; Tanaka et al., 2003). These shared features include severely reduced biomass, brittle tissues, and stunted development. In addition, the maize mutant also has chronically wilted leaves, which would be an expected result of reduced water transport accompanying malformed xylem tissue. A phenotypically similar mutant with abnormal xylem structure was observed in the maize *wilty1* mutant (Postlethwait and Nelson, 1957), however *wilty1* does not map near either of the *Cesa11* locales. Future work will require alternate approaches to determine if the *cesA11* mutation is indeed causal for the wilty phenotype observed. These approaches would include back-crossing the mutant line to the W22 inbred (recently completed) to reduce numbers of other possible mutations segregating in subsequent F-2 progeny (in progress). Another approach will be to quantify *cesA11* mRNA levels of the mutant relative to a wild type sibling to determine if there is a correlation between reduced *cesA11* expression and the mutant phenotype. Finally, restriction enzyme digestion followed by Southern blot analysis can be used to determine if there is a Mu insertion in either of the *cesA11s.* If successful, this work will test the hypothesis that the role of a maize *CesA11* is essential to secondary cell wall formation and stalk integrity, as well as showing that regulation of the *CesAs* extends beyond the identical coding and upstream sequence of these two genes.

Third, future work can further develop the forward genetics approach initially taken to identify genes with critical roles in cell wall biosynthesis by prioritizing lines based on relevant phenotypes. Three lines were selected that had readily visible phenotypes as well as insertion/s in genes that could affect cell wall biosynthesis. These lines were named *shredded* (for its shredded leaves) (Figures A-1 and A2), *flecked* (for its anomalous leaf pigmentation), and *epuf1* (for a kernel phenotype that results when the fruit wall (pericarp) is left empty-looking by minimal development of the single seed within it) (Figure A3). We have yet to identify the causal genes

for these phenotypes through conventional PCR, however high-throughput sequencing technology has provided an alternative approach. Future efforts can effectively use Illumina-based sequencing to identify *Mu* insertions in mutants and wild-type siblings from each line. Flanking sequences from wild-type siblings can be subtracted (*in-silico*) from those of mutants, thus providing a list of potential candidate genes. Association of these candidates with the mutant phenotype of interest will then need to be validated by PCR and co-segregational analysis. If causal genes for any of these three mutants can be identified, then essential roles can be ascribed to their sequences, and further defined by more in-depth analysis of their phenotypes.

Longer-term directions that would be facilitated by this work include testing functional associations between isoforms that may form complexes as indicated by co-expression modules revealed here. Such work would likely require concomitant expression of maize *CesAs* in either an orthologous system, or in a plant system containing an inducible mechanism to silence expression of its own *CesA* family members. In addition, the Gene Balance hypothesis, which we suggest may be governing the retention of specific *CesA* paralogs, can be tested by transforming maize with additional *CesA* "copies" to see if changes in cellulose synthesis and deposition result.

APPENDIX A
FORWARD GENETICS ANALYSIS OF THREE MAIZE MUTANTS

Forward Genetics

Mutants with phenotypes possibly caused by defective cell wall biosynthetic genes were selected from segregating lines in the UniformMu population for further investigation using a forward genetics approach. Lines segregating for mutant phenotypes were identified in the field or from ears after harvest, and prioritized for further analysis depending on whether they contained insertions in cell-wall-associated genes. Lines selected include a *shredded* line (05S-2500), identified by Don McCarty, a *flecked* line (11S-2015), identified by Brent O'Brien, and an *empty-pericarp-UF-1* (*epuf1*) line (09S-3300), identified by Karen Koch and initially characterized by Stephanie Marunich and Gregorio Hueros. The *shredded* line was named for its shredded leaves, the *flecked* line was named for its anomalous leaf pigmentation, and the *epuf1* line for a kernel phenotype that results when the fruit wall (pericarp) is left empty-looking by minimal development of the single seed within it. These mutant phenotypes were characterized to an initial level, and mutant sequences within them were tested for potential causality. The candidate insertions were identified by in-silico subtraction of ancestral insertions from the total of those identified in parental lines.

Characterization of the *shredded* Mutant

The *shredded* phenotype was selected for analysis because the characteristic lesions that formed between major vascular bundles and eventually caused separation of tissue seemed likely to add insights into cell wall synthesis.

These lesions extended to varying lengths along the longitudinal axis of a leaf, parallel to the midrib (Figure A-1). Leaves of *shredded* mutants thus had alternating vertical stripes of normal and affected tissue that were separated by vascular bundles (Figure A-2). Affected tissue progressed through three stages. First, previously-unaffected, green tissue became chlorotic, then lost all color, turning white and eventually translucent (Figures A-1 and A-2). At the second stage of lesion formation, cell shape, cell size, and cell organization became abnormal (Figure A-2B), and affected vertical stripes showed wave-like undulations (Figure 4-2A). In addition, aberrant stomatal distribution, as well as underdeveloped stomata were observed (Figure A-2B). At the third stage of lesion formation, cells within the affected tissue separated, usually parting along a single vertical axis in a given region, opening splits in the leaf that ranged from a few centimeters long to the full length of the leaf blade. Leaves were often split severely enough to justify the name "shredded" (Figure A-2A).

When these leaves were stained with acetocarmine for contrast, unaffected areas stained pink and had a normal distribution of vascular bundles, whereas first-stage lesion tissue did not take up the stain and had a reduced number of vascular bundles (Figure A-2C). Also, boundaries between normal and lesion tissues were clearly defined by vascular bundles (Figures A-2B and C). Other characteristics of the *shredded* mutant included a reduced plant size relative to WT (Figure A-1), and variable intensity of the phenotype that appeared dependent on environmental conditions.

Families segregating for the shredded phenotype were genotyped to test for co-segregation with Mu insertions in genes considered best candidates for causal mutations (17

genes with *Mu* insertions were tested), but co-segregation analyses did not identify a causal insertion among these. This mutant has been further back-crossed to the W22 inbred, and is being tested for presence of other *Mu* insertions not identified by earlier methods.

The phenotype of the *shredded* mutant raised several questions about the developmental progression of stripe-type lesions and the demarcation of boundaries between affected and unaffected tissues. The observation that cell size and shape were aberrant in affected tissue, indicates that the lesion phenotype probably results from defects in cell division and expansion that arise early in leaf development. This hypothesis is supported by the observation that cells in affected tissue can be either smaller or larger than normal cells in unaffected, neighboring tissue, and that the cell files of affected tissue are highly disorganized (Figure A-2B). Additionally, distribution and development of stomata in pre-lesion tissue was atypical, with fewer total stomata per unit area and several stomata being severely underdeveloped.

Another interesting feature of *shredded* plants is that the borders between lesion tissue and normal tissue were defined by the large vascular bundles. This may indicate that the defective, early development of lesion tissue is the result of some mobile signal that does not pass readily beyond the larger vascular bundles that delimit a given region (Figures A-2B and C). Another possibility is that the sugar status of affected tissues is responsible for abnormal development. The lack of minor vascular bundles and apparent degradation or incomplete formation of large vascular bundles in pre-lesion tissue (Figure A-2C) raises the question of whether the bundles failed to form, or formed correctly and were subsequently degraded. Alternatively, the stain used to show contrast between normal tissue and affected tissue may not have moved effectively into pre-lesion tissue, thus giving a false-negative result for the presence of vascular bundles.

The causal insertion for this mutation has yet to be identified, and may be more readily accessed by methods currently under development. Initially, insertions in this line were identified by a TAIL PCR method, which identifies less than a full complement of insertions. A high-throughput sequencing approach can now be used, although this too is PCR-based and thus potentially sensitive to amplification biases that could favor some flanking sequences at the expense of others.

Characterization of the *bz*-linked *flecked* Mutant

The *flecked* mutant was selected for analysis because several aspects of its phenotype suggested cell-wall physiology might be altered. Its short stature is typical of mutants such as those in *CesA* mutants of rice and *Arabidopsis* (Tanaka et al., 2003; Taylor et al., 2003). Cell wall components can also affect development of lesions such as those seen here. Aside from growing to only half the size of WT plants, the *flecked* mutant is also characterized by slightly yellowish, drab-olive colored leaves with a dull appearance on the adaxial side. As mutants matured, numerous, small (0.5-1 mm) yellow spots developed on the leaves, similar to the phenotypes of lesion-mimic mutants, but without the clearly defined lesion boundaries. Additionally, varying degrees of male sterility were evident in *flecked* plants. At anthesis, visible appearance of anthers indicated that they were fully developed, but collapsed, and also devoid of pollen.

In addition, genetic analysis of the *flecked* mutant indicated that the causal gene was linked to the *bz* color marker. Plants growing from bronze and purple kernels of a single ear from a self pollinated *flecked* parent showed a 100% correspondence between bronze kernels and the *flecked* phenotype (25 plants tested, 5 bronze). Thus far, genotyping and co-segregation analysis

of candidate insertions has yet to identify the causal gene. However, candidate genes remain to be tested including those for a calmodulin-binding protein (GRMZM2G429807), and an MSF (mitochondrial stimulation factor)–type transporter (GRMZM2G104942). In addition, linkage of this mutation to the *Bz* gene should facilitate future analyses.

The *flecked* mutant is particularly interesting because it is one of the few mutations to come out of the UniformMu population that is known to be linked to the *bz* color marker locus. This is a relatively recent observation that will facilitate our search for the causal gene by allowing us eliminate candidates that are not on chromosome 9, or are too distant from the *bz* locus to be in linkage.

Characterization of the *empty-pericarp-uf-1* (*epuf1*) Mutant (line 09S-3300)

The *epuf1* mutant was selected because empty pericarp (ep) phenotypes often have underdeveloped and/or aborted kernel tissues, which in turn may arise from defects in cell wall formation.

As the name implies, *epuf1* had kernels with empty-appearing pericarps that, in this case, did not expand to full size. Also, instead of being completely "empty", these pericarps surrounded an underdeveloped endosperm and apparently intact aleurone (Figure A-3A). Presence and location of starch in the *epuf1* endosperm was determined by staining with Lugol's solution. As in WT kernels, the *epuf1* endosperm stained deep purple, indicating the presence of abundant starch. A major difference was observed in starch distribution of the mutant relative to WT (Figure A-3B), with proportionately less starch in the basal area of the *epuf1* endosperm (Figure A-3B).

Embryo formation was also affected in the *epuf1* mutant, however the severity of defective embryo development was variable. Kernels were stained with acetocarmine for contrast in cell type since the small cells of the embryo are more resistant to uptake of stain than the endosperm and surrounding tissues. Results showed a clearly defined embryo in WT kernels, whereas mutant kernels had severely-reduced embryos or completely lacked visibly-detectable embryos (Figure A-3C). The causal insertion for this mutant has yet to be identified through genotyping for candidate genes and co-segregational analysis.

Identification of Mu-Flanking Sequence Tags

Sequences flanking Mu insertion were identified by the UniformMu group as described by Settles et al. (Settles et al., 2004; 2007).

Acetocarmine and Lugol's Solution staining of the *shredded* and *empty-pericarp-uf-1* mutants

Acetocarmine solution (1%) was prepared by dissolving 10 g carmine (Fisher CAT# C579-25) in 100 mL glacial acetic acid. Boileezers (Fischer Scientific, Fair Lawn, NJ) were added, and the solution was refluxed for 24 h. Tissues were stained by submerging in 1% acetocarmine solution for 2 to 3 min, then rinsing with water. Lugol's solution was prepared by dissolving 10 g potassium iodide in 100 mL of water, then adding 5 g iodine crystals and mixing until dissolved. Samples were stained by immersing in Lugol's solution for 2 min then rinsing with water. Images were captured with an RT SPOT camera (Diagnostic Instruments) mounted on a Leica MZ 12-5 dissection microscope or an Olympus BH2 light microscope.

Figure A-1. The maize *shredded* mutant 05S-2500 under field conditions. Visible phenotypic features of the *shredded* mutant include longitudinal strips of tissue that turn chlorotic and "rippled" before splitting between vascular bundles (left), and small plant stature with lighter green leaves than the wild type (right). Wild type plants are visible in the adjacent row. Photos by Brent O'Brien.

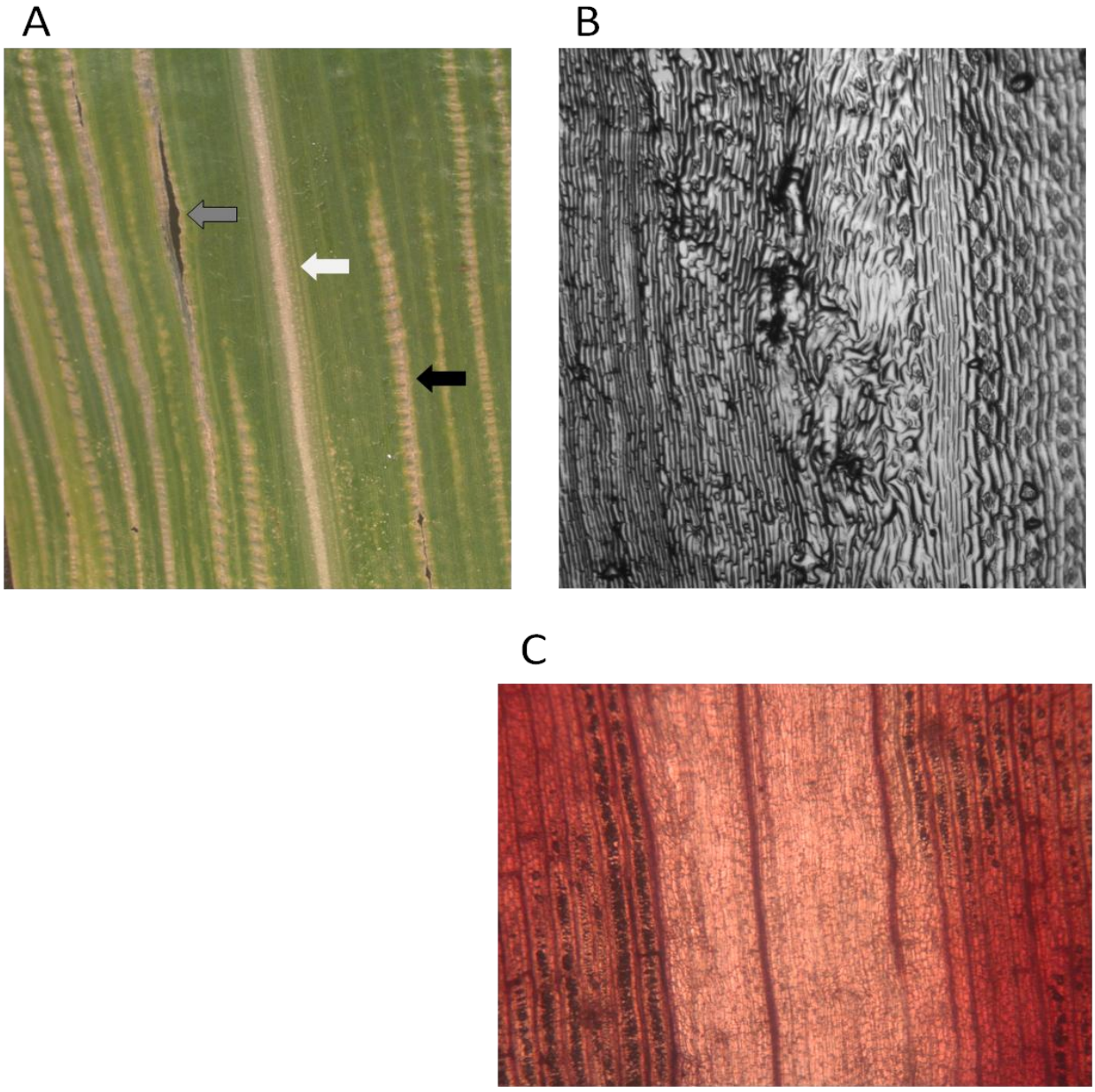

Figure A-2. The *shredded* phenotype. A) The three stages of the *shredded* leaf phenotype viewed under a dissection microscope. Longitudinal strips between major vascular bundles first became chlorotic, eventually turning white and translucent (white arrow). Affected tissue then formed undulations and "ripples" (black arrow) before tissue finally separated (grey arrow). B) Cyano-acrylate impression of the boundary between affected and unaffected leaf tissue. Cell files and stomatal distribution appeared normal (right side of B), however tissue to the left of the vascular bundle showed aberrant cell shape, size, and arrangement, with disorganized cell-files and under-developed stomata. C) A portion of leaf stained with acetocarmine for contrast. Affected (white) and unaffected (red) areas were clearly defined, with absence and/or deterioration of vascular bundles in chlorotic zones. Photos by Brent O'Brien.

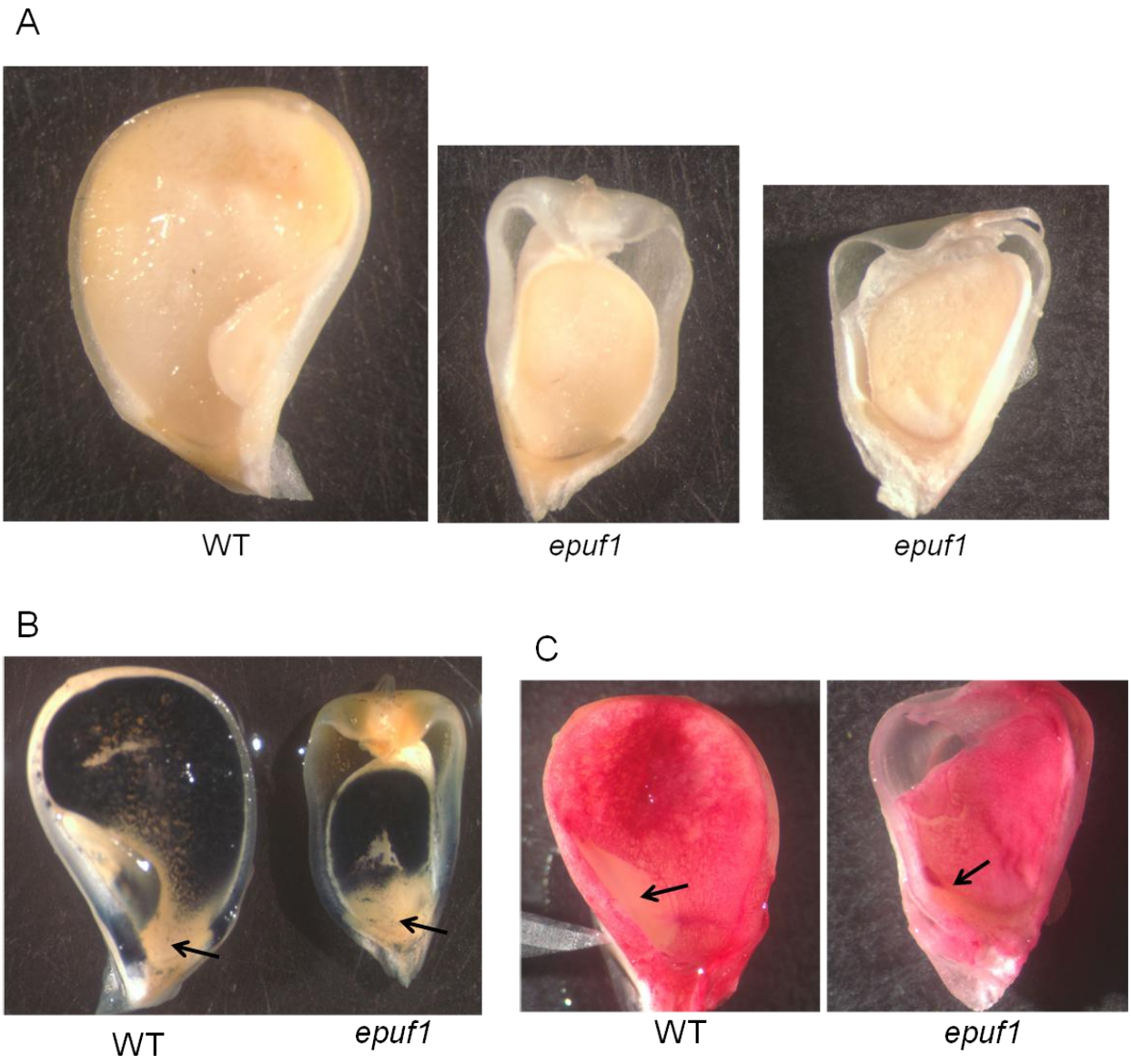

Figure A-3. Characteristics of the *empty pericarp-UF* (*epuf1*) mutant line 09S-3300. A) Longitudinal sections of WT and *epuf1* kernels at 20 days after pollination. The mutant phenotype was characterized by small kernels, and underdeveloped endosperm surrounded by expanded pericarp. B) Wild type and *epuf1* kernels stained for starch with Lugol's solution. Both kernels produced starch in the endosperm, however the (starchless) basal endosperm in the mutant comprised a greater portion of the whole relative to WT (arrows). C) Mutant and WT kernels stained with acetocarmine for contrast. Embryo tissue can be seen in the WT as a prominent area of unstained tissue (arrow), however *epuf1* kernels had either an underdeveloped or aborted embryo as shown (arrow), or no visible embryo. Photos by Brent O'Brien.

APPENDIX B
SEQUENCES OF GENE-SPECIFIC PRIMERS USED FOR QRTPCR ANALYSIS

Table B-1. Sequence of primers used for qRTPCR analysis.

Primer	Sequence
RTCESA1 F	GCCTCGTCGGTGTTGGTGT
RTCESA1 R	CTC CCA CCG AGA CGG CT
RTCESA2 F	GCCTCGTCGGTGTCGGT
RTCESA2 R	CAT CTC CGC GCT CCT CCT A
RTCESA3 F	TAGTGCCTGTTTCATGTTGACTGTCGT
RTCESA3 R	GTT ACA TCA CGA CAG TCC AGA GCC
RTCESA4 F	ATACCCAGACGTGTGGCATCAACT
RTCESA4 R	CACG TGG TAT TCC TCC GTT TCT ACA AAG
RTCESA5 F	AGCGAGCTCCACCACTTGC
RTCESA5 R	AGG CAG AAG CAG AGG CAG C
RTCESA6 F	GATCTTCTCGCTGCTTTGGGTCC
RTCESA6 R	CAG GGG ACC ATC ATC CTT CGC
RTCESA7-F	CGG TCT GTG GCC GAC TC
RTCESA7-R	CCA CGG CCG TAG CTC ATG T
RTCESA7 Paralog-F	ATG TGC ATC TGC CAG TGG AAC AGA
RTCESA7 Paralog-R	TTC CTA GTA TAG ACG AAC ATG TAA TGA AGT TTG T
RTCESA8 F	GCTGTAGATAGAAACCACATGTCCACGG
RTCESA8 R	GGC ACC TCT CTC CTG CTC C
RTCESA9 F	GAAACAGAGAGATACCACGAATGTGCCG
RTCESA9 R	ACG CCA CCT GCC TAT ATA ACT TAC TAA CAG
RTCESA10 F	CGTTTGGACATACAGGCACTTTTGGG
RTCESA10 R	GAG TGA ATT CCA TCA CAG TTC TTA CAC CC
RTCESA11 F	ATCTCGCATCTGGGCTTTTGCC
RTCESA11 R	CCG AAT TTT AAC ATT TCA GGT TTC ACC ACC A
RTCESA12 F	TCAGGCAGTGTGGCATCAATTGC
RTCESA12 R	CCG ACA ATT CTG GGT ACC ATA ACA TTA CAG AC
RT-MPI F	TAG CCG CTA TTT CCT TTC CTT GCC
RT-MPI R	TGA GAA TTC ACA CAT CCA TTA TTC GGC ATG C

LIST OF REFERENCES

Abedon, B.G., Hatfield, R.D., and Tracy, W.F. (2006). Cell wall composition in juvenile and adult leaves of maize (*Zea mays* L.) J. Agric Food Chem **54:** 3896–3900.

Albrecht, G., and Mustroph, A. (2003). Localization of sucrose synthase in wheat roots: increased in situ activity of sucrose synthase correlates with cell wall thickening by cellulose deposition under hypoxia. Planta **217:** 252–260.

Altschul, S.F., Gish, W., Miller, W., Myers, E.W., and Lipman, D.J.(1990). Basic local alignment search tool. J. Mol. Biol. **215:** 403-10.

Amano, Y., and Kanda, T. (2002). New insights into cellulose degradation by cellulases and related enzymes. Trends Glycosci. Glycotechnol. **14:** 27–34.

Amor, Y., Haigler, C.H., Johnson, S., Wainscott, M., and Delmer, D.P. (1995).A membrane associated form of sucrose synthase and its potential role in synthesis of cellulose and callose in plants. Proc. Natl Acad. Sci. USA **92:** 9353-9357.

Andrew Carroll, A., and Specht, C.D. (2011). Understanding plant cellulose synthases through a comprehensive investigation of the cellulose synthase family sequences. Front. Plant Sci. **2:** doi:10.3389/fpls.2011.00005

Appenzeller, L., Doblin, M., Barreiro, R., Wang, H.Y., Niu, X.M., Kollipara, K., Carrigan, L., Tomes, D., Chapman, M., and Dhugga, K.S., (2004). Cellulose synthesis in maize: isolation and expression analysis of the cellulose synthase (*CesA*) gene family. Cellulose. **11:** 287-299.

Arioli, T. et al. (1998). Molecular analysis of cellulose biosynthesis in *Arabidopsis*. Science **279**: 717–720.

Atalla, R. H. and VanderHart, D. L. (1989). Studies on the structure of cellulose using Raman spectroscopy and solid state 13C NMR. Cellulose Wood Chem. Tech. 169-188.

Aziz, A., Gauthier, A., Bezier, A., Poinssot, B., Joubert, J.M., Pugin, A., Heyraud, A., and Baillieul, F. (2007). Elicitor and resistance-inducing activities of beta-1,4 cellodextrins in grapevine, comparison with beta-1,3 glucans and alpha-1,4 oligogalacturonides. J. Exp. Bot. **58:** 1463–1472.

Bacic, A. (2006). Breaking an impasse in pectin biosynthesis. Proc. Natl. Acad. Sci. **103:** 5639-5640.

Bacic, A., and Stone, B.A. (1981). Chemistry and organization of aleurone cell wall components from wheat and barley. Aust. J. Plant Physiol. **8:** 475–495.

Beeckman, T., Przemeck, G.K.H., Stamatiou, G., Lau, R., Terryn, N., De Rycke. R., Inze, D., and Berleth, T. (2002). Genetic complexity of cellulose synthase a gene function in *Arabidopsis* embryogenesis. Plant Physiol. **130**: 1883–1893.

Bennetzen, J.L. (2000). Transposable element contributions to plant genome evolution. Plant Mol. Biol. **42:** 251-269.

Bessueille, L., Sindt, N., Guichardant, M., Djerbi, S., Teeri, T.T., and Bulone, V. (2009). Plasma membrane microdomains from hybrid aspen cells are involved in cell wall polysaccharide biosynthesis. Biochem. J. **420:** 93-103.

Betancur, L., Singh, B., Rapp, R.A., Wendel, J.F., Marks, M.D., Roberts, A.W., and Haigler, C.H. (2010). Phylogenetically distinct cellulose synthase genes support secondary wall thickening in *Arabidopsis* shoot trichomes and cotton fiber. J. Integrative Plant Biol. **52:** 205-220.

Bewley, J.D. (1997). Breaking down the walls: a role for endo-ß-mannanase in release from seed dormancy. Trends Plant Sci. **2:** 464-469.

Birchler, J.A., and Veitia, R.A. (2010). The Gene Balance Hypothesis: implications for gene regulation, quantitative traits and evolution. New Phytol. **186:** 54–62.

Blaschek, W., Haass, D., Koehler, H., and Franz, G. (1981). Cell wall regeneration by *Nicotiana tabacum* protoplasts: chemical and biochemical aspects. Plant Sci. Lett. **22:** 47 -57.

Boerjan, W., Ralph, J., and Baucher, M. (2003). Lignin biosynthesis. Ann. Rev. Plant. Biol. **54:** 519-546.

Bouton, S., Leboeuf, E., Mouille, G., Leydecker, M. T., Talbotec, J., Granier, F., Lahaye, M., Höfte, H., and Truong, H.-N. (2002). *QUASIMODO1* encodes a putative membrane-bound glycosyltransferase required for normal pectin synthesis and cell adhesion in *Arabidopsis*. Plant Cell **14:** 2577–2590.

Bradley, D.J., Kjellbom, P., and Lamb, C.J. (1992). Elicitor- and wound-induced oxidative cross-linking of a proline-rich plant cell wall protein: A novel, rapid defense response. Cell **70:** 21-30.

Brett, CT. (2000). Cellulose microfibrils in plants: biosynthesis, deposition and integration into the cell wall. Int. Rev. Cyt. **199**: 161–199.

Briggs, C. L. (1996). An ultrastructural study of the embryo/endosperm interface in the developing seeds of *Solanum nigrum* L. zygote to mid torpedo stage. Ann. Bot. **78**, 295-304.

Brown, R. M., and Saxena, I. M. (2000). Cellulose biosynthesis: A model for understanding the assembly of biopolymers. Plant Physiol. Biochem. **38:** 57-67.

Brown, R.M. Jr. (2004). Cellulose structure and biosynthesis: what is in store for the 21st century? J. Polymer Sci. Part A: Polymer Chem. **42**: 487–495.

Bruneau, A.H., and Qu, R. (2010). Tissue culture-induced morphological somaclonal variation in St. Augustinegrass [*Stenotaphrum secundatum* (Walt.) Kuntze]. Plant Breeding **129:** 96-99.

Brutnell, T.P. (2002). Transposon tagging in maize. Funct. Integr. Genom. **2:** 4-12.

Burn, J.E., Hocart, C.H., Birch, R.J., Cork, A.C., and Williamson RE. (2002). Functional analysis of the cellulose synthase genes *CesA1*, *CesA2*, and *CesA3* in *Arabidopsis*. Plant Physiol. **129**, 797–807.

Burton, R. A., Shirley, N. J., King, B. J., Harvey, A. J., and Fincher, G. B. (2004). The *CesA* gene family of barley. Quantitative analysis of transcripts reveals two groups of coexpressed genes. Plant Physiol. **134:** 224-236.

Burton, R.A., Farrokhi, N., Bacic, A., and Fincher, G.B. (2005). Plant cell wall polysaccharide biosynthesis: real progress in the identification of participating genes. Planta **221:** 309-312.

Burton, R.A., Wilson, S.M., Hrmova, M., Harvey, A.J., and Shirley, N.J., Medhurst, A., Stone, B.A., Newbigin, E.J., Bacic, A., and Fincher, G.B. (2006). Cellulose Synthase-Like *CslF* genes mediate the synthesis of cell wall (1,3;1,4)-ß-D-Glucans. Science **311:** 1940–1942.

Burton, R.A., Ma, G., Baumann, U., Harvey, A.J., and Shirley, N.J. et al. (2010). A customized gene expression microarray reveals that the brittle stem phenotype *fs2* of barley Is attributable to a retroelement in the *HvCesA4* cellulose synthase gene. Plant Phys. **153:** 1716–1728.

Campbell, J.A., Davies, G.J., Bulone, V., and Henrissat, B. (1997). A classification of nucleotide-diphospho-sugar glycosyltransferases based on amino acid sequence similarities. Biochem J. **326:** 929–939.

Cano-Delgado, A., Penfield, S., Smith, C., Catley, and M., Bevan, M. (2003). Reduced cellulose synthesis invokes lignification and defense responses in *Arabidopsis thaliana*. Plant J. **34**: 351–362.

Cantatore, J.L., **Murphy, S.M.**, **and Lynch, D.V.** Compartmentation and topology of glucosylceramide synthesis. Biochem. Soc. Trans. **28:** 748-750.

Carpita, N.C. (1984). Fractionation of hemicelluloses from maize cell walls with increasing concentrations of alkali. Phytochem. **23:** 1089–1093.

Carpita, N.C. (1986). Incorporation of proline and aromatic amino acids into cell walls of maize coleoptiles. Plant Physiol. **80:** 660–666.

Carpita, N.C. (1996). Structure and biogenesis of the cell walls of grasses. Ann. Rev. Plant Physiol. Plant Molec. Biol. **47:** 445-476.

Carpita, N.C., and Gibeaut, D.M. (1993). Structural models of primary cell walls in flowering plants: consistency of molecular structure with the physical properties of the walls during growth. Plant J. **3:** 1-30.

Cavez, D., Hachez, C., and Chaumont, F. (2009). Maize black Mexican sweet suspension cultured cells are a convenient tool for studying aquaporin activity and regulation. Plant Signal Behav. **4:** 890–892.

Chen, K., and Rajewsky, N. (2007). The evolution of gene regulation by transcription factors and microRNAs. Nat. Rev. Genet. **8:** 93-103.

Chen, L.M., Carpita, N.C., Reiter, W.D., Wilson, R.W., Jeffries, C., and McCann, M.C. (1998). A rapid method to screen for cell wall mutants using discriminant analysis of Fourier transform infrared spectra. Plant J. **8:** 375-382.

Chen, S.L., Ehrhardt, D.W., and Somerville, C.R. (2010). Mutations of cellulose synthase (CESA1) phosphorylation sites modulate anisotropic cell expansion and bidirectional mobility of cellulose synthase. Proc. Natl. Acad. Sci. USA **107:** 17188-17193.

Chomet, P., Lisch, D., Hardeman, D.J., Chandler, V.L., and Freeling, M. (1991). Identification of a regulatory transposon that controls the *Mutator* transposable element system in maize. Genetics **129**: 261-270.

Chourey, P.S., Chen, Y.C., and Miller, M.E. (1991). Early cell degeneration in developing endosperm is unique to the shrunken mutation in maize. Maydica **36:** 141-146.

Chu, C.C., et al. (1975). Establishment of an efficient medium for anther culture of rice through comparative experiments on the nitrogen sources. Sci. Sinica **18:** 659-668.

Cocuron, J.C., Lerouxel, O., Drakakaki, G., Alonso, A.P., Leipman, A.H., Keegstra, K., Raikhek, N., and Wilkerson, C.G. (2007). A gene from the cellulose synthase-like C family encodes a β-1,4 glucan synthase. Proc. Natl. Acad. Sci. **104:** 8550-8555.

Cordero, M.J., Raventós, D., and San Segundo, B. (1994). Expression of a maize proteinase inhibitor gene is induced in response to wounding and fungal infection: systemic wound-response of a monocot gene. Plant J. **6:** 141–150.

Cosgrove, D.J. (1999). Enzymes and other agents that enhance cell wall extensibility. Ann. Rev. Plant Physiol. Plant Mol. Biol. **50:** 391–417.

Cosgrove, D.J. (2003). Expansion of the plant cell wall. The Plant Cell Wall (JKC Rose ed). 237-263.

Delmer, D.P., and Amor, Y. (1995). Cellulose biosynthesis. Plant Cell **7:** 987–1000.

Delmer, D. P. (1999). Cellulose biosynthesis: exciting times for a difficult field of study. Annu. Rev. Plant Physiol. Plant Mol. Biol. **50:** 245–276.

Desprez, T., Juraniec, M., Crowel,l E.F., Jouy, H., Pochylova, Z., Parcy., **F., Hofte, H., Gonneau, M., and Vernhettes, S.** (2007). Organization of cellulose synthase complexes involved in primary cell wall synthesis in *Arabidopsis thaliana*. Proc. Natl. Acad. Sci. USA **104:** 15572–15577.

Dhugga, K. S. (2001). Building the wall: genes and enzyme complexes for polysaccharide synthases. Curr. Opin. Plant Biol. **4:** 488-493.

Dhugga, K. S. (2005). Plant Golgi cell wall synthesis: From genes to enzyme activities. Proc. Natl. Acad. Sci. USA **102:** 1815-1816.

Diao, X.M., and Lisch, D. (2006). *Mutator* transposon in maize and MULEs in the plant genome. Acta Genetica Sinica **33:** 477-487.

Dietrich, C.R., Cui, F., Packila, M.L., Li, J., Ashlock, D.A., Nikolau, B.J., and Schnable, P.S. (2002). Maize *Mu* transposons are targeted to the 5` untranslated region of the *gl8* gene and sequences flanking Mu target-site duplications exhibit nonrandom nucleotide composition throughout the genome. Genetics **160:** 697-716.

Ding, S.Y., and Himmel, M.E. (2006). The maize primary cell wall microfibril: A new model derived from direct visualization. J. Agric. Food Chem. **54:** 597–606.

Doblin, M.S., Durek, I., Jacob-Wild, D., and Delmer, D. P. (2002). Cellulose biosynthesis in plants: from genes to rosettes. Plant Cell Physiol. **43:** 1407-1420.

Dubois, M., Gilles, D.A., Hamilton, J.K., Rebers, P.A., and Smith, F. (1956). Colorimetric method for the determination of sugars and related substances. Anal. Chem. **28:** 350-356.

Edwards, G.E., Lilley, R.M., Craig, S., and Hatch, M.D. (1979). Isolation of intact and functional chloroplasts from mesophyll and bundle sheath protoplasts of the C4 plant *Panicum miliaceum*. Plant Physiol. **63:** 821-827.

Elbein, A.D., Forsee, W.T., Shultz, J.C., and Laine, R.A. (1975). Biosynthesis and structure of glycosyl diglycerides, steryl glucosides, and acylated steryl glucosides. Lipids. **10**: 427-436.

Endo, S., Pesquet, E., Yamaguchi, M., Tashiro, G., Sato, M., Toyooka, M., Nishikubo, N., Udagawa-Motose, M., Kubo, M., Fukuda, H., and Demura, T. (2009). Identifying new components participating in the secondary cell wall formation of vessel elements in *Zinnia* and *Arabidopsis.* Plant Cell **21**: 1155-1165.

Engels, F. M., and Jung, H. G. (1998). Alfalfa stem tissues: Cell-wall development and lignification. Ann. Bot. **82:** 561-568.

Faik, A., Price, N.F., Raikhel, N.V., and Keegstra, K. (2002). Arabidopsis gene encoding an α-xylosyltransferase involved in xyloglucan biosynthesis. Proc. Natl. Acad. Sci. **99:** 7797-7802.

Falconer, M.M., and Seagull, R.W. (1985). Immunofluorescent and calcofluor white staining of developing tracheary elements in *Zinnia elegans* L. suspension cultures. Protoplasma **125:** 190-198.

Farrokhi, N., Burton, R.A., Brownfield, L., Hrmova, M., and Wilson, S.M., Bacic, A, and Fincher, G.B. (2006). Plant cell wall biosynthesis: genetic, biochemical and functional genomics approaches to the identification of key genes. Plant Biotech. J. **4:** 145-167.

Fincher, G.B. (2009). Revolutionary times in our understanding of cell wall biosynthesis and remodeling in the grasses. Plant Physiol. **149:** 27-37.

Fleischer, A., Titel, C., and Ehwald, R. (1998). The boron requirement and cell wall properties of growing and stationary suspension-cultured *Chenopodium album L*. cells. Plant Physiol. **117:** 1401–1410.

Fowler, J.E., and Quatrano, R.S. (1997). Plant cell morphogenesis: Plasma membrane interactions with the cytoskeleton and cell wall. Annu. Rev. Cell Dev. Biol. **13:** 697–743.

Freshour, G., Clay, R.P., Fuller, M.S., Albershein, P., Darvill, A.G., and Hahn, M.C. (1996). Developmental and tissue-specific structural alterations of the cell-wall polysaccharides of *Arabidopsis thaliana* roots**.** Plant Physiol. **110:** 1413–1429.

Frost, D.J., Read, S.M., Drake, R.R., Haley, B.E., and Wasserman, B.P. (1990). Identification of the UDP-glucose-binding polypeptide of callose synthase from *Beta vulgaris* L. by photoaffinity labeling with 5-azido- UDP-glucose. J. Biol. Chem. **265:** 2162-2167.

Fry S.C. (2004). Primary cell wall metabolism: tracking the careers of wall polymers in living plant cells. New physiol. **161:** 641-675.

Fujii, S., Hayashi, T., and Mizuno, K. (2010). Sucrose synthase is an integral component of the cellulose synthesis machinery. Plant Cell Physiol **51:** 294-301.

Fukuda, H. (1997). Tracheary element differentiation. Plant Cell **9:** 1147–1156.

Galletti, R., De Lorenzo, G., and Ferrari, S. (2009). Host-derived signals activate plant innate immunity. Plant Signal Behav. **4:** 33–34.

Giddings, T.H., Brower, D.L., and Staehelin, L.A. (1980). Visualization of particle complexes in the plasma membrane of *Micrasterias denticulata* associated with the formation of cellulose fibrils in primary and secondary cell walls. J. Cell Biol. **84:** 327–339.

Gomez, J., Sanchez-Martínez, D., Stiefel, V., Rigau, J., Puigdomenech, P., and Pages, M. (1988). A gene induced by the plant hormone abscisic acid in response to water stress encodes a glycine-rich protein. Nature **334:** 262-264.

Gómez, L.D., Baud, S., Gilday, A., Li, Y., and Graham, I.A. (2006). Delayed embryo development in the *Arabidopsis* Trehalose-6-Phosphate Synthase 1 mutant is associated with altered cell wall structure, decreased cell division and starch accumulation. Plant J. **46:** 69-84.

Gorshkova, T.A., Salnikov, V.V., Pogodina, N.M., Chemikosova, S.B., Yablokova, E.V., Ulanov, A.V., Ageeva, M.V., Van Darn, J.E.G., and Lozovaya, V.V. (2000). Composition and distribution of cell wall phenolic compounds in flax (*Linum usitatissimum* L.) stem tissues. Annal. Bot. **85:** 477- 486.

Gould, J.H., Palmer, R.L., and Dugger, W.M. (1986). Isolation and culture of cotton ovule epidermal protoplasts (prefiber cells) and analysis of the regenerated wail. Plant Cell Tiss. **6:** 47-59.

Grabber, J. H. (2005). How do lignin composition, structure, and cross-linking affect degradability? A review of cell wall model studies. Crop Sci. **45:** 820-831.

Gu, Y., Kaplinsky, N. , Bringmann, M. , Cobb, A., Carroll, A., Sampathkumar, A. , Baskin, T.I. , Persson, S. , and Somerville, C.R. (2010). Identification of a cellulose synthase-associated protein required for cellulose biosynthesis. Proc. Natl. Acad. Sci. USA **29:** 12866-12871.

Gutierrez, R., Lindeboom, J.J., Paredez, A.R, Mie, A.M.C., Ehrhardt, D.W. (2009). Arabidopsis cortical microtubules position cellulose synthase delivery to the plasma membrane and interact with cellulose synthase trafficking compartments. Nat. Cell Biol. **11:** 797-806.

Ha, M.A., Apperley, D.C., Evans, B.W., Huxham, M., Jardine, W.G., Vietor, R.J., Reis, D., Vian, B., and Jarvis, M.C. (1998). Fine structure in cellulose microfibrils: NMR evidence from onion and quince. Plant J. **16:** 183–190.

Hall, Q. , and Cannon, M.C. (2002). The cell wall hydroxyproline-rich glycoprotein RSH is essential for normal embryo development in arabidopsis. Plant Cell **14:** 1161-1172.

Hansen, K.M., Truesen, A.B., and Soderberg, J.R. (2001). Enzyme assay for identification of pectin and pectin derivatives, based on recombinant pectate lyase. J.A.O.A.C. Int. **84:** 1851-1854.

Harris, P.J., and Hartley, R.D. (1980). Phenolic constituents of the cell walls of monocotyledons. Biochem. System. Ecol. **8:**153–160.

Hatfield R., and Vermerris W. (2001). Lignin formation in plants. The dilemma of linkage specificity.Plant Physiol. **126:** 1351-1357.

Hernandez-Blanco, C., Feng, D.X., Hu, J. *et al.* (2007). Impairment of cellulose synthases required for *Arabidopsis* secondary cell wall formation enhances disease resistance. Plant Cell **19:** 890–903.

Herth, W. (1983) Arrays of plasma-membrane 'rosettes' involved in cellulose microfibril formation in spirogyra. Planta **159**: 347–356.

Herth, W. (1985). Plasma membrane rosettes involved in localized wall thickening during xylem vessel formation of *Lepidium sativum* L. Planta **164:** 12–21.

Hirose, E., Kimura, S., Itoh, T., and Nishikawa, J. (1999). Tunic of pyrosomas, doliolids and salps (Thaliacea, Urochordata): morphology and cellulosic components. Biol. Bull. **196:**113–120.

Holland, N., Holland, D., Helentjaris, T., Dhugga, K. S., Xoconostle-Cazares, B., and Delmer, D. P. (2000). A comparative analysis of the plant cellulose synthase (*CesA*) gene family. Plant Physiol. **123:** 1313-1323.

Horine, R.K., and Ruesnik, A.W. (1972). Cell wall regeneration around protoplasts isolated from *Convolvulus* tissue culture. Plant Physiol.**50:** 438-445.

Huang, R.F., and Lloyd, C.W. (1999). Gibberellic acid stabilises microtubules in maize suspension cells to cold and stimulates acetylation of α-tubulin1. FEBS Lett. **443:** 317-320.

Hughs, R., and Street, H.E. (1974). Galactose as an inhibitor of the expansion of root cells. Annals Bot. **38:** 555-564.

Iwai, H., Masaoka, N., Ishii, T., and Satoh, S. (2002). A pectin glucuronyltransferase gene is essential for intercellular attachment in the plant meristem Proc. Natl. Acad. Sci. USA **99:** 16319–16324.

Jackson, P., Galinha, C., Pereira, C., Fortunato, A., Soares, N., Amâncio, S. and Ricardo, C.P. (2001). Rapid deposition of extensin during the elicitation of grapevine callus cultures is specifically catalised by a 40kDa peroxidase. Plant Physiol. **127:** 1065-1076.

Jang, J.C., and Sheen, J. (1994). Sugar sensing in higher plants. Plant Cell **6**, 1665-1679.

Joshi, C.P., Thammannagowda, S., Fujino, T., Gou, J., and Avci, U. et al. (2011). Perturbation of Wood Cellulose Synthesis Causes Pleiotropic Effects in Transgenic Aspen. Mol. Plant **4:** 331-345.

Juge, N. (2006). Plant protein inhibitors of cell wall degrading enzymes. Trends Plant Sci. **11:** 359-367.

Jung, H.G., and Casler, M. D. (2006). Maize stem tissues: Cell wall concentration and composition during development. Crop Sci. **46:** 1793-1800.

Kapitonov, V.V., and Jurka, J. (2001). Rolling-circle transposons in eukaryotes. Proc. Natl. Acad. Sci. USA **98:** 8714–8719.

Kawagoe, Y., Delmer, D.P. (1997). Cotton CelA1 has a LIM like Zn binding domain in the N-terminal cytoplasmic region. Plant Physiol **114:** S–85.

Kawano Y , Saotome T , Ochiai Y, Katayama M , Narikawa R , Ikeuchi M (2011). Cellulose accumulation and a cellulose synthase gene are responsible for cell aggregation in the cyanobacterium *Thermosynechococcus vulcanus* RKN. Plant Cell Physiol. **52:** 957-966.

Keegstra, K., and Walton, J. (2006). β-Glucans--brewer's bane, dietician's delight. Science **311:** 1872-1873.

Koch, K.E. (2004). Sucrose metabolism: regulatory mechanisms and pivotal roles in sugar sensing and plant development. Curr. Opin. Plant Biol**. 7:** 235-246.

Lampe L. (1931). A microchemical and morphological study of the developing endosperm in maize. Bot. Gaz. **91:** 337-376.

Lee, M., and Phillips, R.L. (1988). The chromosomal basis of somaclonal variation. Annu. Rev. Plant Physiol. Plant Mol. Biol. **39:** 413–437.

Lerouxel, O., Cavalier, D.M., Liepman, A.H., and Keegstra, K. (2006). Biosynthesis of plant cell wall polysaccharides – a complex process. Cur. Opin. Plant Biol. **9:** 621–630.

Liepman, A. H., Wilkerson, C. G., and Keegstra, K. (2005). Expression of cellulose synthase-like (*Csl*) genes in insect cells reveals that *CslA* family members encode mannan synthases. Proc. Natl. Acad. Sci. USA **102:** 2221–2226.

Ling, A.P.K., Phua, G.A.T., Tee, C.S., and Hussein, S. (2010). Optimization of protoplast isolation protocols from callus of *Eurycoma longifolia*. J. Med. Plants Res. **4:** 1778-1785.

Lingwood, D., and Simons, K. (2007). Detergent resistance as a tool in membrane research. Nat. Protocols **2:** 2159 – 2165.

Lisch, D. (2002). *Mutator* transposons. Trends Plant Sci. **7:** 498-504.

Liu, S. et al. (2009). *Mu* transposon insertion sites and meiotic recombination events co-localize with epigenetic marks for open chromatin across the maize genome. PLoS Genet. 5: e1000733. doi:10.1371/journal.pgen.1000733

Lozovaya, V., Gorshkova, T., Yablokova, E., Zabotina,O., Ageeva, M., Rumyantseva, N., Kolesnichenko, E., Waranuwat, A., and Widholm, J. (1996). Callus cell wall phenolics and plant regeneration ability. Plant Physiol. **148:** 711-717.

Ludwig, S. R., Somers, D.A., and Peterson, W.L. (1985). High frequency callus formation from maize protoplasm. Theor. Appl. Genet. **71:** 344-350.

Margulies, M., Egholm1, M., Altman1, W.E., Attiya1, S, and Bader, J.S et al. (2005). Genome sequencing in microfabricated high-density picolitre reactors. Nature. **437:** 376-80.

Mathew, S., and Abraham, T.E. (2004). Ferulic acid: an antioxidant found naturally in plant cell walls and feruloyl esterases involved in its release and their applications. Crit. Rev. Biotechnol. **24:** 59-83.

Matthysse, A.G., White, S., and Lightfoot, R. (1995). Genes required for cellulose synthesis in *Agrobacterium tumefaciens*. J. Bacteriol. **177:** 1069-1075.

May, B.P. Liu, H., Vollbrecht, E., Senior, L., Rabinowicz, P.D., Roh, D., Pan, X., Stein, L., Freeling, M., Alexander, D., and Martienssen, R. (2003). Maize-targeted mutagenesis: A knockout resource for maize. Proc. Natl. Acad. Sci. **100:** 11541-11546.

McCabe, P.F., and Leaver, C.J. (2000). Programmed cell death in cell cultures Plant mol. biol. **44:** 359-368.

McCarty, D.R., Settles, A.M., Suzuki, M., Tan, B.C., and Latshaw, S. et al. (2005). Steady-state transposon mutagenesis in inbred maize. Plant J. **44:** 52-61.

McCarty, D.R., and Meeley, R.B. (2009). Transposon resources for forward and reverse genetics in maize. Handbook of Maize. J.L. Bennetzen, and S. Hake eds (New York, NY: Springer) pp. 561-584.

McClintock, B. (1947). Chromosome organization and gene expression. Cold Spring Harb. Symp. Quant. Biol. **16:**13-47.

Meeley, R.B., Briggs, S.P. (1995). Reverse genetics for maize. Maize Genet Coop Newsl **69:** 67-82.

Moreno, A.B., Peñas, G., Rufat, M., Bravo, J.M., Estopà, M., Messeguer, J., and San Segundo, B. (2005). Pathogen-induced production of the antifungal AFP protein from *Aspergillus giganteus* confers resistance to the blast fungus *Magnaporthe grisea* in transgenic rice. Mol. Plant-Microbe Interactions **18:** 960-972.

Murashige, T., and Skoog, F. (1962). A revised medium for rapid growth and bioassays with tobacco cultures. Physiol. Plant. **15:** 473-497.

Nieuwland, J., Feron, R., Huisman, B.A.H., Fasolino, A., Hilbers, C.W., Derksen, J., and Mariani, C. (2005). Lipid transfer proteins enhance cell wall extension in tobacco. Plant Cell. **17:** 2009–2019.

Nishiyama, Y., Sugiyama, J., Chanzy, H., and Langan, P. (2003). Crystal structure and hydrogen bonding system in cellulose I_α from synchrotron X-ray and neutron fiber diffraction. J. American Chem. Soc. **125:** 14300–14306.

Nishiyama, Y., Johnson, G..P, French, A.D., Forsyth, V.T., and Langan, P. (2008). Neutron crystallography, molecular dynamics, and quantum mechanics studies of the nature of hydrogen bonding in cellulose I_b. Biomacromolecules **9:** 3133–3140.

Nobles, D.R., Romanovicz, D.K., and Brown, R.M. Jr. (2001). Cellulose in cyanobacteria. Origin of vascular plant cellulose synthase? Plant Physiol. **127:** 529-542.

Nolte, K.D., Hendrix, D.L., Radin, J.W., and Koch, K.E. (1995). Sucrose synthase localization during initiation of seed development and trichome differentiation in cotton ovules. Plant Physiol. **109:** 1285–1293.

Oda,Y., Mimura, T., and Hasezawa, S. (2005). Regulation of secondary cell wall development by cortical microtubules during tracheary element differentiation in *Arabidopsis* cell suspensions. Plant Physiol. **137:** 1027-1036.

Offler, C.E., McCurdy, D.W., Patrick, J.W., and Talbot, M.J. (2003).Transfer cells: Cells specialized for a special purpose. Ann. Rev. Plant Biol. **54:** 431-454.

Ohashi-Ito, K., Oda, Y., and Fukuda, H. (2010). *Arabidopsis* VASCULAR-RELATED NAC-DOMAIN6 directly regulates the genes that govern programmed cell death and secondary wall formation during xylem differentiation. Plant Cell **22:** 3461-3473.

Oomen, R.J.F.J., Bergervoet, M. J.E.M., Bachem, C.W.B., Visser, R.J.F., and Vincken, J.P. (2003). Exploring the use of cDNA-AFLP with leaf protoplasts as a tool to study primary cell wall biosynthesis in potato. Plant Physiol. Biochem. **41:** 965-971.

Palmer, E., and Freeman, T. (2004). Investigation into the use of C- and N-terminal GFP fusion proteins for subcellular localization studies using reverse transfection microarrays. Comp. Funct. Genom. **5:** 342-353.

Pandey, S., Wang, X-Q., Coursol, S.A., and Assmann, S.M. (2002). Preparation and applications of *Arabidopsis* thaliana guard cell protoplasts. New Phytol. **153:** 517–526.

Park, Y.W., Tominaga, R., Sugiyama, J., Furuta, Y., Tanimoto, E., Samejima, M., Sakai, F., and Hayashi, T. (2003). Enhancement of growth by expression of poplar cellulase in *Arabidopsis thaliana*. Plant J. **33:** 1099-1106.

Paredez, A.R., Somerville, C.R., and Ehrhardt, D.W. (2006). Visualization of cellulose synthase demonstrates functional association with microtubules. Science, **312:** 1491–1495.

Pauly, M., Albersheim, P., Darvill, A., and York, W.S. (1999). Molecular domains of the cellulose/xyloglucan network in the cell walls of higher plants. Plant J. **20:** 629-639.

Pauly, M., and Keegstra, K. (2009). Cell-wall carbohydrates and their modification as a resource for biofuels. Plant J. **54:** 559-568.

Pear, J.R., Kawagoe, Y., Schreckengost, W.E., Delmer, D.P., and Stalker, D.M. (1996). Higher plants contain homologs of the bacterial *celA* genes encoding the catalytic subunit of cellulose synthase. Proc. Natl. Acad. Sci. USA. **93**(22)**:** 12637-12642.

Peng, L., Kawagoe, Y., Hogan, P., and Delmer, D. (2002). Sitosterol-β-glucoside as primer for cellulose synthesis in plants. Science **295:** 147-150.

Perrin, R., Wilkerson, C., and Keegstra, K. (2001). Golgi enzymes that synthesize plant cell wall polysaccharides: finding and evaluating candidates in the genomic era. Plant Molec. Biol. **47:** 115-130.

Perrin, R.M., DeRocher, A.E., Bar-Peled, M., Zeng, W. and Norambuena, L. (1999). Xyloglucan fucosyltransferase, an enzyme involved in plant cell wall biosynthesis. Science **18:** 1976–1979.

Persson, S., Paredez, A., Carroll, A., Palsdottir, H., Doblin, M., Poindexter, P., Khitrov, N., Auer, M., and Somerville, C.R. (2007). Genetic evidence for three unique components in primary wall cell-wall cellulose synthase complexes in *Arabidopsis.* Proc. Natl. Acad. Sci. USA **104:** 15566–15571.

Philippe, S., Barron, C., Robert, P., Devaux, M.F., Saulnier, L., and Guillon, F. (2006). Characterization using Raman microspectroscopy of arabinoxylans in the walls of different cell types during the development of wheat endosperm. J. Agric. Food Chem. **54:** 5113–5119.

Pilet, P.E., Blaschek, W., Senn, A., and Franz, G. (1984). Comparison between maize root cells and their respective regenerating protoplasts: wall polysaccharides. Planta **161:** 465-469.

Postlethwait, S.N., and Nelson, O.E. (1957). A chronically wilted mutant of maize. Am. J. Bot. **44:** 628–633.

Potrykus, I. (1991). Gene transfer to plants: Assessment of published approached and results. Annu. Rev. Plant Physiol. Plant Mol. Biol. **42:** 205-225.

Priefert, H., Rabenhorst, J., and Steinbuchel, A. (2001). Biotechnological production of vanillin. Appl. Microbiol. Biotechnol. **56:** 296-314.

Raizada, M.N., and Walbot, V. (2000). The late developmental pattern of *Mu* transposon excision is conferred by a cauliflower mosaic virus 35S-driven MURA cDNA in transgenic maize. Plant Cell **12:** 5-22.

Ralph, J., Quideau, S., Grabber, J.H., and Hatfield, R.D. (1994). Identification and synthesis of new ferulic acid dehydrodimers present in grass cell walls. J. Chem. Soc. Perkin Transactions1 **23:** 3485–3498.

Ramakrishna, P., and Amritphale, D. (2005). The perisperm-endosperm envelope in *Cucumis*: Structure, proton diffusion and cell wall hydrolysing activity. Ann. Bot. **96:** 769-778.

Ramsden, M. J., and Blake, F. S. R. (1997). A kinetic study of the acetylation of cellulose, hemicellulose and lignin components in wood. Wood Sci. Tech. **31:** 45-50.

Reid, J.S.G., and Edwards, M.E. (1995). Galactomannans and other cell wall storage polysaccharides in seeds. Food polysaccharides and their applications. A.M. Stephen, ed.(Boca Raton, FL: CRC Press) pp. 155–186.

Richmond, P.A. (1991). Occurrence and functions of native cellulose. Biosynthesis and biodegradation of cellulose. C.H. Haigler, and P.J. Weimer, eds (New York, NY: Marcel Dekker) pp. 5–23.

Richmond, T**.A., and Somerville, C.R.** (2000). The cellulose synthase superfamily. Plant Physiol. **124:** 495-498.

Ridley, B. L., O'Neill, M. A., and Mohnen, D. (2001). Pectins: structure, biosynthesis, and oligogalacturonide-related signaling. Phytochem. **57:** 929–967.

Roberts, E., and Roberts, A.W. (2009). A cellulose synthase (*CesA*) gene from the red alga *Porphyra Yezoensis* (Rhodophyta). J. Phycol., **45:** 203-212.

Robertson, D.S. (1978). Characterization of a mutator system in maize. Mutat. Res. **51:** 21–28.

Rose, J.K.C., and Bennett, A.B. (1999). Cooperative disassembly of the cellulose-xyloglucan network of plant cell walls: parallels between cell expansion and fruit ripening. Trends Plant Sci. **4:** 176–183.

Rose, J.K.C., Saladié, M., and Catalá, C. (2004). The plot thickens: new perspectives of primary cell wall modification. Curr. Opin. Plant Biol. **7:** 296-301.

Ross, P., Mayer, R. and Benziman, M. (1991). Cellulose biosynthesis and function in bacteria Microbiol. Rev. **55:** 35-58.

Ruan, Y.L., Llewellyn, D.J., and Furbank, R.T. (2003). Suppression of sucrose synthase gene expression represses cotton fiber cell initiation, elongation and seed development. Plant Cell **15:** 952–964.

Sampedro, J., and Cosgrove, D. J. (2005). The expansin superfamily. Genome Biol. **6:** 242.1–242.11.

Sato S, et al. (2001). Role of the putative membrane-bound endo-1,4-beta-glucanase KORRIGAN in cell elongation and cellulose synthesis in *Arabidopsis thaliana*. Plant Cell Physiol. **42:** 251-63.

Saxena, I.M., Brown, R.M. Jr., Fevre, M., Geremia, R.A., and Henrissat, B. (1995). Multidomain architecture of β-glycosyltransferases: implications for mechanism of action. J Bacteriol. **177:** 1419–1424.

Saxena, I.M., Brown, R.M. Jr.,and Dandekar, T. (2001). Structure-function characterization of cellulose synthase: relationship to other glycosyltransferases. Phytochem. **57:** 1135–1148.

Saxena, I. M., and Brown, R. M. (2005). Cellulose biosynthesis: Current views and evolving concepts. Ann. Bot. **96:** 9-21.

Schaffner, A.R., and Sheen, J. (1991). Maize *rbcS* promoter activity depends on sequence elements not found in dicot rbcS promoters. Plant Cell **3:** 997-1012.

Scheible, W.R., and Pauly M. (2004). Glycosyltransferases and cell wall biosynthesis: novel players and insights. Curr. Opin. Plant Biol. **7:** 285-295.

Schnable, J.C., Springer, N.M., and Freeling, M. (2011). Differentiation of the maize subgenomes by genome dominance and both ancient and ongoing gene loss. Proc. Natl. Acad. Sci. doi/10.1073/pnas.1101368108

Schnable, P.S., Ware, D., Fulton, R.S., Stein, J.C., and Wei, F. et al. (2009). The B73 maize genome: complexity, diversity, and dynamics. Science **326:** 1112-1115.

Schrick, K., Fujioka, S., Takatsuto, S., Stierhof, Y.D., and Stransky, H., Yoshida, S., and Jurgens, G. (2004). A link between sterol biosynthesis, the cell wall, and cellulose in Arabidopsis. Plant J. **38:** 227-243.

Seifert, G.J. (2004). Nucleotide sugar interconversions and cell wall biosynthesis: how to bring the inside to the outside. Curr. Opin. Plant Biol. **7:** 277–284.

Seifert, G.J., and Blaukopf, C. (2010). Irritable walls: The plant extracellular matrix and signaling. Plant Physiol. **153:** 467-478.

Settles, A.M., Latshaw, S., and McCarty, D.R. (2004). Molecular analysis of high-copy insertion sites in maize. Nucl. Acids Res. **32:** e54. doi: 10.1093/nar/gnh052

Settles, A.M. et al. (2007). Sequence-indexed mutations in maize using the UniformMu transposon-tagging population. BMC Genomics. **8:** 116.

Shatil-Cohen, A., and Menachem Z.A. (2011). Bundle-sheath cell regulation of xylem-mesophyll water transport via aquaporins under drought stress: a target of xylem-borne ABA? Plant J. 72–80.

Shea, E.M., Gibeaut, D.M., and Carpita, N.C. (1989). Structural analysis of the cell walls regenerated by carrot protoplasts. Planta **179:** 293-308.

Singh, B., Cheek, H.D., and Haigler, C.H. (2009). A synthetic auxin (NAA) suppresses secondary wall cellulose synthesis and enhances elongation in cultured cotton fiber. Plant Cell Rep. **28:** 1023–1032.

Skoog, F., and Miller, C.O. (1957). Chemical regulation of growth and organ formation in plant tissues cultured in vitro. Symp. Soc. Exp. Biol. **54:** 118–130.

Somerville,C., Bauer, S., Brininstool, G., Facette, M., and Hamann,, T., Milne, J., Osborne, E., Paredez, A., Persson, S., Raab, T., Vorwerk, S., and Youngs, H. (2004). Toward a systems approach to understanding plant cell walls. Science **306:**, 2206–2211.

Stafford, A., and Warren, G. (1991). Plant Cell and Tissue Culture. (Buckingham, UK: Open University Press) pp. 48-81.

Sterling, J. D., Atmodjo, M. A., Inwood, S. E., Kumar Kolli, V. S., Quigley, H. F., Hahn, M. G., and Mohnen, D. (2006)**.** From the cover: Functional identification of an *Arabidopsis* pectin biosynthetic homogalacturonan galacturonosyltransferase. Proc. Natl. Acad. Sci. USA **103:** 5236–5241.

Stone, E.A., and Ayroles, J.F. (2009) Modulated Modularity Clustering as an exploratory tool for functional genomic inference. PLoS Genet 5(5): e1000479. doi:10.1371/journal.pgen.1000479

Subbaiah, C.C., Bush, S.D., and Sachs, M.M. (1998). Mitochondrial contribution to the anoxic $Ca2^{+}$ signal in maize suspension-cultured cells. Plant Physiol. **118:** 759–771.

Swigonova, Z., Lai, J., Ma, J., Ramakrishna, W.,Llaca, V., Bennetzen, J., and Messing, J. (2004). Close split of sorghum and maize genome progenitors. Genome Res. **14:** 1916-1923.

Szymanska-Chargot, M., Cybulska, J., and Zdunek, A. (2011). Sensing the structural differences in cellulose from apple and bacterial cell wall materials by Raman and FT-IR spectroscopy. Sensors **11:** 5543-5560.

Tamaru, Y., Ui, S., Murashima, K., Kosugi, A., Chan, H., Doi, R. H., Liu, B. (2002). Formation of protoplasts from cultured tobacco cells and *Arabidopsis thaliana* by the action of cellulosomes and pectate lyase from *Clostridium cellulovorans*. Appl. Environ. Microbiol. **68:** 2614-2618.

Tamura, K., Dudley, J., Nei, M., and Kumar, S. (2007). MEGA4: molecular evolutionary genetics analysis (MEGA) software version 4.0. Mol. Biol. Evol. **24**: 1596-1599.

Tanaka, F., and Iwata, T. (2006). Estimation of the elastic modulus of cellulose crystal by molecular mechanics simulation. Cellulose **13:** 509–517.

Tanaka, K., Murata, K., Yamazaki, M., Onosato, K., and Miyao, A. et al. (2003).Three distinct rice cellulose synthase catalytic subunit genes required for cellulose synthesis in the secondary wall. Plant Physiol.**133:** 73-83.

Tanurdzic, M. et al. (2008). Epigenomic consequences of immortalized plant cell suspension culture. PLoS Biol. **6:** e302. doi:10.1371/journal.pbio.0060302

Taylor, N.G., Laurie, S., and Turner, S.R. (2000). Multiple cellulose synthase catalytic subunits are required for cellulose synthesis in *Arabidopsis*. Plant Cell **12:** 2529–2539.

Taylor, N.G., Howells, R.M., Huttly, A.K., Vickers, K., and Turner, S.R. (2003). Interactions among three distinct CesA proteins essential for cellulose synthesis. Proc. Natl. Acad. Sci. USA **100:** 1450–1455.

Taylor, N.G. (2008). Cellulose biosynthesis and deposition in higher plants. New Phytol. **178:** 239–252.

Thompson, J.E., and Fry, S.C. (2001). Restructuring of wall-bound xyloglucan by transglycosylation in living plant cells. The Plant J. **26:** 23-34.

Thorpe, M.R., Macrae, E.A., Minchin, P.E.H., and Edwards, C.M. (1999). Galactose stimulation of carbon import into roots is confined to the Poaceae. J. Exp. Bot. **50:** 1613-1618.

Turner, S., Gallois, P., and Brown, D. (2007). Tracheary element differentiation. Annu. Rev. Plant Biol. **58:** 407–433.

Valla, S., Coucheron, D.H., Fjaervlk, E., Kjosbakken, J., and Welnhouse, H. et al. (1989). Cloning of a gene involved in cellulose biosynthesis in *Acetobacter xylinum*: Complementation of cellulose-negative mutants by the UDPG pyrophosphorylase structural gene. Mol. Gen. Genet. **217:** 26-30.

Varner, J.E., and Lin, L. (1989). Plant cell wall architecture. Cell **56:** 231-239.

Veit, B., Vollbrecht, E., Mathern, J., and Hake, S. (1990). A tandem duplication causes the *Knl-O* allele of Knotted, a dominant morphological mutant of maize. Genetics **125:** 623-631.

Vicient, C.M. (2010). Transcriptional activity of transposable elements in maize. BMC Genom. **11:** 601doi:10.1186/1471-2164-11-601

Vietor, R.J., Newman, R.H., Ha, M.A., Apperley, D.C., and Jarvis, M.C. (2002). Conformational features of crystal-surface cellulose from higher plants. Plant J. **30:** 721–731.

Vollbrecht, E., **Duvicka, J., Scharesa, J.P., Ahernb, K.R., and Deewatthanawong, P. et al.** (2010). Genome-wide distribution of transposed Dissociation elements in maize. Plant Cell **22:** 1667-1685.

Walley, J.W., , Coughlan, S., Hudson, M.E., Covington, M.F., and Kaspi R, et al. (2007) Mechanical stress induces biotic and abiotic stress responses via a novel cis-element. PLoS Genet. **3:** e172. doi:10.1371/journal.pgen.0030172

Walbot, V. (2000). Saturation mutagenesis using maize transposons. Curr. Opin. Plant Biol. **3:** 103-107.

Walbot, V., and Rudenko, G.N. (2002). *MuDR/Mu* transposable elements of maize. In Mobile DNA II. N.L. Craig, R. Craigie, M. Gellert, and A. Lambowitz, eds (Washington, DC: American Society of Microbiology), pp. 533–564.

Wang, H., Slater, G.P., Fowke, L.C., Saleem, M., Cutler, A.J. (1991). Comparison of cell wall regeneration on maize protoplasts isolated from leaf tissue and suspension cultured cells**.** In Vitro Cell. Dev. Biol. **27:** 70-77.

Wang, J., Elliott, J.E., and Williamson, R.E. (2008). Features of the primary wall CESA complex in wild type and cellulose-deficient mutants of *Arabidopsis thaliana*. J. Exp. Bot. **59:** 2627-2637.

Wang, L., Guo, K., Li, Y., Tu, Y., Hu, H., Wang, B., Cui, X., and Peng, L. (2010). Expression profiling and integrative analysis of the *CESA*/*CSL* superfamily in rice. BMC Plant Biol. doi/10.1186/1471-2229-10-282

Wang, Q.H. , Zhang, X., Li, F.G., Hou, Y.X., Liu, X.L., and Zhang, X.Y. (2011). Identification of a UDP-glucose pyrophosphorylase from cotton (*Gossypium hirsutum L.*) involved in cellulose biosynthesis in *Arabidopsis thaliana.* Plant Cell Rep. **30:** 1303-1312.

Wei, F., Coe, E., Nelson, W., Bharti, A.K., Engler, F. et al. (2007). Physical and genetic structure of the maize genome reflects its complex evolutionary history. PLoS Genet. **7:** e123. doi:10.1371/journal.pgen.0030123

Whitney, S.E.C., Gothard, M.G.E., Mitchell, J.T., and Gidley, M.J. (1999). Roles of cellulose and xyloglucan in determining the mechanical properties of primary plant cell walls. Plant Physiol. **121:** 657–663.

Wicker, T. et al. (2007). A unified classification system for eukaryotic transposable elements. Nature Rev. Genet. **8:** 973-982.

Wilkie, K.C.B. (1979). The hemicelluloses of grasses and cereals. Adv. Carbohydrate Chem. Biochem. **36:** 215–64.

Williams-Carrier, R., Stiffler, N., Belcher, S., Kroeger, T., Stern, D.B., Monde, R.A., Coalter, R., and Barkan, A. (2010). Use of Illumina sequencing to identify transposon insertions underlying mutant phenotypes in high-copy *Mutator* lines of maize. Plant J. **63:** 167-77.

Wu, A., Hu, J.S., and Liu, J.Y. (2009). Functional analysis of a cotton cellulose synthase A4 gene promoter in transgenic tobacco plants. Plant Cell Reports **28:** 1539-1548.

Wu, C.T., Leubner-Metzger, G., Meins, F., and Bradford, K.J. (2001). Class I β-1,3-glucanase and chitinase are expressed in the micropylar endosperm of tomato seeds prior to radicle emergence. Plant Physiol. **126:** 1299-1313.

Xin, Z., and Li, P.H. (1992). Abscisic acid-induced chilling tolerance in maize suspension-cultured cells. Plant Physiol. **99:** 707–711.

Yamamoto, R. (1987). Effect of galactose on auxin-induced cell elongation in oat coleoptile segments in mannitol solutions. J. Plant Res. **100:** 43-49.

Yamazaki, T., Kawamura, Y., Minami, A., and Uemura, M. (2008). Calcium-dependent freezing tolerance in *Arabidopsis* involves membrane resealing via synaptotagmin SYT1. Plant Cell **20:** 3389-3404.

Ye, H., Song, Y.R., Marcus, A., and Varner, J.E. (1991). Comparative localization of three classes of cell wall proteins. Plant J. **1:** 175-183.

Yim, K.O. and Bradford, K.J. (1998). Callose deposition is responsible for apoplastic semipermeability of the endosperm envelope of muskmelon seeds. Plant Physiol. **118:** 83-90.

Yokoyama R. and Nishitani K. (2001). A comprehensive expression analysis of all members of a gene family encoding cell-wall enzymes allowed us to predict cis-regulatory regions involved in cell-wall construction in specific organs of *Arabidopsis*. Plant Cell Physiol. **42:** 1025-33.

Yong W. P. et al. (2003). Enhancement of growth by expression of poplar cellulose in Arabidopsis thaliana. Plant J. **33:** 1099-1106.

Yoo, S.-D., Cho, Y.-H., and Sheen, J. (2007). Arabidopsis mesophyll protoplasts: a versatile cell system for transient gene expression analysis. Nature Protocols **2:** 1565-1572.

Yu, S.M. (1999). Cellular and genetic responses of plants to sugar starvation. Plant Physiol. **121:** 687-693.

Zeiger, E., Hepler, P.K. (1979). Blue light induced intrinsic vacuolar fluorescence in onion guard cells. J. Cell Sci. **37:** 1-10.

Zhong et al. (2003). Expression of a mutant form of cellulose synthase *AtCesA7* causes dominant negative effect on cellulose biosynthesis. Plant Physiol. **132:** 786-795.

BIOGRAPHICAL SKETCH

Brent O'Brien was born in 1982 in Davenport Iowa. The oldest child in a family of five, Brent grew up in several locations due to to his father's military career. Before beginning college in Florida, he had spent 4 years in Jamaica, 8 years in Okinawa, Japan, and 7 years in Jacksonville, North Carolina. Brent began his post-high school academic career in 2000 at Embry-Riddle Aeronautical University with a focus on aeronautical engineering. His interests soon shifted, however, and he transferred to the University of Florida in 2002. He graduated cum laude with a Bachelor's degree in Plant Science, (with a focus in biotechnology) in 2004, and remained at the University of Florida for graduate school. Brent was awarded an Alumni Fellowship to enroll in the Plant Molecular and Cellular Biology program, and received his PhD in December, 2011.